On the origin and nature of brown dwarfs and massive planets

Dissertation
zur
Erlangung des Doktorgrades (Dr. rer. nat)
der
Mathematisch-Naturwissenschaftlichen Fakultät
der
Rheinischen Friedrich-Wilhelms-Universität Bonn

vorgelegt von

Ingo Thies
aus
Niebüll

Bonn, 2010

Angefertigt mit Genehmigung der Mathematisch-Naturwissenschaftlichen Fakultät der Rheinischen Friedrich-Wilhelms-Universität Bonn.

1. Referent: Prof. Dr. P. Kroupa
2. Referent: Prof. Dr. R. Izzard

Tag der Promotion: 9. Februar 2011
Erscheinungsjahr: 2011

I believe in intuition and inspiration. Imagination is more important than knowledge. For knowledge is limited, whereas imagination embraces the entire world, stimulating progress, giving birth to evolution. It is, strictly speaking, a real factor in scientific research.

Albert Einstein

To all the people who will have left this universe before the universe will leave us

Summary

In this thesis the apparent peculiarities of brown dwarfs (BDs) are pointed out which force us to treat them as a population apart from, but yet still related to the stellar population. In particular, the properties that make BDs so special are deduced from the observational evidence in Chapter 1: 1. The *brown dwarf desert*, i.e. the apparent dearth of substellar, non-planetary companions to stars, 2. the truncated distribution of the semi-major axes of BD-BD binaries (Fig. 1.1), 3. the unusually top-heavy mass ratio distribution of BD-BD binaries, compared to star-star binaries (Fig. 1.11), and 4. the theoretical difficulties to explain a star-like, i.e. isolated formation scenario for BDs (Adams & Fatuzzo 1996; Goodwin & Whitworth 2007). These combined facts effectively rule out star-like formation as the predominant mechanism of BD formation. In addition, some fraction of very-low-mass stars may also have a non-star-like origin. As an immediate consequence, a separate population, here called *BD-like*, is introduced. Although the present observational data do not yet allow a precise determination of the mass range of this population, a steep descent of the BD-like initial mass function between 0.1 and 0.2 $M_\odot$ as well as a steep onset of the stellar IMF slightly below the hydrogen-burning mass, $m_\mathrm{H} = 0.075\,M_\odot$, appears to be in good agreement with the lower end of the observational mass function if it has been corrected for unresolved binaries (see Section 1.2.2). This two-populations model results necessarily in a discontinuity in the overall IMF of BDs and stars together. This discontinuity may be hidden in the observed mass function unless the mass function is corrected for unseen binaries.

In Chapter 2 the issue is revised for the case of a high abundance of BD-BD binaries. It is shown that the discontinuity persists even if a star-like BD-BD binary fraction of up to 60 % is assumed. This further supports the two-populations model.

In Chapter 3 a probable formation scenario of BDs (as well as for massive gas planets) is presented. Earlier work by Stamatellos et al. (2007) and subsequent studies had shown that fragmentation of massive circumstellar disc beyond 100 AU is a valid mechanism to form substellar companions. My research now shows that less massive (and thus more frequent) discs can also fragment upon a tidal perturbation. While direct hydrodynamic perturbation in disc-disc collisions (Shen et al. 2010) requires two colliding massive discs, rendering such a scenario highly improbable, a tidal perturbation by a low-mass star with no disc or only a negligibly small disc (i.e. a typical protoplanetary disc in contrast to a massive extended one) appears to be reasonably probable for encounter distances around 500 AU, as estimated by Thies et al. (2005) and briefly revisited in Section 3.2 in Chapter 3.

This thesis is based on the following publications:

- Thies & Kroupa 2007, ApJ, 671, pp. 767–780. *A Discontinuity in the Low-Mass Initial Mass Function*(Chapter 1),
- Thies & Kroupa, 2007 MNRAS, 390, pp. 1200–1206. *A discontinuity in the low-mass IMF - the case of high multiplicity*(Chapter 2), and
- Thies et al., 2010 ApJ, 717, pp. 577-585. *Tidally Induced Brown Dwarf and Planet Formation in Circumstellar Disks*(Chapter 3).

Some preliminary work has also been published in Thies, Kroupa & Theis 2005 MNRAS, 364, pp. 961-970. *Induced planet formation in stellar clusters: a parameter study of star-disc encounters.*
Supplementary content like movies from our calculations can be downloaded from the AIfA download page,
http://www.astro.uni-bonn.de/~webaiub/german/downloads.php

Contents

List of Figures

List of Tables

Introduction

Understanding the origin of stars as well as of substellar objects like brown dwarfs (BDs) and planets is deeply related to the understanding the origin of ourselves. BDs are stars from a hydrodynamical point of view, but lack the central conditions (temperature and density) to sustain thermonuclear fusion of hydrogen. BDs thus are thought to form like stars from the collapse of a molecular cloud core but ultimately cool to low luminosities. Planets, on the other hand, are believed to form in the gas and dust discs surrounding young stars. They form either through direct gravitational collapse or through the coagulation of dust to larger bodies which then begin to accrete from the circumstellar disc.

Research on planet formation has made great progress in the recent decades while the investigation of brown dwarfs has been advanced mainly in the recent 15 years after the first confirmed discovery of such bodies between the planetary and stellar mass range in 1995.

The first brown dwarf directly observed is Gliese 229B and was discovered in 1995 (Nakajima et al. 1995). In the same year, the first extrasolar planet (or *exoplanet*), 51 Pegasi (Mayor & Queloz 1995), was found via Doppler spectroscopy. Since then, about one thousand brown dwarfs[1] and several hundred exoplanets[2] have been discovered.

In this thesis I investigate different aspects of the origin and formation mechanisms of planets and brown dwarfs in the context of the natural environment of star formation. In the past, the evolution of stars and their circumstellar material have mostly been treated in isolation, i.e. without any interference with their environment. The fact that most stars form in clusters rather than in isolation (Lada & Lada 2003; Kroupa 2005), however, forces some paradigm change in this topic.

The thesis begins with an analysis of the observational facts about the nature of brown dwarfs and very-low-mass stars (i.e. stars which have masses only slightly above the hydrogen-burning limit of 0.075 $M_{\odot}$). In the first two chapters the implications of the evident dearth of BD companions to normal stars and the different statistical properties of stellar and BD/VLMSs binaries are analysed. Based on the observational fact that BDs/VLMSs and ordinary stars essentially do not pair-up in close binaries we propose the existence of (at least) two separate populations in star clusters: a *starlike* population that originates from the standard model of cloud fragmentation, collapse and accretion, and a *BD-like* population the members of which form through different channels like the ejection of unfinished protostars from dynamically unstable multiple systems (the so-called *embryo ejection* model, Reipurth & Clarke 2001) or as widely

[1] http://simbad.u-strasbg.fr/simbad/
[2] http://exoplanet.eu/catalog-all.php

separated substellar companions that got separated from their host star by dynamical interactions with other stars or companions (Goodwin & Whitworth 2007).

This hypothesis is further supported by peculiarities in the orbital statistics of BD-BD binaries. While stellar binaries have a widespread distribution of orbital separations, ranging from near-contact orbits (< 0.01 AU) up to thousands of AU, with a most likely separation around 30 AU, the distribution of BD and VLMS binaries is truncated above ≈ 15 AU and peaks at ≈ 4 AU. This cannot be explained by simple downscaling from the stellar regime but may fit with a formation in systems of a smaller scale than the typical star-forming cluster. Such subsystems may be multiple protostar systems with at least three members (since such systems are dynamically unstable in most cases) or dense sub-protostellar gas filaments in the prestellar cloud.

The assumption of two separate populations has severe implications on the mass distribution of stars and brown dwarfs. In particular, the initial mass function (IMF), which describes the outcome of star formation, has to be split into two separate regimes to cover the star-like regime as well as the realm of BD-like bodies. Although these regimes probably overlap between about 0.07 and 0.15 $M_\odot$ the presence of two separate IMFs implies a discontinuity in this mass range. By varying basic parameters of the separate IMFs (in particular, the BD-to-star ratio, the slope of the BD-like IMF and its upper mass limit) the fundamental underlying IMFs are fitted to the Orion Nebula Cluster (ONC), the Taurus-Auriga association (TA), IC 348 and the Pleiades. The fitting takes also into account that the majority of binaries are not resolved in typical star cluster surveys, making a numerical correction of this "binary error" necessary. The resulting system IMFs are fitted against the observed mass functions of all clusters. As a major result, a discontinuity emerges in the true (individual object) IMFs for all clusters under study.

Chapter 2 refines the study of the Chapter 1 for the case of a high BD-BD multiplicity and shows that the discontinuity found there is still present for a binary fraction up to 60 per cent (i.e. comparable to that of stars) among BDs.

One of the most important mechanisms of perturbation of a forming star by its environment is the gravitational (or, more accurately, tidal) influence of other stars in the star cluster. In a typical star cluster with several thousand stars per cubic parsec the average distance between two stars is of the order of $\lesssim 0.1$ pc or $\lesssim 20\,000$ AU. This is sufficient to prevent significant tidal perturbation even by the most massive stars during most of the time. However, star clusters are dynamical systems where encounters between two stars at much closer distances occur from time to time. In Chapter 3 the effects of moderately close encounters between 500 and 1000 AU on massive circumstellar discs is analysed via a 3D smoothed particle hydrodynamics (SPH) code with radiative heat transfer treatment. It is shown that such encounters do not prohibit the formation of brown dwarfs via fragmentation but, instead, even support fragmentation in otherwise stable discs. Fragmentation thus requires less massive discs than assumed by Goodwin & Whitworth (2007); Stamatellos et al. (2007); Stamatellos & Whitworth (2009a) for isolated disc fragmentation. It is further shown that, similar to the embryo-ejection model, the least massive companions formed this way are prone to dynamical ejection while more massive ones tend to keep bound within a few 100 AU. Also the formation of

BD and VLMS binaries through dynamical interaction of such newborn companions is demonstrated and shown to be consistent with the observed properties of very-low-mass binaries. In addition, I show that the perturbing star accretes a considerable amount of gas from the target star's circumstellar disc which may allow the formation of randomly aligned planets around it.

This work then closes with an outlook on the future work, in particular, the analysis of new observational data available in future as well as an extended parameter study of planet and BD formation to create a sufficient statistical basis for further analysis and predictions.

1 Brown dwarfs and very-low-mass stars – do they form a separate population?

(based on Thies & Kroupa 2007, ApJ, 671, pp. 767–780. *A Discontinuity in the Low-Mass Initial Mass Function*)

The origin of brown dwarfs (BDs) is still an unsolved mystery. While the standard model describes the formation of BDs and stars in a similar way recent data on the multiplicity properties of stars and BDs show them to have different binary distribution functions. Here we show that proper treatment of these uncovers a discontinuity of the multiplicity-corrected mass distribution in the very-low-mass star (VLMS) and BD mass regime. A continuous IMF can be discarded with extremely high confidence. This suggests that VLMSs and BDs on the one hand, and stars on the other, are two correlated but disjoint populations with different dynamical histories. The analysis presented here suggests that about one BD forms per five stars and that the BD-star binary fraction is about 2 %–3 % among stellar systems.

1.1 Introduction

Traditionally, brown dwarfs (BDs) are defined as (sub)stellar bodies with masses below the hydrogen burning mass limit (HBL), $m_{\rm H} = 0.075\,M_\odot$ for solar composition, and consequently they cool indefinitely after formation (Burrows et al. 1993; Chabrier & Baraffe 2000). Several attempts have been made to explain the formation of BDs by the same mechanisms as for stars, i.e. via fragmentation of a gas cloud and subsequent accretion (Adams & Fatuzzo 1996; Padoan & Nordlund 2002, 2004). If a gas cloud in a star-forming region fragments there will be a certain number of gas clumps with masses below the HBL. Unless the mass of the fragment is below the local Jeans mass it will contract in essentially the same way as higher mass clumps and finally produce a single or multiple BD. This scenario predicts similar multiplicities and also a substellar initial mass function (IMF) as a continuous extension of the stellar one (e.g. the standard model with BDs in Kroupa et al. 2003).

However, recent observations have shown that there is a lack of BD companions to low-mass stars (McCarthy, Zuckerman & Becklin 2003). Grether & Lineweaver (2006) found a star-BD binary fraction among solar-type primaries of less than 1 % for close companions, the *brown dwarf desert*. This implies two populations of stellar and sub-

stellar objects, and that binaries are formed in each population separately (except for pairing due to post-formation dynamical exchanges). Observations e.g. by Reid et al. (2006) also show that most BD binaries have a primary-to-companion mass ratio of $q > 0.8$, in contrast to the mass ratio distribution of stellar binaries which has typically $q < 0.4$ (Duquennoy & Mayor 1991).

There are indications, e.g. Metchev & Hillenbrand (2005), that the BD desert may not be as dry for larger separations (> 30 AU) as it is for smaller ones. Since new surveys using adaptive optics or new instruments like the upcoming James Webb Space Telescope might reveal more substellar companions to stars, the fraction of star-BD systems may increase.

Apart from the BD desert there are more hints for a separate population. For example, BDs and VLMSs have a relatively low binary fraction of about 15 % (Bouy et al. 2003; Close et al. 2003; Martín et al. 2003; Kraus, White & Hillenbrand 2006; Law et al. 2007). By comparison, the stellar binary fraction is close to 100 % for the very young Taurus-Auriga association (TA, about 1 Myr; Duchêne 1999; Luhman et al. 2003) and about 40 %–50 % for other clusters and field stars (Lada 2006). The BD and VLMS binary fraction can be increased to a star-like binary fraction if there are a large fraction of $\lesssim 5$ AU binaries, e.g. as deduced by Jeffries & Maxted (2005). But such a semi-major axis distribution would again imply a discontinuity of its form between low-mass stars and VLMSs/BDs and is not supported by the radial-velocity survey of Joergens (2006). We therefore do not consider the star-like formation as a major mechanism for BDs.

It has also been argued that the low binary fraction of BDs can be understood as a continuous extension of a trend that can already be recognised from G dwarfs to M dwarfs (Luhman 2004a; Sterzik & Durisen 2003). Therefore, the binary fraction alone cannot be taken as a strong evidence to introduce a separate population.

The most striking evidence for two separate populations is the empirical fact that the distribution of the separations and therefore the binding energies of BD binaries differs significantly from that in the stellar regime (Bouy et al. 2003; Burgasser et al. 2003; Martín et al. 2003; Close et al. 2003). This is shown in Figures 1.1 and 1.2. The solid line is a Gaussian fit to the central peak of the histogram while the dash-dotted one refers to (Basri & Reiners 2006, a compressed Fischer & Marcy 1992 fit). BDs and very low-mass stars (VLMS) have a semi-major axis distribution limited to $\lesssim 15$ AU, whereas M, K, and G dwarfs have a very broad and similar distribution (*long-dashed and short-dashed curves*; Close et al. 2003; Law, Hodgkin & Mackay 2007; Goodwin et al. 2007). There is also a dearth of BDs below 1 AU. Recent findings, e.g. by Guenther & Wuchterl (2003) and Kenyon et al. (2005), suggest a low number of such very close BD/VLMSs binaries. The semi-major axis distribution of BDs/VLMSs binaries based on the data from Close et al. (2003) can be modelled with a $\log a$ Gaussian centered at 4.6 AU ($\log a = 0.66$) with a half-peak width of $\sigma = 0.4$. It corresponds to an overall BD/VLMS binary fraction of $f_{\rm BD} = 0.15$. If data from Luhman (2004b), Joergens (2006), and Konopacky et al. (2007) are taken as hints to incomplete data between about 0.02 and 1 AU, the compressed Fischer & Marcy (1992) Gaussian from Figure 4 in Basri & Reiners (2006) may provide an appropriate envelope. However, for an assumed BD mass of 0.07 $M_\odot$ and $f_{\rm BD} = 0.26$ their period distribution corresponds to a

semi-major axis distribution with $\sigma \approx 0.85$ and is therefore still inconsistent with that of M and G dwarfs.

Although Konopacky et al. (2007) have recently found five VLMS binaries in TA with four of them having separations much larger than 15 AU, the sudden change of the orbital properties remains. In particular, they found two binaries with projected separations slightly above 30 AU and two others with separations between 80 and 90 AU. Possible implications of these discoveries are discussed in § 1.5.4. However, the truncation near 15 AU cannot be derived from the stellar distribution through downsizing according to Newton's laws (Close et al. 2003; Bouy et al. 2003). Not even dynamical encounters in dense stellar environments can invoke such a truncation near 15 AU (Burgasser et al. 2003). Using N-body simulations Kroupa et al. (2003) tested the hypothesis that BDs and stars form alike, and mix in pairs, and found that, despite of close dynamical encounters, the distribution of the semimajor axes of BD binaries remains star-like. That is, dynamical encounters even in dense clusters cannot truncate the BD binary distribution near 15 AU. They further found that star-BD binaries would be much more frequent than actually observed. Thus, this classical hypothesis is rejected with high confidence.

With this contribution we study the implications of the observed change of binary properties on the underlying single-object initial mass function (IMF). For this purpose, we analysed the observational mass functions of TA (Luhman et al. 2003a, 2004b), the IC 348 cluster (Luhman et al. 2003), the Trapezium cluster (Muench et al. 2002), and the Pleiades cluster based on data by Dobbie et al. (2002), Moraux et al. (2003), and the Prosser and Stauffer Open Cluster Database.[1] For all the systems we analyst, we refer to the MF as the IMF, although strictly speaking this is not correct for the 130 Myr old Pleiades. In § 1.2.1 we shortly review the definition of the IMF and the role of multiplicity on the shape of the individual body IMF compared to the observed system IMF ($\mathrm{IMF_{sys}}$). We show that the IMF that can be derived from an observed $\mathrm{IMF_{sys}}$ does not need to be continuous even if the $\mathrm{IMF_{sys}}$ does not show any discontinuity. In § 1.3 we describe the statistical method how to fit a model $\mathrm{IMF_{sys}}$ by combining BD and star IMFs as an approximation to the observed $\mathrm{IMF_{sys}}$. § 1.4 presents the results that indicate a discontinuity close to the HBL. Also the BD to star ratio from the model is calculated there. In § 1.5 the results are discussed in the context of four alternative BD formation scenarios, i.e. embryo ejection, disk fragmentation, photoevaporation, and ejection by close stellar encounters.

1.2 The IMF for individual stars and systems

1.2.1 Definition

The IMF is among the most important properties of a stellar population since it gives hints to the processes that form stars and BDs. Although we can only observe stellar

[1] Available at http://www.cfa.harvard.edu/~stauffer/opencl/

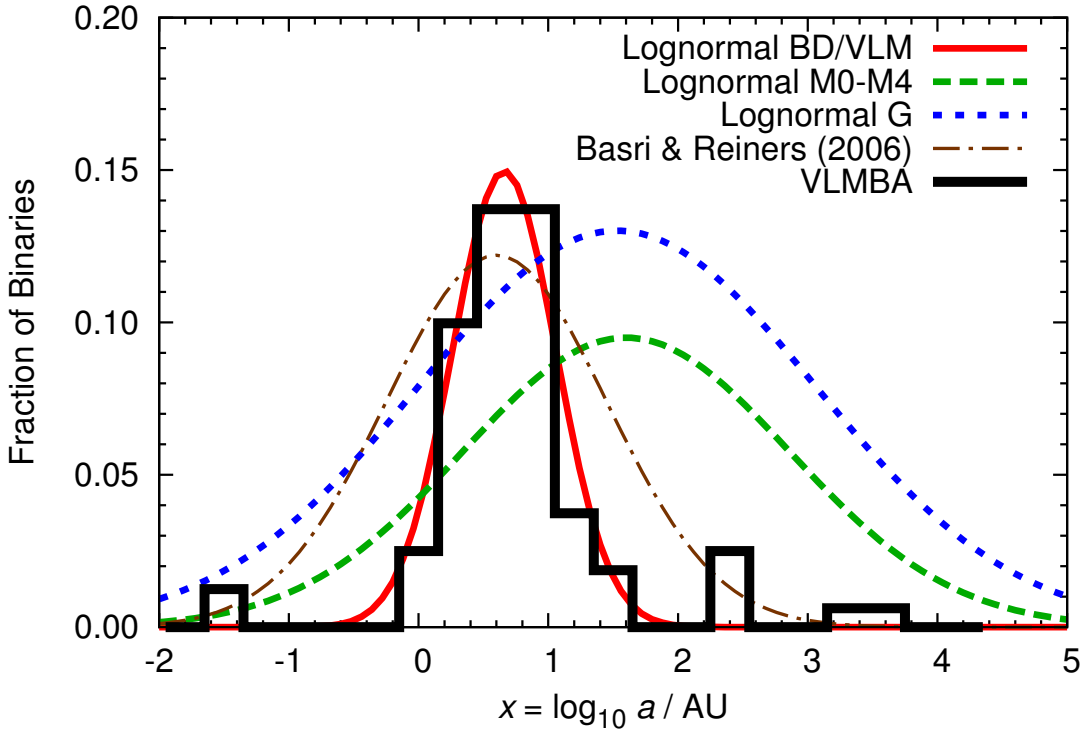

Figure 1.1: The semi-major axis (a) distribution for VLM binaries (VLMBs) with a total mass $m_{\rm bin} < 0.2\,M_\odot$ based on data from Nick Siegler's *Very Low Mass Binaries Archive* (VLMBA, http://paperclip.as.arizona.edu/~nsiegler/VLM_binaries/, version from June 1, 2007; histogram). The data can be fitted with a log-normal distribution. For the VLMBs (solid curve) the Gaussian parameters are $x_{\rm peak} = 0.66$ (corresponding to $a = 4.6\,$AU) and $\sigma = 0.4$ with a normalisation factor (= total binary fraction) $f_{\rm tot} = 0.15$, the binary fraction among BDs and VLMSs. For the M0–M4 dwarf binaries by Close et al. (2003) $x_{\rm peak} = 1.6$ and $\sigma = 1.26$ ($f_{\rm tot} = 0.3$) and for the G dwarf binaries $x_{\rm peak} = 1.53$ and $\sigma = 1.53$ ($f_{\rm tot} = 0.5$; Fischer & Marcy 1992, long-dashed and short-dashed curves, respectively). For VLMBs the gap within $-1.5 \leq \log a/AU \leq 0$ can be interpolated with the compressed Gaussian of Basri & Reiners (2006) with $\sigma = 0.85$ (thin dot-dashed curve), also enveloping wider BD/VLMS binaries found by Konopacky et al. (2007). It corresponds to a total BD/VLMS $f_{\rm BD} = 0.26$. The areas below the histogram and the curves are equal to the corresponding $f_{\rm tot}$ (eq. 1.3).

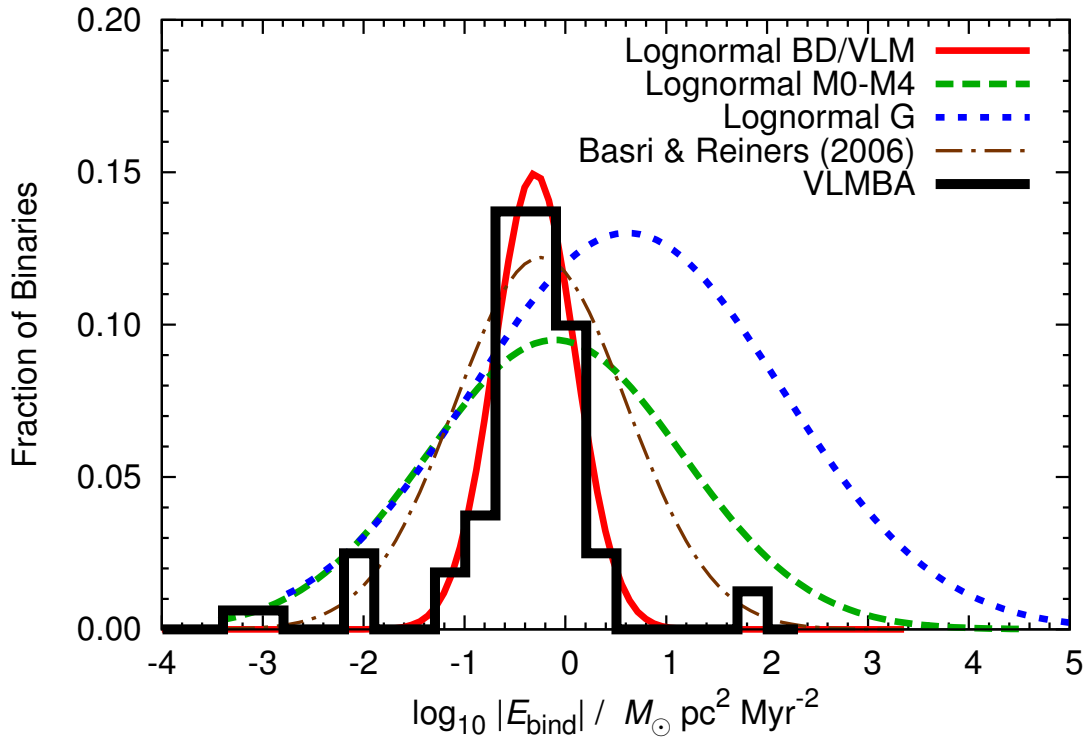

Figure 1.2: The distribution of the orbital binding energy $E_{\rm bind} = -0.5G(m_1 m_2/a)$ for VLM binaries and low-mass stellar binaries. Line types and symbols are the same as in Fig. 1.1. As for the semi-major axes there is a clearly different distribution for BDs/VLMSs on the one hand side and M, K and G dwarf binaries on the other.

populations at their given age there are data of several very young populations where the mass function is probably still very close to the initial one.

In general, the mass distribution of stars and BDs can be approximated by a power law or a combination of several power laws. Salpeter (1955a) estimated the relationship between the stellar mass and the relative number of stars of a given mass as a single power law,

$$\xi(m) = \frac{\mathrm{d}n}{\mathrm{d}m} = k\, m^{-\alpha}\,, \tag{1.1}$$

for $0.4 \lesssim m/M_\odot \lesssim 10$ and with $\alpha = 2.35$ and a normalisation constant k. The IMF is often expressed on the logarithmic mass scale and then becomes

$$\xi_\mathrm{L}(\log m) = \frac{\mathrm{d}n}{\mathrm{d}\log m} = (\ln 10)\; m\,\xi(m) = k_\mathrm{L}\, m^{1-\alpha}\,, \tag{1.2}$$

where k_L is the corresponding normalisation constant for ξ_L. An IMF is said to be *flat* if $\xi_\mathrm{L}(\log m)$ is constant, i.e. $\alpha = 1$. More recent work has shown there to be a flattening in the lower-mass regime of the observed mass function and, in the ξ_L representation, even a turnover near the BD-star transition (Kroupa 2001; Reid, Gizis & Hawley 2002; Chabrier 2003). Here, all objects from BDs to the most massive stars in a cluster are described by a *continuous IMF*, i.e. with a single population containing BDs as well as stars. The universal or "canonical" IMF has $\alpha_\mathrm{BD} \equiv \alpha_0 = 0.3$ $(0.01 \leq m/M_\odot \leq 0.075)$, $\alpha_1 = 1.3$ $(0.075 \leq m/M_\odot \leq 0.5)$, and $\alpha_2 = 2.3$ $(0.5 \leq m/M_\odot \leq m_\mathrm{max})$, where m_max is given by the mass of the host cluster (Weidner & Kroupa 2006). The generally accepted wisdom has been that the IMF is continuous from above 0.01 $M_\odot$ to m_max (e.g. Chabrier 2002).

1.2.2 Unresolved Binaries

Star cluster surveys are usually performed with wide-field telescopes with limited resolution that do not resolve most of the binaries. Hence, they yield, as an approximation, system MFs in which unresolved binary systems are counted as one object. The fraction of unresolved multiples can be taken as the total binary fraction of a cluster,

$$f_\mathrm{tot} = \frac{N_\mathrm{bin,tot}}{N_\mathrm{sng} + N_\mathrm{bin,tot}}\,, \tag{1.3}$$

where N_sng is the number of singles (or resolved individual bodies) and $N_\mathrm{bin,tot}$ the number of (unresolved) binaries. Unresolved binaries increase the number of individual bodies, N_bod, in a cluster such that

$$N_\mathrm{bod} = (1 + f_\mathrm{tot})\, N_\mathrm{sys}\,, \tag{1.4}$$

where $N_\mathrm{sys} = N_\mathrm{sng} + N_\mathrm{bin,tot}$ is the total number of systems. Note that a "system" is either a single body or a binary or a higher order multiple. Here we ignore higher order

multiples, because they are rare (Goodwin & Kroupa 2005). The binary fraction in dependence of the mass of the primary star, $m_{\rm prim}$, is

$$f(m_{\rm prim}) = \frac{N_{\rm bin,tot}(m_{\rm prim})}{N_{\rm sng}(m_{\rm prim}) + N_{\rm bin,tot}(m_{\rm prim})} \ , \tag{1.5}$$

where $N_{\rm bin,tot}(m_{\rm prim})$ and $N_{\rm sng}(m_{\rm prim})$ are, respectively, the number of binaries with primary star mass $m_{\rm prim}$ and single stars of mass $m_{\rm prim}$.

1.2.3 The System Mass Function

The effect of this *binary error* on the appearance of the IMF can be described as follows. Assume a stellar population with $f_{\rm tot} < 1$ and with stellar masses with a minimum mass $m_{\rm min}$ and a maximum mass limit of $m_{\rm max}$. The minimum mass of a binary is $2m_{\rm min}$, while the mass-dependent binary fraction $f(m) = 0$ for $m_{\rm min} \leq m_{\rm sys} < 2m_{\rm min}$. A binary closely above $2m_{\rm min}$ can only consist of two stars near $m_{\rm min}$ making such binaries rare. For higher system masses, where a system can be a multiple or a single star, there are more possible combinations of primary and companion mass, so that the binary fraction increases with the system mass and approaches an upper limit for the most massive objects.

Figure 1.3 shows the general shape of a system IMF for a flat (logarithmic scale) IMF with $m_{\rm min} = 0.1\,M_\odot$, $m_{\rm max} = 1\,M_\odot$, and $f_{\rm tot} = 0.5$. The IMF$_{\rm sys}$ is flat between $m_{\rm min}$ and $2m_{\rm min}$ ($\log m/M_\odot \approx -0.7$) and rises above $2m_{\rm min}$ to a maximum at $m_{\rm max}$. Systems with $m_{\rm sys} < 2m_{\rm min}$ can only be singles and the IMF$_{\rm sys}$ in this region is just the IMF minus the mass function of objects that are bound to a multiple system. For masses $m_{\rm sys} > m_{\rm max}$, on the other hand, only binaries exist, and the IMF$_{\rm sys}$ declines towards zero at $m_{\rm sys} = 2m_{\rm max}$, the highest mass possible for binaries. The sharp truncation of the IMF at $m = m_{\rm max}$ causes the sudden drop at $m_{\rm sys} = m_{\rm max}$, while the minor peak at $m_{\rm sys} = m_{\rm max} + m_{\rm min}$ corresponds to the maximum of the *binary mass function* (IMF$_{\rm bin}$, the IMF of binary system masses). For a binary of this mass the primary and companion mass can be drawn from the whole IMF, and thus the number of possible combinations becomes maximal. It should be noted that natural distributions with smoother boundaries probably do not show such a double peak.

Mathematically and in the case of random pairing, which is a reasonable approximation in the stellar regime (Malkov & Zinnecker 2001; Goodwin, Kroupa, Goodman & Burkert 2007), the binary mass function is just the integral of the product of the normalised IMF, $\hat{\xi} \equiv \xi/N_{\rm bod}$, of each component times the total number of binaries $N_{\rm bin,tot}$. Given the masses of the binary components A and B, $m_{\rm A}$ and $m_{\rm B}$, the binary mass $m_{\rm bin} = m_{\rm A} + m_{\rm B}$. Thus, $m_{\rm B} = m_{\rm bin} - m_{\rm A}$. Thus, IMF$_{\rm bin}$ can now be written as

$$\xi_{\rm bin}(m_{\rm bin}) = N_{\rm bin,tot} \int\limits_{m_{\rm min}}^{m_{\rm bin}-m_{\rm min}} \hat{\xi}(m)\,\hat{\xi}(m_{\rm bin}-m)\,{\rm d}m\,, \tag{1.6}$$

where $m_{\rm min}$ is the lower mass limit of all individual bodies in the population. The upper

limit of the integral, $m_{\rm bin} - m_{\rm min}$, is the maximum mass of the primary component $m_{\rm A}$ corresponding to a secondary component with $m_{\rm B} = m_{\rm min}$.

The other extreme case of assigning the component masses is equal-mass pairing. In that case, equation (1.6) simplifies to the IMF of one of the components and $\mathrm{IMF}_{\rm bin}$ is just the IMF shifted by a factor of 2 in mass and corrected for binarity using equations (1.3) and (1.4):

$$\xi_{\mathrm{bin}_{\rm equal}}(m_{\rm bin} = 2m) = \frac{f_{\rm tot}}{1 + f_{\rm tot}}\,\xi(m)\,. \tag{1.7}$$

This case is more applicable for BD binaries since their mass ratio distribution peaks at a ratio $q = 1$ (Reid et al. 2006). However, due to the low overall binary fraction of BDs the effect of the mass ratio distribution is quite small.

The $\mathrm{IMF}_{\rm sys}$ is just the sum of $\mathrm{IMF}_{\rm bin}$ and the IMF of the remaining single objects, $(1 - f_{\rm tot})\xi$:

$$\xi_{\rm sys}(m) = \xi_{\rm bin}(m) + (1 - f_{\rm tot})\;\xi(m)\,. \tag{1.8}$$

Thus, to obtain the true individual star IMF, $\xi(m)$ has to be extracted from the observed $\xi_{\rm sys}(m)$ for which a model for $\xi_{\rm bin}(m)$ is required. That is $\mathrm{IMF}_{\rm sys}$ has to be corrected for unresolved binaries in the cluster or population under study. This leads to a significant increase of the numbers of objects at the low-mass end because low-mass objects contribute to both low-mass singles and intermediate-mass binaries and thus more individual objects are required to reproduce the observed $\mathrm{IMF}_{\rm sys}$ (Kroupa et al. 1991; Malkov & Zinnecker 2001). In the mass range $m_{\rm min}$–$2m_{\rm min}$, systems can only be single because the system mass is the sum of the masses of the system members. Increasing the system mass beyond $2m_{\rm min}$ causes the binary contribution to rise quickly and then to asymptotically approximate a maximum value. Thus, the fraction of singles among M dwarfs is higher than for G dwarfs (Lada 2006), as one would expect for a stellar population ($> 0.08\,M_\odot$), i.e. essentially without BDs.

Figure 1.4 schematically shows the effects of correcting a flat continuous observed $\mathrm{IMF}_{\rm sys}$ for unresolved multiples whereby the binary fraction for BDs is smaller than for stars, as is observed to be the case. For a binary fraction of 15 % (i.e. $f_{\rm BD} = 0.15$) among BDs there would thus be $N_{\rm BD} = (1 + f_{\rm BD})N_{\rm sys,BD} = 1.15N_{\rm sys,BD}$ BDs in total, while for stars with $f_{\rm tot} = 0.5$ we would have $1.5N_{\rm sys,star}$. This exemplifies how the change in f leads to a discontinuous $\mathrm{IMF}_{\rm sys}$.

1.3 Computational Method

1.3.1 The Parameter Space

The most straightforward way to calculate the influence of binaries on the stellar/substellar statistics would be the Monte Carlo method (Kroupa et al. 1991, 1993). However, for better (smoother) results and to reduce the computational efforts we do not use a Monte Carlo approach here but a semi-analytical approach in which the binary mass function is calculated via numerical integration of eq. (1.6) for each population. This can be done with a standard quadrature algorithm. This algorithm has been verified with a Monte

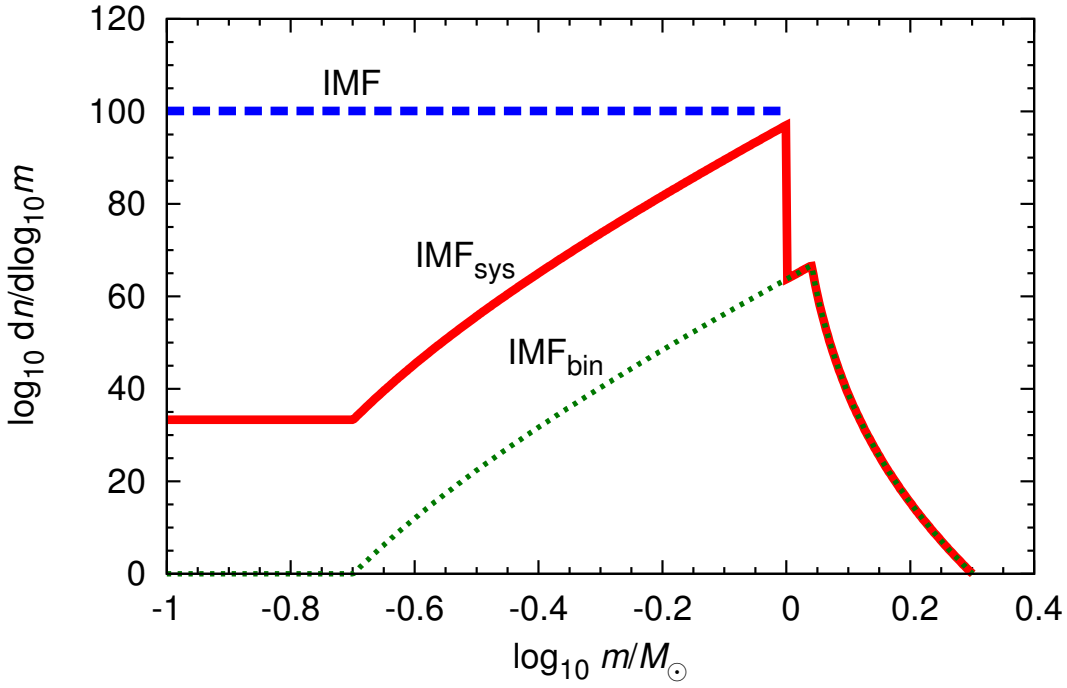

Figure 1.3: The system IMF ($\mathrm{IMF}_{\mathrm{sys}}$ solid line) corresponding to a flat logarithmic IMF (i.e. $\alpha = 1$, dashed line) for $m_{\mathrm{min}} = 0.1 \leq m/M_{\odot} \leq 1 = m_{\mathrm{max}}$ with an overall binary fraction of 50 %. The corresponding binary IMF ($\mathrm{IMF}_{\mathrm{bin}}$ eq. 1.6) is shown by the thin dotted line. The system MF peaks at 1 $M_{\odot}$ and is truncated for higher masses while there is a minor peak at 1.1 $M_{\odot}$ corresponding to the peak of the binary MF at $m_{\mathrm{min}} + m_{\mathrm{max}}$.

Parameter No.	Quantity	varied from	to (approx.)
1	α_{BD}	0	1
2	$m_{\mathrm{max,BD}}$	$m_{0,\mathrm{star}}$	$m_{0,\mathrm{star}} + 0.2$
3	$\log \mathcal{R}_{\mathrm{pop}}$	-1	0

Table 1.1: List of the variable parameters that span the parameter space of a two-population IMF studied in this contribution. Note that α_{BD} is not varied for IC 348 and the Pleiades since it is not well-constrained by the data for these clusters.

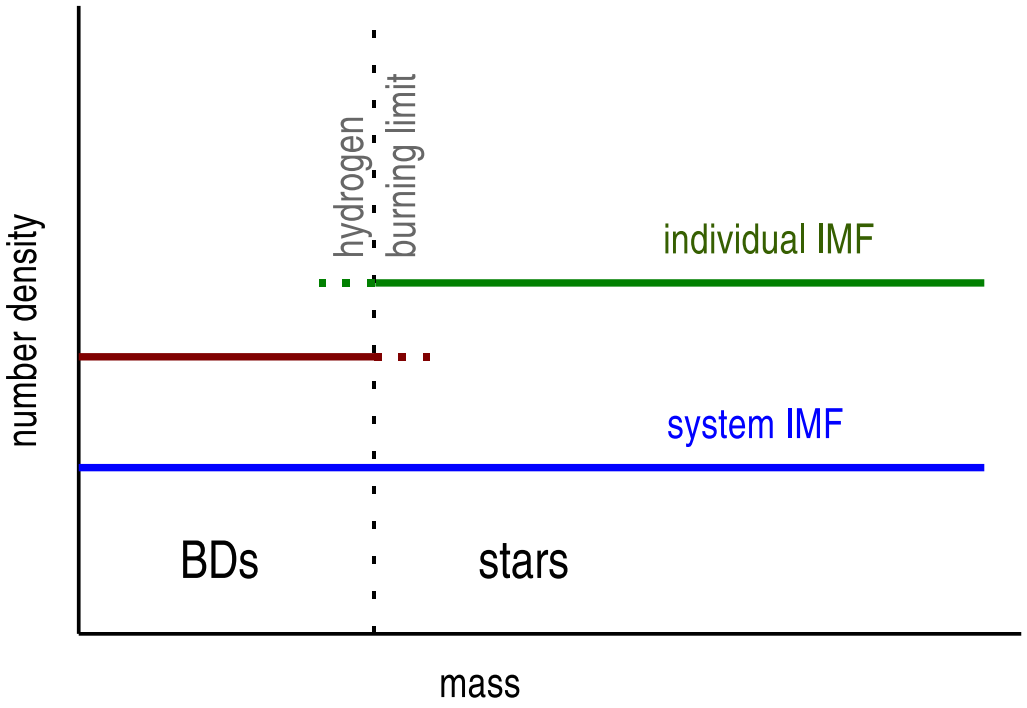

Figure 1.4: A population of stars and BDs with different binary fractions can result in a discontinuous IMF, even if the observed (system) IMF appears to be continuous. The binary fraction of the BDs is lower than that of stars and therefore a lower number, $N_{\rm bod}$, of individual objects is required for the frequency of BD and stellar systems of a given mass being equal (eq. 1.4). Note the overlap region indicated by the horizontal dotted lines: some star-like bodies may actually be physical BDs (upper line) while some BD-likes are indeed very-low-mass stars.

Cluster	$N_{\rm sys}$	$n_{\rm data}$	c	ν
Trapezium	1040	30	3	26
TA	127	9	3	5
IC 348	194	9	2	6
Pleiades	~ 500	19	2	16

Table 1.2: Size of the observed sample, $N_{\rm sys}$ (= the number of observed systems), number of data points (mass bins), $n_{\rm data}$, number of fitting parameters, c, and the number of degrees of freedom, $\nu = n_{\rm data} - 1 - c$, for the four clusters under study.

Carlo simulation of a few million random experiments, each being a random draw from the IMF. The Monte Carlo method is used later to determine the BD-to-star ratio and the total binary fractions within defined mass ranges (§§ 1.4.2 and 1.4.3). It makes use of the *Mersenne Twister* random number generator developed by Matsumoto & Nishimura (1998). Since there are only a few runs to be done (in contrast to hundreds of thousands of runs during an iterated parameter scan, see below) the simple Monte Carlo approach with an appropriately large random sample is fully sufficient for this purpose.

The lack of star-BD binaries and the truncation of the BD binary separation distribution suggest two disjunct populations where binary components are taken only from the same population. For reasons discussed in § 1.5 we call these populations *BD-like* and *star-like*. The binary corrections are therefore applied separately to the stellar and the substellar regime rather than to a combined population. Random pairing over the whole mass regime is not considered further as it leads to too many star-BD binaries (Kroupa et al. 2003).

The approach here requires separate application of normalisations on both populations. For this purpose we define the *population ratio*,

$$\mathcal{R}_{\rm pop} = N_1/N_2 \tag{1.9}$$

where N_1 is the number of individual bodies of the BD-like population ($m_{0,\rm BD} \leq m \leq m_{\rm max,BD}$) and N_2 ($m_{0,\rm star} \leq m \leq m_{\rm max}$) that of the star-like population. This must not be mixed up with the *BD-to-star ratio*, $\mathcal{R}$, (eq. [1.14]) which refers to *physical BDs* and stars separated by the HBL.

The partial IMF for each population can be described by parameters α_i, m_j, and a normalisation constant. In this work a single power law for BDs (i = "BD") and a two-part power law (i=1 or 2) for stars is applied. Thus, there is a mass border, m_{12}, separating the two power law regimes. The parameters of both populations form a three-dimensional parameter space of the IMF model for each cluster. It has been found that the lower mass limits of the BD-like population, $m_{0,\rm BD} = 0.01\,M_\odot$, and that of the star-like population, $m_{0,\rm star} = 0.07\,M_\odot$, are suitable for all studied clusters. Furthermore, we focus on the canonical stellar IMF (Kroupa 2001) with $\alpha_1 = 1.3$ for $m \leq 0.5 M_\odot \equiv m_{12}$ and $\alpha_2 = 2.3$ for $m > 0.5 M_\odot$. The reason is that this canonical IMF has been verified with high confidence by other observations as well as theoretically. Thus, only the BD-like power law, $\alpha_{\rm BD}$, the normalisation of the BD-like population against the stellar one, $\mathcal{R}_{\rm pop}$, and the upper mass border, $m_{\rm max,BD}$, of the BD-like regime are the parameters to be varied. Because of the sparse and probably incomplete data sets for IC 348 and the Pleiades, $\alpha_{\rm BD}$ has also been set to the canonical value (i.e. $\alpha_{\rm BD} = \alpha_0 = 0.3$) for these clusters, varying only $\mathcal{R}_{\rm pop}$ and $m_{\rm max,BD}$.

Table 1.1 lists the variables and their range of variation for the Trapezium, IC 348, and the Pleiades. As the upper mass limits of stars in the clusters one can either take the maximum observed mass or a theoretical mass limit, as given by Weidner & Kroupa (2006). Because in our model the IMF is cut sharply rather than declining softly as shown in that work, we here set the mass limit somewhat below the Weidner & Kroupa (2006) limits. For the Trapezium we set an upper limit of 10 $M_\odot$, 1.5 $M_\odot$ for TA, 3 $M_\odot$

for IC 348 and 5 $M_\odot$ for the Pleiades. Note that the observed most massive star in the Trapezium has a mass of $\approx 50\,M_\odot$, but varying $m_{\rm max}$ to this value does not affect the results significantly.

Little is known about non-planetary substellar objects below the standard opacity limit for fragmentation, $0.01 M_\odot$, making this a reasonable lower mass limit for our BD statistics. The lower-mass limit for stars, however, is chosen somewhat arbitrarily but is justified by a smaller test study that finds less agreement with observational data used here if the stellar mass is lowered too much below $0.08 M_\odot$. As will be shown later, the extreme case of a stellar mass range that includes the BD mass range leads to poor fits to the observational MFs as well as to some inconsistency with the observed binary fraction. This is discussed later in §§ 1.4 and 1.5. In general, the choice of the mass ranges also influences the mass ratio distribution, since for random-pairing each component is distributed via the IMF. Thus, for a given primary mass out of a chosen population, the companion mass distribution is just equal to $\xi(m)$ within the mass interval $m_{\rm min} \leq m \leq m_{\rm prim}$.

The overall binary fraction is taken as a constant for each population. For the stars we adopt an unresolved binary fraction of 80 % for TA ($f_{\rm ST} = 0.80$) and 40 % for the others ($f_{\rm ST} = 0.40$), in accordance to the observational data. For BDs we choose a value of 15 % for all cases ($f_{\rm BD} = 0.15$). Furthermore, we found the need to introduce an overlap of the BD and star regimes between 0.07 and about 0.15–$0.2 M_\odot$. Indeed, there is no reason why the upper mass border of the BD-like population should coincide with the lower mass border of the star-like population. The physical implications of this required overlap region are discussed in § 1.5.

1.3.2 χ^2 Minimisation

In § 1.3.1 a parameter space of three (Trapezium, TA) and two (IC 348, Pleiades) dimensions of individually adjustable quantities has been defined. For each cluster, the quality of a set of fitting parameters is characterised via the χ^2 criterion,

$$\chi^2 = \sum_i^{n_{\rm data}} \frac{\left(N_i - N\xi_{\rm sys}(m_i)\right)^2}{\sigma_i^2}\,, \tag{1.10}$$

where $\xi_{\rm sys}(m_i)$ is $\mathrm{IMF}_{\rm sys}$ at the midpoint of the ith bin of the observational histogram that is taken as the reference and $n_{\rm data}$ is the number of mass bins in the observational histogram (Tab. 1.2). The values σ_i represent the error bars of the observational data, or, if none are given, the Poisson errors, and N_i is the number of systems found in the ith mass bin. The fitted $\mathrm{IMF}_{\rm sys}$ is normalised to the total number of systems in the cluster.

That set of c fitting parameters that minimises the reduced χ^2 value, $\chi^2_\nu = \chi^2/\nu$, defines our best-fit model. Here $\nu = n_{\rm data} - c - 1$ is the number of degrees of freedom. The values for $n_{\rm data}$, c, ν, and the sample sizes for the studied clusters are listed in Table 1.2. The reduction of ν by 1 is due to the normalisation of the total number of stars and BDs against the observational data. For the two-component model the

fitting parameters are the power in the BD regime, $\alpha_{\rm BD}$, the upper mass border of the BD population, and the ratio $\mathcal{R}_{\rm pop}$; thus, $c = 3$ (2, for IC 348 and the Pleiades). The probability, P, that the model has a reduced χ^2, $\chi^2_\nu = \chi^2/\nu$, as large as or larger than the value actually obtained is calculated from the incomplete Gamma function (Press et al. 1992),

$$Q(\chi^2_\nu|\nu) = P(\tilde{\chi}^2_\nu \leq \chi^2_\nu)\,. \tag{1.11}$$

The logarithmic mass error is not mentioned in the sources, but is given by the photometric measurements and to a larger degree by uncertain theoretical models of stars and BDs. We assumed a value of $\Delta \log m = 0.05$ for the Trapezium and $\Delta \log m = 0.1$ for the others, corresponding to a relative error in the mass estimates of 12 % and 26 %, respectively. This error has been estimated from the width of the logarithmic bins in the observational data for the Trapezium, TA and IC 348. For the Pleiades, for which non-equally spaced data from different sources are given, we assume the same log mass error as for TA, and IC 348. To take this into account the $\log m$ values have been smoothed by a Gaussian convolution corresponding to a log-normal smearing of the masses.

After generating the model IMFs for both populations a binary mass function (eq. [1.6]) is derived separately from the stellar and substellar IMF, i.e. there are formally no BD-like companions to star-like primaries, in accordance with the observations. This leads to consistency with the observed binary fraction (§ 1.4.3) and the BD desert. Note, though, that as a result of the required overlap both the BD-like and the star-like population contain stars as well as BDs; thus, we do have star-BD pairs in our description (more on this in § 1.5).

The addition of the two resulting system IMFs leads to an overall $\mathrm{IMF}_{\rm sys}$ for the whole mass range. By adjusting the power law coefficients and the population ratio $\mathcal{R}_{\rm pop}$, the $\mathrm{IMF}_{\rm sys}$ is fitted against the observational data such that χ^2 is minimised. The prominent substellar peak in the Trapezium cluster below 0.03 $M_\odot$ (Muench et al. 2002) is ignored here because it is well below the BD–star mass limit and therefore does not interfere with any feature there. Furthermore, it is possibly an artefact of the BD mass-luminosity relation (Lada & Lada 2003).

1.3.3 Error Estimation

The errors of the parameters are estimated from the marginal distribution of each parameter within the parameter space (Lupton 1993). The marginal probability density distribution, p, is

$$\begin{aligned} p(A_i) &= \mathrm{d}P(A_i)/\mathrm{d}A_i \\ &= \int_{-\infty}^{\infty}\int_{-\infty}^{\infty} \mathcal{L}(A_1, A_2, A_3)\,\mathrm{d}A_k \mathrm{d}A_j\,, \end{aligned} \tag{1.12}$$

where A_1, A_2 and A_3 correspond to $\alpha_{\rm BD}$, $\mathcal{R}_{\rm pop}$, $m_{\rm max,BD}$ and $i = 1, \ldots, 3$; $j, k \neq i$. The likelihood $\mathcal{L}$ is defined as

$$\mathcal{L}(A_1, A_2, A_3) = \mathcal{N} e^{-\chi^2/2}\,, \tag{1.13}$$

where the normalisation constant $\mathcal{N}$ is such that the integral over the whole range is one. Note that χ^2 instead of χ^2_ν is used here. The integral is approximated by summation

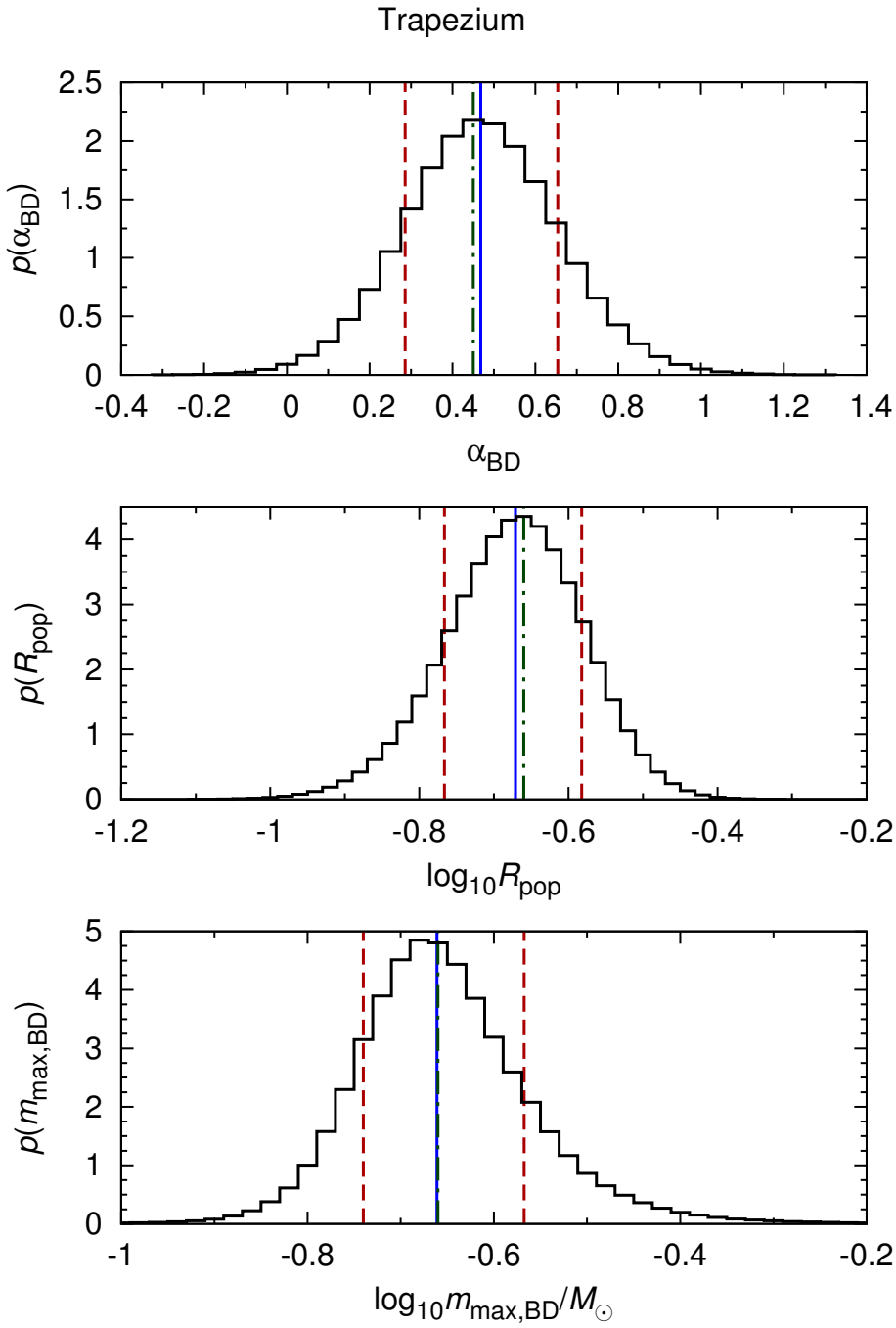

Figure 1.5: The marginal probability density distributions of the parameters α_{BD}, $\log \mathcal{R}_{\mathrm{pop}}$ and $\log\left(m_{\mathrm{max,BD}}/M_{\odot}\right)$ as an estimate of the errors for the Trapezium cluster fit (see § 1.3.3). The peak-width engulfing 68 % of the whole parameter sample (thus referring to $\approx 1\sigma$, dashed vertical lines) is taken as the error for each parameter. Because the median (solid vertical line) of the sample does not match the best-fit value (dash-dotted line) in all cases, both are listed in Table 1.3.

	Median $\pm1\sigma$			Best fit				
Cluster	$\alpha_{\rm BD}$	$\log \mathcal{R}_{\rm pop}$	$m_{\rm max,BD}$	$\alpha_{\rm BD}$	$\log \mathcal{R}_{\rm pop}$	$m_{\rm max,BD}$	χ^2_ν	P
Trapezium	$0.47^{+0.18}_{-0.19}$	$-0.67^{+0.10}_{-0.09}$	$0.22^{+0.04}_{-0.05}$	0.45	-0.66	0.22	0.23	0.99998
TA	$-0.08^{+0.63}_{-1.05}$	$-0.68^{+0.13}_{-0.14}$	$0.11^{+0.03}_{-0.04}$	0.00	-0.62	0.12	2.69	0.020
IC 348	—	$-0.57^{+0.23}_{-0.19}$	$0.22^{+0.06}_{-0.08}$	0.3 (c)	-0.51	0.22	1.01	0.416
Pleiades	—	$-0.82^{+0.44}_{-0.11}$	$0.07^{+0.02}_{-0.20}$	0.3 (c)	-0.80	0.06	1.20	0.257

Table 1.3: The best-fit BD-like power law coefficients, $\alpha_{\rm BD}$, population ratios, $\mathcal{R}_{\rm pop}$, and BD-like upper mass limits, $m_{\rm max,BD}$. The uncertainties are derived in § 1.3. Note that $\alpha_{\rm BD}$ is set to the canonical value for IC 348 and the Pleiades.

with equidistant stepping of each parameter. We conservatively rejected all parameter sets with $P < 0.27\,\%$ (corresponding to $\chi^2_\nu > \pm 3\,\sigma$; § 1.3.2).

As an example, the parameter distribution for the Trapezium is illustrated in Figure 1.5. The interval around the median which contains 68 % of the scanned parameter sets is taken as the σ measure of the errors. The interval limits and the medians are shown among the best-fit results in Table 1.3. Apparently, the median of the probability density distribution does not always coincide with the best-fit value. The reason for this is that the distribution is slightly asymmetric for most parameters and clusters with the Pleiades being the by far worst case. This results in asymmetric error bars. Note that there are sets of $\alpha_{\rm BD}$, $\mathcal{R}_{\rm pop}$, and $m_{\rm max,BD}$ that are within these error limits but with a $\chi^2 > 3\sigma$, and thus the error limits may be slightly over-estimated.

Another possibility to illustrate the statistical significance of a fit is by its confidence contours within a two-dimensional subspace of the parameter space, as is shown later in § 1.4.2.

1.4 Results

1.4.1 The IMF for BDs and Stars

Figure 1.6 demonstrates the results for different models (continuous IMF, two-component IMF with and without overlap region) for the Trapezium cluster. The continuous IMF is shown for illustration only. Its underlying model assumes a single population containing BDs as well as stars (Kroupa et al. 2003). Instead of an overlap as for the two-component model the mass border between the regime of the BD slope $\alpha_{\rm BD}$ and the (canonical) stellar regime is varied. The total binary fraction, $f_{\rm tot}$, is set to 0.4 with random pairing among the entire population. Our calculations give a best fit with $\alpha_{\rm BD} = -0.4 \pm 0.2$, $m_{\rm max,BD} \equiv m_{\rm 0,star} = 0.093 \pm 0.01$ (and canonical stellar IMF) which is comparable to the canonical IMF for BDs and stars (Kroupa 2001). As already mentioned in § 1.1, it leads to a high number of star-BD binaries, $f_{\rm star-BD} = 15\,\% \pm 4\,\%$ altogether (see §1.4.3), while Kroupa et al. (2003) found 7 %–15 % star-BD binaries with $a \gtrsim 30\,{\rm AU}$ in their standard model with stars and BDs. Furthermore, the different orbital properties

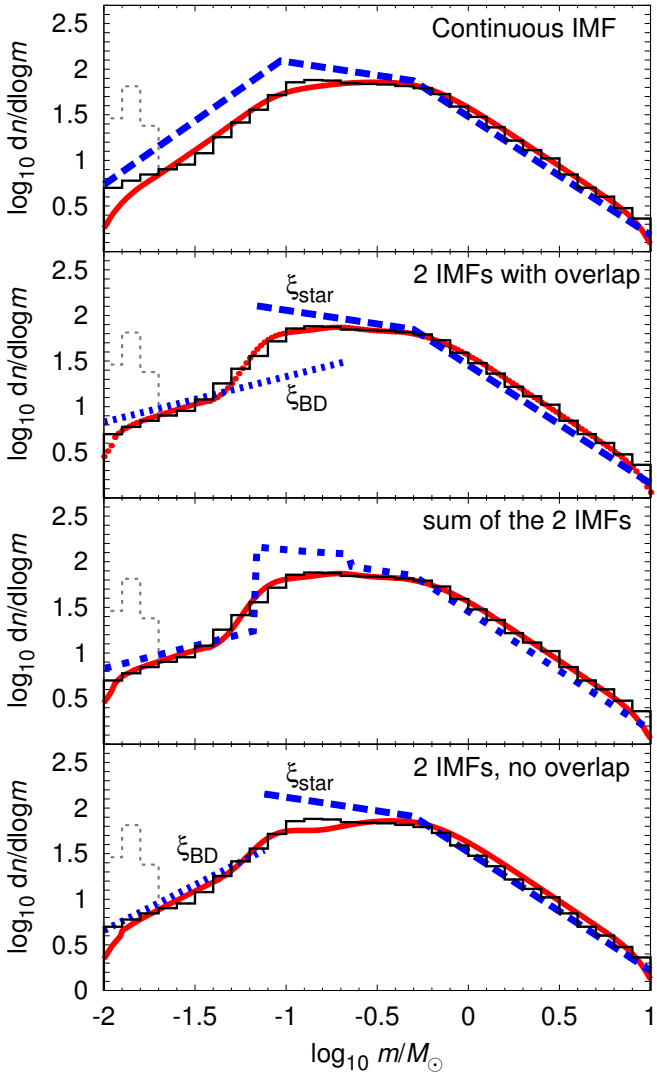

Figure 1.6: Four different IMF models applied to the Trapezium cluster. Top panel: A classical continuous-IMF fit (dashed line) for the Trapezium cluster with random pairing over the whole BD and stellar mass range. The method of converting the IMF to the $\mathrm{IMF_{sys}}$ (solid curve) is essentially the same as for the two-component IMFs discussed in this paper but with no allowance for an overlap or a discontinuity in the BD-star transition region. Although the general shape of the observational histogram (thin steps) is represented by this fit this model leads to an unrealistic high fraction of star-BD binaries and is therefore discarded. Second panel: The Trapezium IMF fitted with two separate IMFs, ξ_{BD} (dotted line) and ξ_{star} (dashed line), as in Figure 1.7 (the two-component IMF). Third panel: The same but with the sum IMF of both component IMFs shown here as the possible appearance of the IMF if all binaries could be resolved. Apparently, there is a "hump" between about 0.07 $M_{\odot}$ and 0.2 $M_{\odot}$ bracketing the probable overlap region of the BD-like and star-like populations. Bottom panel: Trapezium fitted with two separate IMFs but with no overlap. The binary correction leads to the dip near the hydrogen-burning limit. However, the fit is only slightly worse than that one with an overlap.

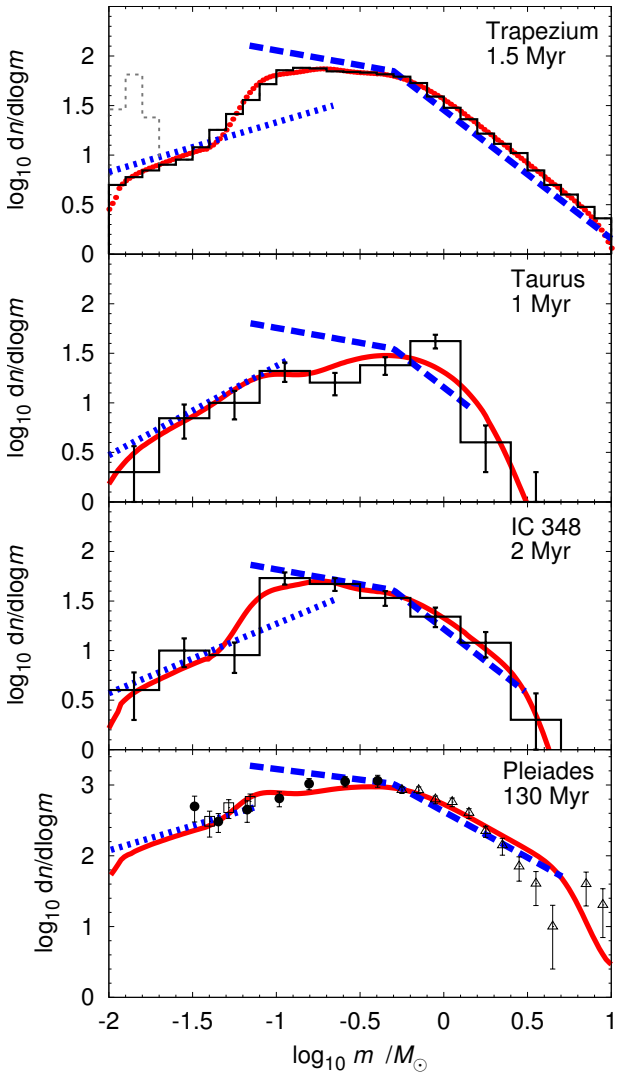

Figure 1.7: Two-component IMFs of the Trapezium, IC 348, and TA clusters based on observational data by Luhman (2004a), Luhman et al. (2003) and Muench et al. (2002) (solid histograms), as well as for the Pleiades cluster using data from Moraux et al. (2003) (filled circles), Dobbie et al. (2002) (open squares) and from the Prosser and Stauffer Open Cluster Database (from which only those for $\log m/M_\odot \leq 0.55$ are used for fitting). For all clusters the stellar IMF, shown here as the dashed line, has the canonical or standard shape after Kroupa (2001), i.e. $\alpha_1 = 1.3$ below 0.5 $M_\odot$ and $\alpha_2 = 2.3$ above 0.5 $M_\odot$. The Trapezium IMF is fitted without the substellar peak indicated by the faint dotted steps. The dotted lines show the optimised binary-corrected BD-like body IMFs (distribution of individual BD-like bodies). The resulting model system IMFs are represented by the solid curves. Ages are from Luhman et al. (2003), Luhman et al. (2003), Hillenbrand et al. (2001) and Barrado y Navascués et al. (2004) for TA, IC 348, Trapezium and the Pleiades, respectively. Note that the BD-like IMF of IC 348 and the Pleiades are set to the canonical slope $\alpha_{\rm BD} = 0.3$ since they are not well constrained due to the lack of BD data for these clusters.

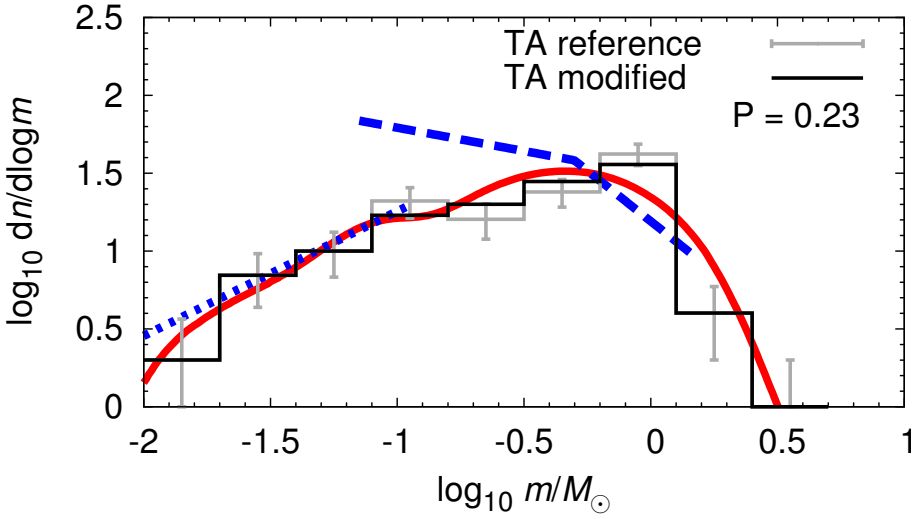

Figure 1.8: The two-component model with canonical stellar IMF for a slightly modified TA observational histogram (black solid steps). The peak at 1 $M_\odot$ and the dent around 0.3 $M_\odot$ have been slightly flattened without leaving the error bars of the original data (grey steps and bars). This fit has a reasonable confidence of about $P = 0.25$, about 12 times larger than for the original histogram ($P = 0.02$, see Tab. 1.3).

of BD-BD and star-star binaries (Fig. 1.1) cannot be explained by a single-population model without further assumptions. Therefore, it is not considered further here.

The two-component IMF model (Fig. 1.6, *second panel*) accounts for the empirical binary properties of BDs and stars. Apart from this it also fits the observational data (Fig. 1.6, *histogram*) slightly better than the continuous model, especially in the BD/VLMS region and the "plateau" between 0.1 and 0.5 $M_\odot$.

Objects with equal mass and composition appear as equal in observations, even if they have been formed in different populations. Thus, it is hard to determine their formation history. A high-resolution survey that resolves most of the multiples would yield an overall mass function from the lowest mass BDs to the highest mass stars. However, if such a resolved individual mass function is composed of two overlapping populations, it may be possible to detect its imprints as an excess of objects within the overlap region. To illustrate this ((Fig. 1.6, *third panel*), we construct such an overall IMF by simply adding the two IMF components from the second panel. BDs and stars are paired separately from their respective mass range. It is clear that the addition of the two IMFs leads to discontinuities, i.e. in the overlap region the continuous IMF increases steeply at the minimum stellar mass and drops again at the upper mass limit of the BD-like regime. Even with a smoother drop at each end of the BD-like and star-like IMF it is likely to be detectable once most of the multiples have been resolved. Thus, a discovery of such a "hump" within the resolved IMF would strongly support the two-component model.

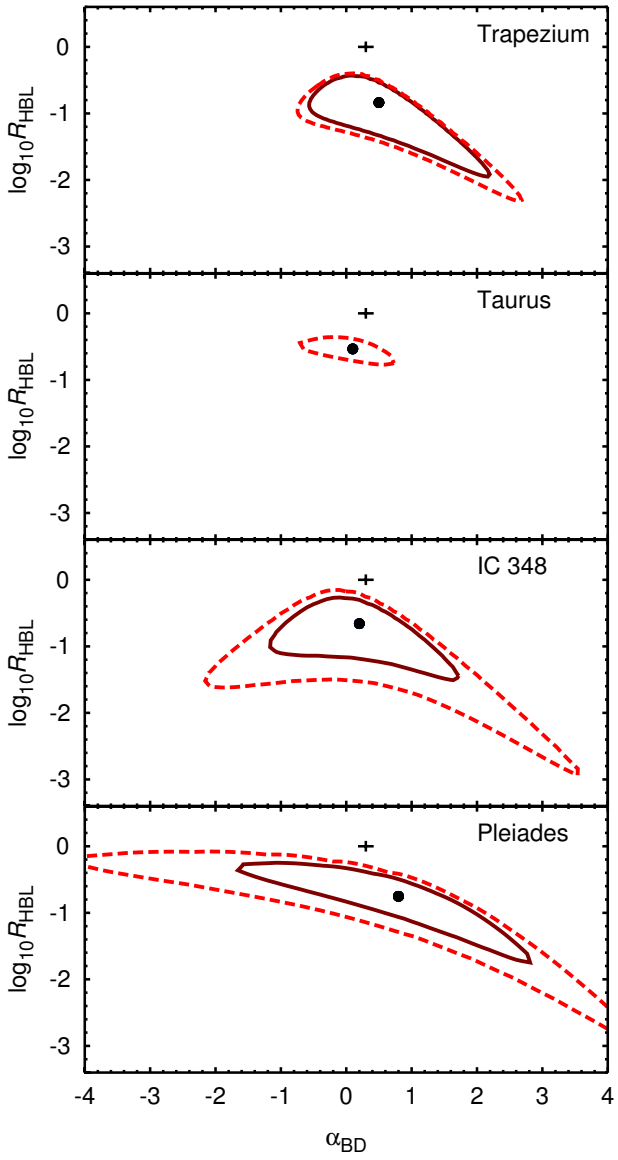

Figure 1.9: Contour plots of 5 % and 1 % significance levels from χ^2 fitting (see § 1.3 for details) of $\alpha_{\rm BD}$ and the BD-like to star-like ratio $\mathcal{R}_{\rm HBL}$ at $m = 0.075\,M_\odot$ (eq. 1.15) for the Trapezium, TA, IC 348 and the Pleiades. The stellar IMF is canonical, i.e. $\alpha_1 = 1.3$ and $\alpha_2 = 2.3$ while the upper BD mass limits, $m_{\rm max,BD}$, are the best-fit values from Table 1.3. All fitting parameters outside the solid line are rejected with 95 %, and those outside the dashed line are rejected with 99 % confidence. The optimum of the Trapezium and TA is marked by the filled circle while the cross marks the standard/canonical configuration with a continuous IMF (i.e. $\log \mathcal{R}_{\rm HBL} = 0$) and $\alpha_{\rm BD} = 0.3$. As can be seen, it is well outside both levels (even for arbitrary $\alpha_{\rm BD}$). For the Pleiades it is still well outside at least for reasonable choices of $\alpha_{\rm BD}$. Note that the optimum for $\alpha_{\rm BD}$ for IC 348 and the Pleiades does exist in this 2D cross section but not in the full 3D parameter space.

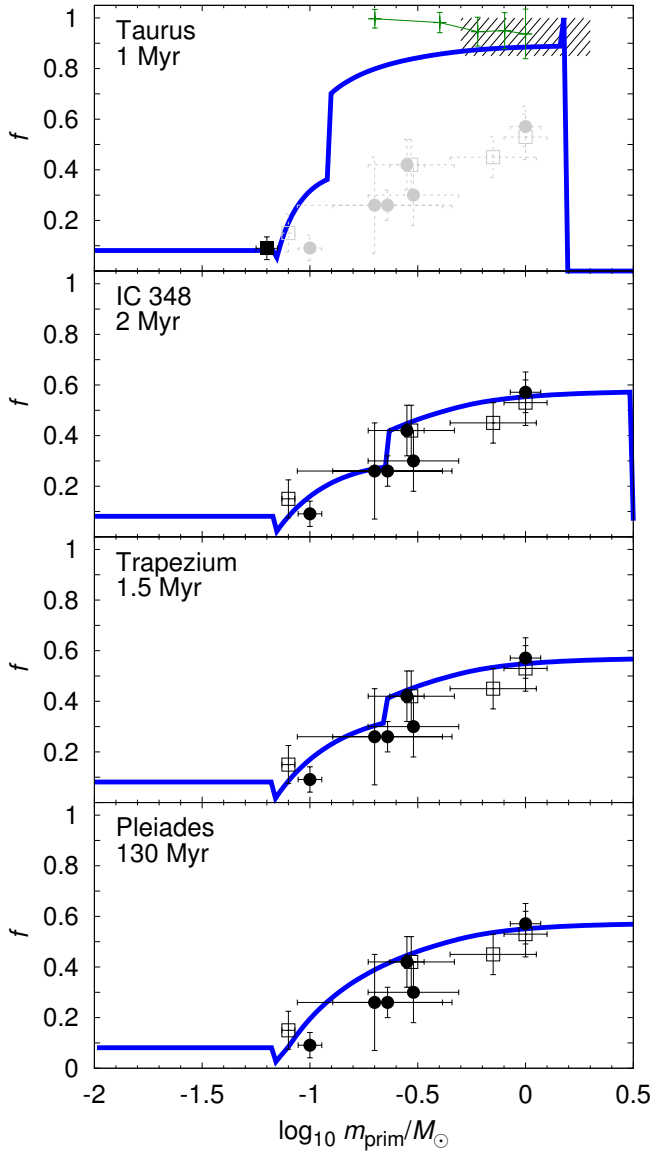

Figure 1.10: The binary fraction f (eq. 1.5) of the four discussed clusters as a function of primary mass, $m_{\rm prim}$, for the two-component best-fit IMF model (with canonical stellar IMF) is shown by the solid line. The BD binary fraction appears flat due to the equal-mass pairing used in our algorithm. Since merely very sparse data is available for low-mass BDs, only the higher-mass end of the curve should be taken into account. For comparison, the average binary fractions of G, K, M and L type stars in the solar neighbourhood (average age ~ 5 Gyr; filled circles: Lada 2006, open squares: Kroupa et al. 2003) have been added to each panel. The shaded region in the top panel indicates the approx. 1 Myr old pre-main sequence data (Duchêne 1999) while the thin solid line represents the initial TA-like dynamical model from Kroupa et al. (2003). The single filled square in the top panel at $\log m \approx -1.2$ is the VLMS/BD datum inferred by Kraus et al. (2006) for TA. Note that the stars in TA have a binary fraction near 100 % (Duchêne 1999; Kroupa et al. 2003).

To illustrate the effect of the overlap region, a two-component IMF without an overlap is shown in the bottom panel of Figure 1.6. Like the continuous IMF this approach gives a slightly worse fit, especially between 0.1 and 0.2 $M_\odot$ ($-1 \leq \log m/M_\odot \leq -0.7$). However, the "dip" in this region is only weak.

The results of the two-component IMF model for all clusters are shown in Figure 1.7, the power law coefficients being listed in Table 1.3. For the Pleiades and IC 348 the BD IMF slope has been kept standard, i.e. $\alpha_{\rm BD} = 0.3$ (Kroupa 2001), because the sparse, and in the case of the Pleiades most probably incomplete data, do not allow useful confidence limits to be placed on $\alpha_{\rm BD}$. For the same reason the highly uncertain observational data for $\log(m/M_\odot) \geq 0.65$ have not been used for fitting (but are still plotted for completeness).

As can be seen the BD/VLMS and stellar IMFs do not meet at the BD-star boundary. The number density of individual BDs near the BD-star border is about one third of that of individual low-mass M dwarfs. This discontinuity cannot be seen directly in the observational data because it is masked by the different binary fractions for different masses (§1.2.3), but the IC 348 data (histogram in the third panel of Figure 1.7) may indeed be showing the discontinuity (compare third panel of Figure 1.6).

Furthermore, there are large uncertainties in the mass determination of stars in stellar groups such as TA which may probably lead to even larger error bars of the bins than shown in the observational data. Even within the given error bars certain variations of these data provide a much better fit to the canonical stellar IMF with $P = 0.25$ (original: $P = 0.02$, Table 1.3). This has been done in Figure 1.8 by lowering the peak near 1 $M_\odot$ and somewhat rising the "valley" around 0.3 $M_\odot$corresponding to the re-shuffling of 9 stars out of 127 (Tab. 1.1) by 0.1 to 0.4 $M_\odot$ (one bin width), e.g. through measurement errors. This suggests that, in agreement with Kroupa et al. (2003), the TA IMF might not necessarily be inconsistent with the canonical IMF.

Except for the Pleiades all clusters show features near the peak in the low-mass star region that are slightly better fitted with a separate BD population *and* an overlap region. Although these features alone do not reject the continuous IMF model, they might be taken as a further support of the argumentation towards a two-populations model.

It should be mentioned that the continuous IMF model (Fig. 1.6, *first panel*) still fits the observed Trapezium and Pleiades MF with high confidence (while failing for the other clusters) but leads to VLMS binary properties that are inconsistent with the observed properties as mentioned in § 1.1. A possible extension of our modelling would thus be to fit both the observed IMF *and* the observed binary statistics.

1.4.2 BD to Star Ratio

We analysed the BD-to-star ratio $\mathcal{R}$ of TA, Trapezium and IC 348, defined as

$$\mathcal{R} = \frac{N(0.02\text{–}0.075\,M_\odot)}{N(0.15\text{–}1.0\,M_\odot)}\,, \tag{1.14}$$

where N is the number of bodies in the respective mass range. The mass ranges are chosen to match those used in Kroupa & Bouvier (2003a) in their definition of $\mathcal{R}$. Since BDs below 0.02 $M_\odot$ are very difficult to observe and since TA and IC 348 do not host many stars above 1 $M_\odot$ (in contrast to Trapezium and the Pleiades), we restricted the mass ranges to these limits.

The Pleiades cluster is difficult to handle due to a lack of BD data. Moreover, at an age of about 130 Myr (Barrado y Navascués, Stauffer & Jayawardhana 2004) it has undergone dynamical evolution, and massive stars have already evolved from the main sequence which affects the higher mass end of the IMF (Moraux et al. 2004).

Another relevant quantity is the ratio $\mathcal{R}_{\rm HBL}$ of BD-like to star-like objects at the HBL, i.e. the classical BD-star border,

$$\mathcal{R}_{\rm HBL} = \frac{\xi_{\rm BD}(0.075\,M_\odot)}{\xi_{\rm star}(0.075\,M_\odot)}\,. \tag{1.15}$$

In the classical continuous IMF approach it is one by definition, because otherwise the IMF would not be continuous. In a two-component IMF its value depends on the shapes of the BD-like and the star-like IMF, as well as on the BD-to-star ratio. The evaluation of equation (1.15) yields $\mathcal{R}_{\rm HBL} = 0.17$ for the Trapezium, $\mathcal{R}_{\rm HBL} = 0.30$ for TA, $\mathcal{R}_{\rm HBL} = 0.22$ for IC 348, and $\mathcal{R}_{\rm HBL} = 0.3$ for the Pleiades. Although $\mathcal{R}_{\rm HBL}$ is not an input parameter here but is calculated from the two IMFs and their relative normalisation, $\mathcal{R}_{\rm pop}$, it could easily be used as one instead of $\mathcal{R}_{\rm pop}$ while calculating the latter from $\mathcal{R}_{\rm HBL}$.

Figure 1.9 shows the contour plots of the 5 % and 1 % significance ranges in the $\alpha_{\rm BD} - \mathcal{R}_{\rm HBL}$ space for Trapezium, TA, IC 348, and the Pleiades. The significance values are calculated from χ^2_ν via the incomplete Gamma function as described in § 1.3. The contours mark the regions outside which the hypothesis of a two-component IMF with a single power law for BDs and a double power law for stars has to be rejected with 95 % or 99 % confidence. Also shown (by a cross) is the standard configuration with $\alpha_{\rm BD} = 0.3$ and $\log \mathcal{R}_{\rm HBL} = 0$ for the continuous standard IMF. This point is outside both levels for all three clusters, and at least for Trapezium and TA it is well outside even for arbitrary $\alpha_{\rm BD}$. In other words, *the corresponding hypothesis of a continuous IMF has to be rejected with at least 99 % confidence.*

The size of the non-rejection areas can be used for an estimate of the errors of $\alpha_{\rm BD}$ and $\mathcal{R}_{\rm HBL}$. However, one has to keep in mind that these are only maximum possible deviations with all the other parameters kept at the optimum. The non-rejection areas in the full three-dimensional parameter space are therefore expected to be somewhat narrower.

1.4.3 Binary Fraction

Additionally, the binary fraction for each cluster as well as the total binary fraction is calculated for the best-fit models. The fraction of binaries as a function of the primary mass, $f(m_{\rm prim})$, among all systems is shown in Figure 1.10. For stars the binary fraction is a monotonic function of the primary mass in agreement with the data (Lada 2006), at least for the Trapezium, IC 348, and the Pleiades. For BDs, however, it is flat due to

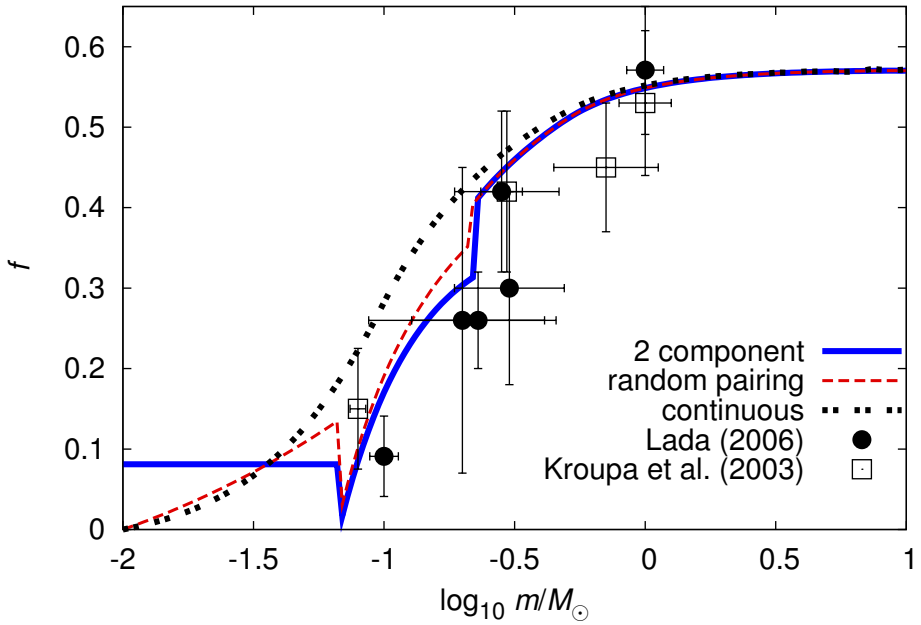

Figure 1.11: The binary fraction $f(m_{\rm prim})$ of our best fit 2-component IMF for the Trapezium (solid line) with $\alpha_{\rm BD} = 0.5$ in comparison with the binary fraction, $f_{\rm c}(m_{\rm prim})$, of the best continuous IMF model (dotted line, see also top panel in Figure 1.6). The 2-component model assumes random pairing of stars but equal-mass pairing for BD binaries. The continuous model, on the other hand, assumes random pairing of companions chosen randomly from the canonical IMF ($\alpha_{\rm BD} = 0.3$, $\alpha_1 = 1.3$ and $\alpha_2 = 2.3$). This model is merely shown for illustrative purposes and has already been discarded (§ 1.1). The thin dashed line refers to the same two-component IMF as the solid line, but with random-pairing instead of equal-mass pairing for BDs. The visible jumps in $f(m_{\rm prim})$ at $\log(m/M_\odot) = -1.15$ and -0.7 are due to the truncation at the upper and lower mass limit of the BD-like and the star-like population with their different binary properties. The global shapes of the continuous and the two-component IMF curves are similar but $f_{\rm c}(m_{\rm prim})$ is significantly higher than $f(m_{\rm prim})$ in the low-mass star and VLMS regime and outside the uncertainties of the data by Lada (2006).

the equal-mass pairing. In the case of random pairing it would approach zero for very low mass BDs (Fig. 1.11). The true mass ratio function grows monotonically with the mass ratio and becomes very steep near $q = 1$, as shown by Reid et al. (2006). Thus, for BDs the true binary fraction is probably closer to the equal-mass case than the random pairing case.

For comparison, Figure 1.11 also shows the binary fraction, $f_{\rm c}(m_{\rm prim})$, for the Trapezium that would result from a continuous IMF. Although the overall shape is very similar to that of the two-component model the binary fraction near the BD-star transition is significantly higher for low-mass stars than the observed values while being approximately equal for stars above 1 $M_\odot$. Thus, a continuous IMF cannot fit the observational data as good as a two-population IMF even if $f_{\rm tot}$ is reduced.

The total fractions of BD-BD binaries, $f_{\rm BD}$, of star-star binaries, $f_{\rm ST}$, and the fraction of (very low mass) star-BD binaries, $f_{\rm star-BD}$, are of further interest. Pairs of the latter type consist of two objects of the BD-*like* or star*like* population (see § 1.5 for the motivation and definition of the populations) but where the primary object is a star ($m_{\rm prim} \geq 0.075\,M_\odot$) within the BD-VLMS overlap region between 0.07 and 0.15 $M_\odot$, while the companion is a true, physical BD with a mass below 0.075 $M_\odot$.

For each cluster we define

$$f_{\rm BD} = \frac{N_{\rm BD-BD}}{N_{\rm sys,BD}} \tag{1.16}$$

$$f_{\rm MD-MD} = \frac{N_{\rm MD-MD}}{N_{\rm sys,MD}} \tag{1.17}$$

$$f_{\rm ST} = \frac{N_{\rm star-star}}{N_{\rm sys,star}} \tag{1.18}$$

$$f_{\rm star-BD} = \frac{N_{\rm star-BD}}{N_{\rm sys,star}}\,, \tag{1.19}$$

where $N_{\rm BD-BD}$ is the number of all BD-BD binaries (i.e. all objects have masses $\leq 0.075\,M_\odot$), $N_{\rm MD-MD}$ that of all M dwarf–M dwarf (MD-MD) binaries, $N_{\rm star-star}$ that of all star-star binaries, and $N_{\rm star-BD}$ the number of mixed (star-BD) binaries (composed of a VLMS and a BD). Furthermore, $N_{\rm sys,BD}$ is the number of all BD systems (including single BDs), $N_{\rm sys,MD}$ that of all M dwarf systems, and $N_{\rm sys,star}$ the number of all systems with a star as primary and with a stellar, BD, or no companion. As for the BD-to-star ratio we also applied the (primary) mass ranges from Kroupa & Bouvier (2003a) on the BD and star sample from each cluster but with no gap between the BD and the stellar regime, i.e. $0.02\,M_\odot \leq m_{\rm prim} \leq 0.075\,M_\odot$ for BDs and $0.075\,M_\odot \leq m_{\rm prim} \leq 1\,M_\odot$ for stars. In addition, the binary fraction of M dwarfs is calculated in the same way as the stellar one but in the mass range $0.075\,M_\odot \leq m_{\rm prim} \leq 0.5\,M_\odot$. The uncertainty limits of the binary fractions and BD-to-star ratios have been derived from those of the IMF slopes by applying the minimum and maximum slopes.

The results are shown in Table 1.4. The binary fractions for BDs vary only slightly between 12 % and 15 %, while the stellar binary fraction, $f_{\rm ST}$, is about 70 % for TA and 30 %–40 % for the others. They are apparently slightly lower than the binary fractions

Cluster	$f_{\rm BD}$	$f_{\rm MD-MD}$	$f_{\rm ST}$	$f_{\rm star-BD}$	$\mathcal{R}$	$\mathcal{R}_{\rm HBL}$
Trapezium	0.13 ± 0.01	0.30 ± 0.01	0.34 ± 0.01	0.023 ± 0.002	0.18 ± 0.03	0.17 ± 0.04
TA	0.15 ± 0.01	0.64 ± 0.06	0.69 ± 0.05	0.046 ± 0.005	0.27 ± 0.09	0.30 ± 0.11
IC 348	0.13 ± 0.02	0.29 ± 0.02	0.33 ± 0.02	0.021 ± 0.004	0.20 ± 0.10	0.22 ± 0.11
Pleiades	0.13 ± 0.02	0.33 ± 0.03	0.37 ± 0.03	0.025 ± 0.002	0.28 ± 0.18	0.28 ± 0.18

Table 1.4: Binary fractions $f_{\rm BD}$ for BD-BD, $f_{\rm MD-MD}$ for MD-MD, $f_{\rm star-BD}$ for star-BD and $f_{\rm ST}$ for star-star binaries in the studied clusters. Note that the star-BD binaries result from the pairing in the overlap region between about 0.075 and 0.15 $M_\odot$. Thus, for example, in IC 348 2.1 % of all stars are expected to have a physical BD as a companion. In addition, the BD-to-star ratio between 0.02 and 1.0 $M_\odot$ $\mathcal{R}$, and at the HBL, $\mathcal{R}_{\rm HBL}$, is listed. Note that the numerical uncertainties of $f_{\rm star-BD}$ are probably much smaller than true ones since $f_{\rm star-BD}$ largely depends on $m_{0,\rm star}$.

that are set for the star-like population because of the non-constant distribution binary as shown in Figure 1.10. The binary mass function (eq. [1.6]) is smaller in the mass region below 1 $M_\odot$ and thus the binarity is below average if the focus is set on this region.

Furthermore, in the overlap region the relatively low binary fraction of VLMSs from the BD-like population also contributes to $f_{\rm ST}$, which results in an even lower value of $f_{\rm ST}$. This trend is more emphasised for the M dwarf binary fraction, $f_{\rm MD-MD}$, which is about 10 % lower than $f_{\rm ST}$ for each cluster but still much larger than $f_{\rm BD}$.

The star-BD binary fraction $f_{\rm star-BD}$ is of special interest since it is the measure for the "dryness" of the BD desert. Note that due to the equal-mass pairing used here for BD-like binaries, the BD-like population formally does not contribute to $f_{\rm star-BD}$. All star-BD binaries are from the star-like regime which extends down to $m_{0,\rm star} = 0.07\,M_\odot$, i.e. into the BD mass regime. For the Trapezium, IC 348, and the Pleiades our two-component models yield values between 2 % and 2.5 %, whereas TA shows $f_{\rm star-BD} \approx 5\,\%$. For comparison, the continuous IMF from the top panel of Figure 1.6 corresponds to $f_{\rm star-BD} = 15\,\% \pm 4\,\%$. For mass ratio distributions other than equal-mass pairing we expect a higher $f_{\rm star-BD}$, consisting mostly of binaries from the BD-like population with primary masses slightly above the HBL and companion masses below. For random pairing of BD-like binaries this increment is between 0.01 and 0.03. Also the lower mass limit of the star-like population slightly influences $f_{\rm tot}$. It should also be noted that the size of the error limits for $f_{\rm star-BD}$ are calculated from the uncertainties of the IMF model (Tab. 1.3) but do not include the uncertainties of $m_{0,\rm star}$.

1.5 Discussion: Brown dwarfs as a separate population?

1.5.1 An Apparent Discontinuity

By correcting the observed MFs for unresolved multiple systems a discontinuity in the IMF near the BD/VLMS region emerges. We have also tried to model continuous single-body IMFs, but we find this hypothesis of continuity to be inconsistent with the observed MFs given the observational data on the binary properties of stars and BDs. We have shown that the *empirically determined* difference in the binary properties between BDs/VLMSs on the one hand side and stars on the other, and the *empirical finding* that stars and BDs rarely pair, implies a discontinuity in the IMF near the BD/VLMSs mass.

Thus, the discontinuity in binary properties, which has already been interpreted to mean two separate populations (Kroupa & Bouvier 2003a), also implies a discontinuity in the IMF. This relates the probably different formation mechanism more clearly to the observational evidence.

We have performed a parameter survey allowing the IMF parameters $\alpha_{\rm BD}$, $\mathcal{R}_{\rm pop}$, and $m_{\rm max,BD}$ to vary finding that the canonical stellar IMF ($\alpha_1 = 1.3$ and $\alpha_2 = 2.3$) cannot be discarded even for TA, and that the BD/VLMS discontinuity is required for all solutions. The discontinuity uncovered in this way, if measured at the classical BD-star border, is of a similar magnitude for the stellar clusters studied ($0.17 \leq \mathcal{R}_{\rm HBL} \leq 0.30$), supporting the concept of a universal IMF, which is, by itself, rather notable.

We recommend calling these populations *BD-like* and *star-like* with respect to their formation history. These populations have probably overlapping mass ranges since there is no physical reason for the upper mass limit of the BD-like population to match the lower mass limit of the star-like one. Furthermore, the best-fit models suggest such an overlap between 0.07 $M_\odot$ and about 0.2 $M_\odot$. According to this classification through the formation history, BD-like objects would include VLMSs, while star-like ones would include massive BDs.

The overlap region implies that BD-like pairs can consist of a VLMS-BD pair, and that a star-like binary can consist of a stellar primary with a massive BD as a companion. As can be seen from Table 1.4, the star-BD fractions are similar (except for the dynamically unevolved TA) and that the star-BD binary fraction, $f_{\rm star-BD}$, is about 2 %–3 %. This is somewhat higher than the value of < 1 % BD companion fraction Grether & Lineweaver (2006) found for nearby stars but still far below the value expected for a single population model (at least 7 %-15 % in Kroupa et al. 2003 and 15 % $\pm$ 4 % in our calculations). Simulations by Bate et al. (2003), Bate & Bonnell (2005), and Bate (2005) predict a fraction of about 2 % star-BD binaries (actually one M dwarf with a BD companion out of 58 stars formed in three independent calculations). Note that, in our model, $f_{\rm star-BD}$ is a prediction of the required overlap region and is sensitive to the overlapping range. As our model for the Pleiades IMF suggests, the overlapping range might be considerably smaller than that we have found for the other clusters. Furthermore, we did not fit the lower mass border, $m_{\rm 0,star}$, of the star-like population but simply assumed a value

of 0.07 $M_\odot$ which is well in the BD mass regime (and is the major source of star-BD binaries in our Pleiades model). A slight increase of $m_{0,\mathrm{star}}$ by only 0.01 $M_\odot$ would cause the Pleiades star-BD binary fraction to drop to nearly zero.

Several authors doubt the existence of two separate populations. Most recently, Eislöffel & Steinacker (2007) summarise that the observational community in general prefers the model of star-like formation for BDs. They mention the detection of isolated proto(sub)stellar "blobs" in the Ophiuchus B and D clouds, which may support the theory of star-like formation for BDs. It remains unclear, though, how many of these blobs will actually form BDs instead of dissolving from lack of gravitational binding energy. Goodwin & Whitworth (2007) refer to a private communication with Å. Nordlund stating that the pure turbulence theory predicts about 20,000 transient cores for every actual pre-stellar core of about 0.1 $M_\odot$.

We recall that one of the main reasons for the existence of a separate population is the semi-major axis distribution of BD binaries (Fig. 1.1). But Luhman et al. (2007) also mention a wide binary BD in Ophiuchus with a separation of approximately 300 AU. Indeed, a small number of wide BD binaries are known. However, it can be doubted that the occasional discovery of a wide BD binary may expand the narrow semi-major axis distribution (Fig. 1.1) to a star-like one. The striking evidence posed by the lack of BD companions to stars is a strong indication for two populations. It is usually ignored by the community, though. We note that even if there actually may be some BDs that formed star-like they are most probably a minority.

There is also the interpretation of the BD desert being a "low-q desert" rather than an absolute mass-dependent drop in the companion mass function. Grether & Lineweaver (2006) find a low-mass companion desert of solar-type primary stars between approximately 0.01 and 0.06 $M_\odot$. They find this interval to be dependent on the primary star mass and therefore predict M dwarfs to have BD companions, and that M dwarfs ought to have a companion desert between a few Jupiter masses and the low-mass BD regime. However, this interpretation does not address the different orbital properties of BDs and stars as well as the different q distribution.

1.5.2 Implications for the Formation History

Can the existence of such a discontinuity, i.e. the formation of two separate populations, be understood theoretically? Although BDs and stars appear to be distinct populations the formation of BDs is likely to be connected to star formation. Bate et al. (2002, 2003) show that BDs significantly below 0.07 $M_\odot$ cannot form in a classical way since the minimum mass they need for stellar-type formation would also lead to progressive accretion and growth to stellar mass unless they are in regions with very low mass infall rates. But such regions are very rare, because the prevailing densities and temperatures cannot achieve the required Jeans masses, as also stressed by Goodwin & Whitworth (2007). For this reason, Adams & Fatuzzo (1996) expected BDs to be rare. Only a small fraction of the BDs, especially those at the high-mass end of the BD regime, may form this way if the surrounding gas has been consumed by star formation processes just after the proto-BD has reached the Jeans mass. To explain the actually higher

BD frequency (per star) in recent surveys the accretion process has to be terminated or impeded somehow (Bonnell, Larson & Zinnecker 2007).

Also the above-mentioned differences in the distribution of the semimajor axes between BDs and stars cannot be explained by a scaled-down star formation process, because that would imply a continuous variation and a much broader semi-major axis distribution for BDs and VLMSs that has not been observed (Kroupa et al. 2003). While binary stars show a very broad distribution of their semimajor axes peaking at about 30 AU the semimajor axes of BDs are distributed around about 5 AU with a sharp truncation at 10–15 AU (Fig. 1.1). No smooth transition region between both regimes can be recognised (Close et al. 2003). In a high angular resolution survey Law et al. (2007) found that the orbital radius distribution of binaries with V-K < 6.5 appears to differ significantly from that of cooler (and thus lower mass) objects, suggesting a sudden change of the number of binaries wider than 10 AU at about the M5 spectral type. This is in agreement with our finding of a possible BD-like population that extends beyond the hydrogen-burning mass limit into the VLMS regime.

In a radial-velocity survey of Chamaeleon I, Joergens (2006) has found evidence for a rather low binary fraction below 0.1 AU, while most companions found in that survey orbit their primaries within a few AU. For this reason an extreme excess of close BD binaries that cannot be resolved by imaging surveys appears to be unlikely. A larger binary fraction than about 15 % would thus not be plausible. Basri & Reiners (2006) suggest an upper limit of $26\,\% \pm 10\,\%$ for the BD binary fraction based on their own results ($11\,\%^{+0.07}_{-0.04}$, for separations below 6 AU) and the survey by Close et al. (2003; $15\,\% \pm 7\,\%$, for separations greater than 2.6 AU) by simple addition of the results. This is nearly consistent with a BD binary fraction of 15 %, since the survey is neither magnitude- nor volume-limited. However, they admit that their value may be overestimated since the objects with separations between 2.6 and 6 AU are counted twice. We note further that even a total BD binary fraction of 25 % ($f_{\rm BD} = 0.25$), although outside the error limits of our best-fit models, would only lead to a minor change in the fitted IMFs.

It has been argued (Basri & Reiners 2006) that the lower binary fraction of BDs is just the extension of a natural trend from G dwarfs to M dwarfs (Figs. 1.10 and 1.11). Our contribution has shown that this trend can be understood by the simple fact that there are many fewer possibilities to form a binary near the lower mass end than for higher component masses. The observational data are in better agreement with a minimum mass, $m_{\rm min}$, near the hydrogen-burning mass limit and a low overall binary fraction of BD-like objects than with an "all-in-one" IMF from the lowest mass BDs to the upper stellar mass limit, as shown in Figure 1.11. This observed trend thus appears as an additional enforcement of the two-populations model of BDs and stars.

Given that the conditions for a star-like formation of BDs are very rare (Bate et al. 2003), four alternative formation scenarios for BDs apart from star-like formation can be identified, namely

1. Formation of wide star-BD binaries via fragmentation of a proto- or circumstellar disk and subsequent disruption by moderately close encounters.

2. Formation of BDs as unfinished stellar embryos ejected from their birth system.

3. Removal of the accretion envelopes from low-mass protostars via photoevaporation.

4. Removal of the accretion envelopes due to extremely close stellar encounters (Price & Podsiadlowski 1995).

Scenario 4 can be ruled out as the major BD formation mechanism because the probability of such close encounters, with required flyby distances typically below 10 AU (Kroupa & Bouvier 2003a) for efficient disruption of accretion envelopes (less than a tenth of those proposed by Thies et al. [2005] for triggered planet formation), is far too low for such a scenario being a significant contribution to BD formation. The photo evaporation model, as studied by Whitworth & Zinnecker (2004), also cannot be the major mechanism of BD formation (Kroupa & Bouvier 2003a). It predicts a variation of the IMF with the population number and density of the host cluster. In dense starburst clusters (young globular clusters) with a larger number of O/B stars or even modest clusters such as the ONC with a dozen O/B stars compared to TA, a larger fraction of low-mass stars would have halted in growth. This would result in a bias towards M dwarfs, since many of them would be failed K or G dwarfs. In contrast to this prediction, Briceño et al. (2002) and Kroupa et al. (2003) show that the IMFs of TA and ONC are very similar in the mass range 0.1–1 $M_\odot$, while globular clusters likewise have a low-mass MF similar to the standard form (Kroupa 2001).

1.5.3 Embryo Ejection

Reipurth (2000) and Reipurth & Clarke (2001) introduced the formation of BDs as ejected stellar embryos as the alternative scenario 2. If a forming protostar in a newborn multiple system is ejected due to dynamical instability its accretion process is terminated and the object remains in a protostellar state with only a fraction of the mass compared to a fully developed star. Since the final mass is physically independent of the hydrogen fusion mass limit one would not expect the mass range of ejected embryos to be truncated at the HBL and thus expect an *overlap region* between these populations. This fully agrees with the requirement of having to introduce such an overlap region in order to fit the observed $\mathrm{IMF}_{\mathrm{sys}}$ in § 1.3.

This model gives some hints to understand the low BD binary fraction as well as the truncation of the semimajor axis distribution of BDs. The decay of a young multiple system of three or more stellar embryos typically leads to the ejection of single objects but also to the ejection of a small fraction of close binaries. In order to survive the ejection, the semi-major axis of such a binary must be significantly smaller (by a factor of about 3) than the typical orbital separation within the original multiple system. A similar explanation is that the orbital velocity of the BD binary components has to be higher than the typical ejection velocity in order to keep the interaction cross section of the binary with other system members small. Indeed, the velocity dispersion of BDs in the embryo-ejection model shown in Kroupa & Bouvier (2003a) is $\lesssim 2\,\mathrm{km\,s^{-1}}$ for the majority of the BDs. This is in good agreement with the Keplerian orbital velocity

of each BD-binary member of about 1.5–2 $\mathrm{km\,s^{-1}}$ for an equal-mass binary of 0.05–0.08 $M_\odot$ and $a \approx 10\,\mathrm{AU}$. The majority of BD binaries have smaller separations, and, consequently, higher orbital velocities and are bound tighter. This would set the low binding energy cut near $E_{\mathrm{bind}} = 0.2\,\mathrm{pc^{-2}\,Myr^2}$ in Figure 1.2.

There have been numerical simulations of star formation and dynamics, e.g. by Bate et al. (2003) and Umbreit et al. (2005), in which binaries are produced via ejection that show remarkably similar properties to the actually observed ones. Umbreit et al. (2005) describe the formation of BDs from decaying triple systems. Their simulations predict a semi-major axis distribution between about 0.2 and 8 AU (see Fig. 8 in their paper), peaking at 3 AU. This is slightly shifted towards closer separations compared with the results by Close et al. (2003) but still in agreement with the observational data. In contrast to this, Goodwin & Whitworth (2007) doubt the frequent formation of close BD binaries via ejection, arguing that hydrogen-burning stars which formed via ejection were almost always single.

In further qualitative support of the embryo ejection model, Guieu et al. (2006) describe a deficit by a factor of 2 of BDs near the highest density regions of TA relative to the BD abundance in the less dense regions that can possibly be explained by dynamical ejection and consequently larger velocity dispersion of stellar embryos, i.e. BDs. A star-like fragmentation scenario would result in an opposite trend since the Jeans mass is smaller for higher densities, thus allowing gas clumps of lower mass to form (sub)stellar bodies. Contrary to this, Luhman (2006) did not find any evidence for a different spatial distribution of BDs and stars in TA. Recently, Kumar & Schmeja (2007) have found that substellar objects in both the Trapezium and IC 348 are distributed homogeneously within twice the cluster core radii while the stellar populations display a clustered distribution. They conclude that these distributions are best explained with a higher initial velocity dispersion of BDs, in accordance with Kroupa & Bouvier (2003a), supporting the embryo-ejection model.

However, the embryo-ejection model has a challenge to reproduce the high fraction of significant disks around BDs that have been observed in young clusters. Several studies, e.g. Natta et al. (2004), reveal a considerable number of BDs with an infrared excess that indicates the presence of warm circum(sub)stellar material. While these studies do not show the actual mass of these disks because a small amount of dust in these disks is sufficient to produce these excesses, Scholz, Jayawardhana & Wood (2006) found 25 % of BDs in TA having disks with radii > 10 AU and significant masses (larger than 0.4 M_{J}). For the remaining 75 % no disks were detectable. In simulations, e.g. by Bate et al. (2003), such large disks survive occasionally, but less frequently (about 5 %) than suggested by the observations (Scholz et al. 2006). However, Scholz et al. (2006) point out that their results to not rule out the embryo-ejection scenario and admit that this mechanism may still be relevant for some BDs. In general, the embryo-ejection model is in agreement with at least the existence of low-mass circum-substellar disks up to about 10 AU (Bate et al. 2003; Umbreit et al. 2005; Güdel et al. 2007). Thies et al. (2005) also show that a thin low-mass disk can survive near-parabolic prograde coplanar encounters above about three Hill radii with respect to the disk-hosting BD. This means that a disk with a radius up to about 5 AU (later viscously evolved to about 10 AU, see Bate et al.

2003) can survive a flyby of an equal-mass embryo within about 15 AU while larger disks or widely separated binaries would be disrupted.

Furthermore, Bate et al. (2003) suggest from their simulations that the binary fraction via ejection might by as small as about 5 % (see also Whitworth et al. 2007).

1.5.4 Disk Fragmentation and Binary Disruption

The fragmentation of proto-binary disks with subsequent disruption of a star-BD binary is another promising alternative scenario. A disk can fragment during the accretion process if it reaches a critical mass above which the disk becomes gravitationally unstable against small perturbations. Fragmentation may be triggered by an external perturbation, i.e. infalling gas clumps or a passing neighbour star. The latter mechanism may also be capable of triggering fragmentation in relatively low-mass circumstellar disks resulting in rapid planet formation (Thies et al. 2005). Thus, BD formation via disk fragmentation likely plays an important role in the early ages of the cluster where the frequency of massive disks is highest (Haisch et al. 2001; Whitworth et al. 2007).

Following the argumentation of Goodwin & Whitworth (2007), disk fragmentation may explain the observed distribution of BD binary separations at least as well as the embryo-ejection model. In addition, it may explain the existence of wide star–BD binaries, since a fraction of the initial wide binaries can survive without being disrupted. Because the likelihood of disrupting close encounters depends on the mass and density of the host cluster, one expects a higher fraction of those wide star-BD binaries in smaller and less dense clusters and associations like TA. However, further studies and observations are needed to test this hypothesis.

Whitworth & Stamatellos (2006) show that BDs can actually form as widely separated companions to low-mass stars with mass m at a sufficiently large disk radius, $r_{\rm disk}$,

$$r_{\rm disk} \gtrsim 150\,{\rm AU} \left(\frac{m}{M_\odot} \right) , \tag{1.20}$$

where the disk is cool enough to allow a substellar clump to undergo gravitational collapse. For a primary star below 0.2 $M_\odot$ this minimum radius therefore becomes less than 90 AU which is in remarkable agreement with the two wider VLMS binaries found by Konopacky et al. (2007). Such large distances to the primary star allow the formation of BD-BD binaries as well as the survival of circum-substellar disks up to about 10–30 AU, depending on the total mass of the pre-substellar core and the mass of the primary star. Furthermore, this scenario explains the existence of wide star-BD binaries. In addition, such a wide star-BD binary can be disrupted by moderately close encounters of about 100–200 AU (i.e. a distance similar to the star-BD orbital radius), the disruption of such systems appears to be likely in contrast to the disruption of accretion envelopes as required in the already rejected scenario 4.

1.5.5 Summary

Both the embryo-ejection model and disk fragmentation with subsequent wide binary disruption explain the above-mentioned connection between stars and BDs, since BDs start to form like stars before their growth is terminated due to their separation from their host system or from lack of surrounding material in the outer parts of a circumstellar disk. It is obvious that the formation rate of these embryos is proportional to the total star formation rate.

For these reasons these formation mechanisms appear to be the most likely ones for BDs and some VLMSs and BD/VLMS binaries. It cannot be decided yet which scenario is the dominant mechanism. This may depend on the size and the density of the star-forming region. We expect, on the other hand, the classical star-like formation scenario to be of some importance only for the most massive BDs.

The possibility of two different *alternative* BD formation mechanisms (disk fragmentation and embryo ejection) may lead to another discontinuity in the intermediate mass BD IMF since both scenarios correspond to different binary fractions as mentioned above. The currently available data, however, are far from being sufficient for a verification of this prediction.

1.6 Conclusions

The different empirical binary properties of BDs and stars strongly imply the existence of two separate but mutually related populations. We have shown that if the IMF of BDs and stars is analysed under consideration of their binary properties then there is a discontinuity in the transition region between the substellar and stellar regime that is quite independent of the host cluster. The discontinuity in the IMF near the HBL is a strong logical implication of the disjunct binary properties and suggests splitting up the IMF into two components, the BD-like and the star-like regime. An alternative but equivalent description would be to view the stellar IMF as a continuous distribution function ranging from about 0.07 to 150 $M_\odot$ (Weidner & Kroupa 2004), and a causally connected but disjoint distribution of (probably mostly) separated ultra–low-mass companions and ejected embryos with masses ranging from 0.01 $M_\odot$ to 0.1–0.2 $M_\odot$. While the canonical stellar IMF is consistent with the observed stellar MFs at least for the Trapezium, IC 348, and the Pleiades, the sub-stellar IMF of at least the Trapezium and TA has a power law index that is consistent with the canonical value $\alpha_{\rm BD} = 0.3$. Within the error limits, our analysis does not reject the canonical power law indices for BDs and stars for any cluster.

The discontinuity is often masked in the observational data due to a mass overlap of both populations in the BD-VLMS region as well as the higher apparent masses of unresolved binaries compared to single objects in the observed $\mathrm{IMF}_{\rm sys}$. The discontinuity in the number density near the HBL is a step of approximately a factor of 3–5 (Table 1.4). This implies a general dependency between both populations and is, as far as we can tell, consistent with the scenario of disrupted wide binaries (Goodwin & Whitworth

2007) as well as with the truncated-star scenario (e.g. as an ejected stellar embryo, Reipurth & Clarke 2001), since the number of unready stars is directly correlated with the total amount of star formation in the host cluster. Both embryo-ejection and wide binary disruption are also consistent with the properties of close binary BDs.

Our results (Tab. 1.3) suggest that about one BD is produced per 4–6 formed stars. This suggests the necessity of a distinct description of BDs and stars as well as the connection between these two populations through their formation process.

2 A discontinuity in the low-mass IMF – the case of high multiplicity

(based on Thies & Kroupa, 2007 MNRAS, 390, pp. 1200–1206. *A discontinuity in the low-mass IMF - the case of high multiplicity*)

The empirical binary properties of brown dwarfs (BDs) differ from those of normal stars suggesting BDs form a separate population. Recent work by Thies and Kroupa revealed a discontinuity of the initial mass function (IMF) in the very-low-mass star regime under the assumption of a low multiplicity of BDs of about 15 per cent. However, previous observations had suggested that the multiplicity of BDs may be significantly higher, up to 45 per cent. This contribution investigates the implication of a high BD multiplicity on the appearance of the IMF for the Orion Nebula Cluster, Taurus-Auriga, IC 348 and the Pleiades. We show that the discontinuity remains pronounced even if the observed MF appears to be continuous, even for a BD binary fraction as high as 60 %. We find no evidence for a variation of the BD IMF with star-forming conditions. The BD IMF has a power-law index $\alpha_{\rm BD} \approx +0.3$ and about 2 BDs form per 10 low-mass stars assuming equal-mass pairing of BDs.

2.1 Introduction

The origin of brown dwarfs (BDs) remains the subject of intense discussions. There are two broad ideas on their origin: 1. the classical *star-like* formation scenario of BDs (e.g. Adams & Fatuzzo 1996; Padoan & Nordlund 2004), and 2. BDs and some very-low-mass stars (VLMSs) form as a separate population (hereafter named *BD-like* besides the classical *star-like* population) with a different formation history than stars, e.g. as ejected stellar embryos (Reipurth & Clarke 2001; Kroupa & Bouvier 2003a) or as disrupted wide binaries (Goodwin & Whitworth 2007; Stamatellos et al. 2007). Additionally, the formation of BDs from Jeans instabilities in high-density filaments near the centre of a massive star-forming cloud has been recently suggested implying such BDs to be preferentially located in clusters with strong gravitational potentials (Bonnell et al. 2008).

The star-like formation scenario fails to reproduce the observed different binary properties of BDs and stars. Especially the truncation of the semi-major axis distribution between 10 and 20 AU for BDs and the different mass-ratio distribution of BDs and stars (Bouy et al. 2003; Burgasser et al. 2003; Martín et al. 2003; Kroupa et al. 2003;

Close et al. 2003), as well as the *brown dwarf desert* (McCarthy et al. 2003; Grether & Lineweaver 2006), are difficult to account for if BDs form indistinguishably to stars. This implies the need of treating BDs as a separate population to stars. The assumption of two separate populations would then require two separate initial mass functions (IMFs) of the individual bodies of a star cluster. Although the observed mass function may appear approximately continuous from the lowest mass BDs up to the highest mass stars (Lodieu et al. 2007), a discontinuity in the IMF may be present but be masked by 'hidden' (unresolved) binaries only emerging if the observed MF is corrected for unresolved multiplicity. This issue has been discussed in greater detail in Thies & Kroupa (2007, hereafter TK07) for the case of a low multiplicity of 15 % of the BD-like population. However, a higher BD multiplicity between 20 % and 45 % had been reported by some authors, e.g. Jeffries & Maxted (2005); Basri & Reiners (2006). This raises the need, dealt with this contribution, for including higher multiplicities as well as for an analysis of the general effects of a high multiplicity on the IMF and on the BD-to-star ratio.

In Section 2.2 we review the evidence for a separate BD-like population. Section 2.3 briefly introduces the mathematical method of calculating the IMF including unresolved binaries. In Section 2.4 the new results are presented and compared to those of TK07. The Summary follows in Section 2.5.

2.2 Brown dwarfs as a separate population

2.2.1 Motivation

It may be argued that by treating the BDs as a separate population this forces an IMF discontinuity near the stellar/sub-stellar mass limit by construction. Indeed, the semi-major axis data and binary fraction (here used as a simplification for the multiplicity, neglecting multiples of higher order, Goodwin et al. 2007) as a function of the primary mass can be interpreted to be continuous with no evidence for BDs being a separate population (Burgasser et al. 2007).

Given this argumentation, it is essential to describe the methodology applied in our analysis: We seek one mathematical formulation which is a unification of the binary population for G-, K-, M-dwarfs and VLM-stars and BDs. This is found to be possible for G-, K- and M-dwarfs: thus, for example, G-dwarfs have mostly K- and M-dwarf companions, and the period-distribution functions of G-, K- and M-dwarf primaries are indistinguishable. Further, the mass-ratio and period-distribution functions for G-, K- and M-dwarf primaries derive from a single birth mass-ratio and period distribution which does not differentiate according to the mass of the primary (Kroupa et al. 2003; Goodwin et al. 2007). One single mathematical model can therewith be written down which treats G-, K- and M-dwarfs on exactly the same footing – one can say that G-, K- and M-dwarf stars mix according to one rule (random pairing from the IMF at birth).

If BDs are to be introduced into a similar mathematical formulation which does not differentiate between BDs and stars, then the model fails, because it leads to (1) a too wide BD period-distribution function, (2) too many BD binaries, (3) far too many stellar–BD

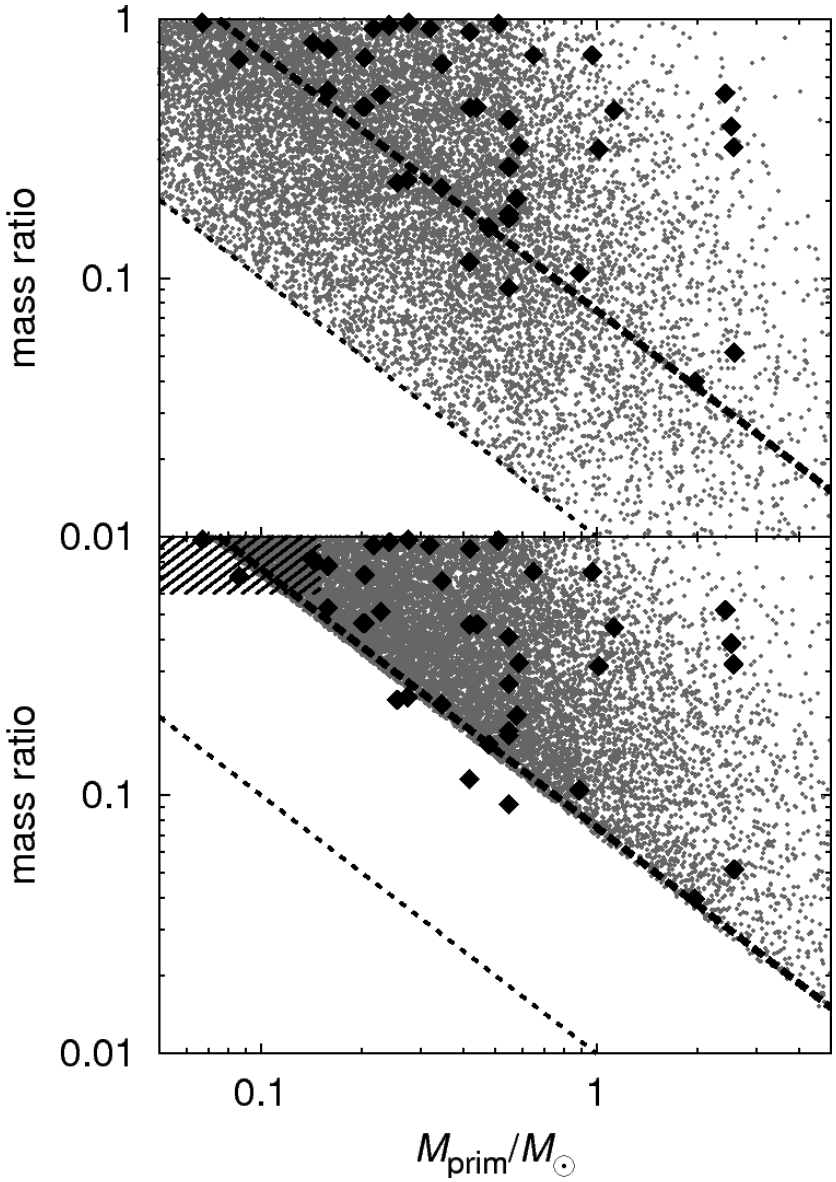

Figure 2.1: Mass-ratio distribution of binaries in a Monte Carlo sample cluster following the canonical stellar mass function (§ 2.3). **Upper panel:** Binaries formed via random pairing over the complete mass range of a single population of BDs and stars (dots). The companions have masses down to 0.01 $M_\odot$ (thin dashed line) for all kinds of primaries. This is in contradiction with observations (Lafrenière et al. 2008, black diamonds). **Lower panel:** Binaries from random pairing within separate populations of BDs between 0.01 and 0.075 $M_\odot$, and stars above 0.075 $M_\odot$, i.e. there are no stellar companions below 0.075 $M_\odot$ (thick dashed line). The resulting mass-ratio distribution fits well to the one observed by Lafrenière et al. (2008) in the stellar regime. The regime of the (approximately equal-mass companion) BD-like binaries is indicated by the shaded region.

binaries, and (4) far too few star–star binaries (Kroupa et al. 2003). Lafrenière et al. (2008) show that the mass-ratio of binaries depends on the primary-star mass in a way that results in an almost constant lower mass limit of the companions near 0.075 $M_\odot$ for the Chamaeleon I star-forming region (see the figures 7 and 12 in their paper). This distribution can be reproduced by random pairing over the stellar mass range, while global random pairing over BDs and stars yields a different distribution, as shown in Fig. 2.1. In order to avoid these failures, and in particular, in order to incorporate the BD desert ("stars and BDs don't mix, while G, K and M dwarfs do mix") into the mathematical formulation of the population, it is unavoidable to *invent special mathematical rules for the BDs*. That is, stars and BDs *must* be described separately.

TK07 show that this necessarily implies a discontinuity in the IMF, given the observational data. We emphasise that the observational mass distributions lead to this conclusion, once the correct mathematical description is incorporated consistently. However, TK07 assume a rather low binary fraction of the BD-like population of 15 %. Some papers (Guenther & Wuchterl 2003; Kenyon et al. 2005; Joergens 2006) that report the discovery of close BD binaries instead conclude that these may imply a significantly higher binary fraction between 20 % and 45 % (Jeffries & Maxted 2005; Basri & Reiners 2006), the latter being similar to that of stars in dynamically evolved environments (Kroupa 1995c). It is therefore useful to re-address the problem TK07 posed by incorporating a larger BD binary fraction into the analysis.

2.2.2 A short review of binarity analysis

This contribution is, like TK07, part of a series on the theoretical interpretation of observational stellar cluster data. Kroupa et al. (1991, 1993); Kroupa (2001) showed for the first time that the true individual-body stellar IMF is changed significantly by correcting for the bias due to unresolved binary stars. A detailed study in Kroupa (1995a,c,b), in Kroupa, Petr & McCaughrean (1999), and in Kroupa, Aarseth & Hurley (2001) of the *observed* binary properties of field stars, stars in the Orion Nebula Cluster (ONC), the Pleiades and the Taurus-Auriga association (TA) led to a thorough understanding of the energy distribution of binary systems. This work established that simply taking observed distributions can lead to wrong interpretations, unless the counting biases and stellar-dynamical evolution is treated systematically and consistently; the basis of the argument being that Newton's laws of motion cannot be ignored. In a recent paper Reipurth et al. (2007) have supported the predictions made by Kroupa et al. (1999) concerning the binary population in the ONC, by uncovering a radially dependent binary fraction in nice agreement with the theoretically expected behaviour. The late-type stellar binary population is therewith quite well understood, over the mass range between about 0.2 $M_\odot$ and 1.2 $M_\odot$. The above work has also established the necessity to correctly dynamically model *observed* data in order to arrive at a consistent understanding of the physically relevant distribution functions.

Brown dwarfs (BDs), which extend the mass scale down to 0.01 $M_\odot$, have been added into the theoretical analysis in Kroupa & Bouvier (2003b,a); Kroupa et al. (2003). This theoretical study of observational data (Close et al. 2003; Bouy et al. 2003) showed that

BDs cannot be understood to be an extension of the stellar mass regime (as is often but wrongly stated). The hypothesis of doing so leads to incompatible statistics on the star-star, star-BD and BD-BD binary fractions, and on their energy distributions. This work showed that BDs must be viewed as a separate population, and the theoretical suggestion by Reipurth & Clarke (2001), that BDs are ejected stellar embryos, is one likely explanation for this. In fact, their proposition logically implies different binary properties between stars and BDs, because ejected objects cannot have the same binding energies as not-ejected objects. Likewise, the model of Goodwin & Whitworth (2007), according to which BDs are born in the outer regions of massive accretion disks, implies them to have different pairing rules than stars.

TK07 and this contribution are a logical extension of the above findings. Here we repeat parts of the analysis of TK07 with assumed BD-like binary fractions up to 60 % as an upper limit. The clusters we analyse are the ONC (Muench et al. 2002), TA (Luhman 2004a; Luhman et al. 2003), IC 348 (Luhman et al. 2003) and the Pleiades based on data by Dobbie et al. (2002), Moraux et al. (2003) and the Prosser and Stauffer Open Cluster Database[1]. The aim is to check whether our previous results are still valid for a higher binary fraction, and how robust they are for different accounting of unresolved binary masses.

2.3 IMF basics and computational method

The IMFs are constructed from power-law functions similar to that proposed by Salpeter (1955b),

$$\xi(m) = \frac{\mathrm{d}n}{\mathrm{d}m} = k\, m^{-\alpha}\,, \tag{2.1}$$

or in bi-logarithmic form

$$\xi_{\mathrm{L}}(\log_{10} m) = \frac{\mathrm{d}n}{\mathrm{d}\log_{10} m} = \ln(10)\ m\,\xi(m) = k_{\mathrm{L}}\, m^{1-\alpha}\,, \tag{2.2}$$

where k is a normalisation constant and $k_{\mathrm{L}} = \ln(10)k$. While Salpeter found $\alpha \approx 2.35$, the *canonical* stellar IMF, ξ_{star}, is constructed as a two-part-power law after Kroupa (2001), with $\alpha_1 = 1.3$ for a stellar mass $m < 0.5\ M_\odot$ and $\alpha = 2.3$ for higher masses. The substellar IMF, ξ_{BD}, is taken to be a single power-law with cluster-dependent exponent α_{BD}.

The basic assumption is that a large fraction of binaries remains unresolved since cluster surveys are often performed with wide-field surveys with limited resolution. One may be tempted to use the observed IMF (hereafter $\mathrm{IMF_{obs}}$) as a direct representation of the true IMF of individual bodies (simply the IMF hereafter). However, the observed IMF ($\mathrm{IMF_{obs}}$) can differ largely from the IMF, especially at the low-mass end of the population which contains most of the stellar companions. If the companion has a much lower mass than its primary, then its light does not contribute much to the combined

[1] Available at http://www.cfa.harvard.edu/~stauffer/opencl/

luminosity and spectral type, and thus the derived mass is essentially that of the primary. If, however, both components have near-equal masses (as expected from random pairing for very low primary masses), the low-mass region of the $\mathrm{IMF_{obs}}$ may be depressed even further, since the combined luminosity can be up to twice the luminosity of the primary alone. Therefore a fraction of unresolved low-mass binaries is counted as single stars, maybe even of higher mass, while their companions are omitted, attenuating the $\mathrm{IMF_{obs}}$ at the lower mass end.

Possible approximations to the $\mathrm{IMF_{obs}}$ are the system IMF ($\mathrm{IMF_{sys}}$), that is the IMF as a function of system mass (see equations 6 to 8 in TK07), and the primary body IMF ($\mathrm{IMF_{pri}}$), the IMF as a function of the primary object mass, m_{prim},

$$\xi_{\mathrm{pri}}(m_{\mathrm{prim}}) = f_{\mathrm{tot}} N_{\mathrm{bod}} \int_{m_{\mathrm{min}}}^{m_{\mathrm{prim}}} \hat{\xi}(m_{\mathrm{prim}}) \hat{\xi}(m)\, \mathrm{d}m\,, \tag{2.3}$$

where N_{bod} is the total number of objects, m_{min} is the minimum mass of an individual body in the given population, $f_{\mathrm{tot}} \equiv N_{\mathrm{bin,tot}}/(N_{\mathrm{sng}} + N_{\mathrm{bin,tot}})$ is the total binary fraction, and $\hat{\xi}(m) = \xi(m)/N_{\mathrm{bod}}$ is the normalised individual-body IMF.

In TK07 the $\mathrm{IMF_{sys}}$ has been used for the fitting process. However, one may argue that the mass derived from the system luminosity is closer to the mass of the primary star since the luminosity is mainly given by the primary object and the spectral features of the companion are outshone by those of the primary. Therefore, the $\mathrm{IMF_{pri}}$ has been used as the workhorse in the current contribution.

To obtain the true IMF from an observed mass distribution a binary correction has to be applied to each native population (i.e. a population of objects that share the same formation history) the cluster consists of. This is done here via the semi-analytical backward-calculation method and χ^2 minimisation against the observational data introduced in TK07. It assumes two native populations with different IMFs, different overall binary fractions and different mass-ratio distributions (namely the two extreme cases of random pairing and equal-mass pairing for BDs while random pairing is always applied to stars). For each cluster the BD IMF slopes, the population ratio,

$$\mathcal{R}_{\mathrm{pop}} = \frac{N_{\mathrm{BD}}}{N_{\mathrm{star}}}\,, \tag{2.4}$$

and the upper mass limit of the BD-like IMF, $m_{\mathrm{max,BD}}$, are to be fitted, while the lower mass limit of BDs (0.01 $M_\odot$) and of the star-like population (0.07 $M_\odot$) is kept constant. Here, the number of BD-like and star-like objects is given by

$$\begin{aligned} N_{\mathrm{BD}} &= \int \xi_{\mathrm{BD}}(m)\, \mathrm{d}m\,, \\ N_{\mathrm{star}} &= \int \xi_{\mathrm{star}}(m)\, \mathrm{d}m\,, \end{aligned} \tag{2.5}$$

respectively. The IMFs are then transformed into separate primary mass functions. Before being compared to the observational MFs the fitted $\mathrm{IMF_{pri}}$ has been smoothed by a Gaussian convolution along the mass axis in order to simulate the error of the mass

determination (see TK07 for a more detailed description). This process is repeated iteratively until χ^2 reaches a minimum.

For the Pleiades the BD data do not constrain the power-law index, so fixed power-laws with $\alpha_{\rm BD} = 0.3$ (the canonical value) and $\alpha_{\rm BD} = 1$ have been used here. It should be noted that the power-law indices are in rough agreement with the power-law index $\alpha = 0.6$ deduced by Bouvier et al. (1998) and Moraux et al. (2003). Since they use BDs and low-mass stars up to 0.48 $M_\odot$ while only BDs and VLMSs are used in our contribution these values have to be compared with caution.

The crucial point in performing the binary correction is that the assumed number and mass range of a native population largely affects the resulting $\mathrm{IMF_{pri}}$. If, for example, only one overall population is assumed (as in the traditional star-like scenario for BDs and stars) but there are actually two separate BD-like and star-like populations with different mass ranges, then the binarity is corrected for wrongly at the lower mass end of the star-like population since a mixing of binary components between BDs and stars is assumed that does not exist in reality. Reversely, the observed (primary) IMF of a cluster may appear as being continuous while actually consisting of two populations, because the discontinuity is masked by the interference of different probability densities of the populations in the transition or overlap region on the one hand and different binary fractions on the other, as well as being smeared out by measurement uncertainties. Thus, an apparently continuous $\mathrm{IMF_{pri}}$ or $\mathrm{IMF_{sys}}$ may be related to a discontinuous IMF or, more precisely, a composite IMF which can only be revealed by reducing the fraction of unresolved binaries to insignificance by high-resolution observations.

The magnitude of the discontinuity, measured as the number ratio of BD-like to star-like objects at the hydrogen-burning mass limit (HBL), $\mathcal{R}_{\rm HBL}$, is given by

$$\mathcal{R}_{\rm HBL} = \frac{N_{\rm BD}\,(m \approx 0.075\,M_\odot)}{N_{\rm star}\,(m \approx 0.075\,M_\odot)}\,. \tag{2.6}$$

If there is no overlap of the fitted BD-like and the star-like population (which is actually the case for the ONC and the Pleiades), $\mathcal{R}_{\rm HBL}$ is calculated from extrapolation of the BD-like IMF to the HBL. Since $\mathcal{R}_{\rm HBL}$ depends on the binary fraction among each population, the binary fraction is varied from $f_{\rm BD} = 0$ to $f_{\rm BD} = 0.6$ in order to include even the most extreme BD binary fraction. The unresolved stellar binary fraction, $f_{\rm ST}$, is set to 0.4 for the ONC, IC 348 and the Pleiades while that of TA is assumed to be 0.8, as in TK07.

2.4 Results

2.4.1 IMF fitting parameters for different BD binary fractions

For illustration, Fig. 2.2 shows the fitted BD-like and star-like IMFs, $\xi_{\rm BD}$ and $\xi_{\rm star}$ and the resulting $\mathrm{IMF_{pri}}$ for the ONC for an assumed $f_{\rm BD} = 0.15$ (upper panel) and $f_{\rm BD} = 0.45$ (lower panel), both using equal-mass pairing for BD-like binaries and random pairing for star-like ones. Random pairing means, in this context, pairing two stars

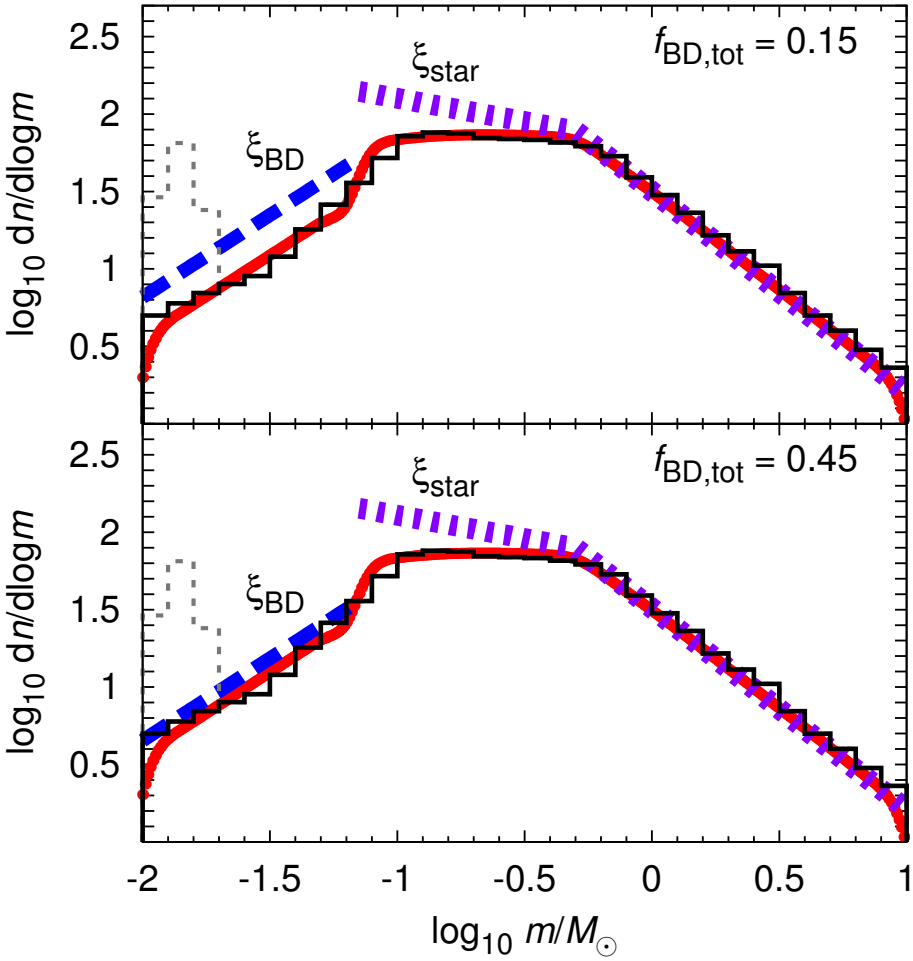

Figure 2.2: The best-fit IMFs for the ONC (Muench et al. 2002, histogram) for $f_{\rm BD}$ = 0.15, as displayed in TK07, and for $f_{\rm BD}$ = 0.45, the upper limit deduced by Jeffries & Maxted (2005). The primary IMFs (solid curves) are being derived from separated BD-like (dashed lines) and star-like (dotted lines) populations consistent with the ejected-embryo hypothesis of Reipurth & Clarke (2001) or the disk-fragmentation hypothesis of Goodwin & Whitworth (2007). The assumed fraction of unresolved star-like binaries is $f_{\rm ST}$ = 0.4. Despite the high binary fraction in the lower panel the discontinuity near the stellar-substellar border is only slightly reduced. The unequal binary fractions for different masses and populations mask the apparent discontinuities of the IMFs in the VLMS region in IMF$_{\rm pri}$ (solid curves). The thin dashed histogram refers to a substellar peak in the data from Muench et al. (2002) which may be due to non-physical artefacts in the mass-luminosity relation used for the mass calculation (Lada & Lada 2003).

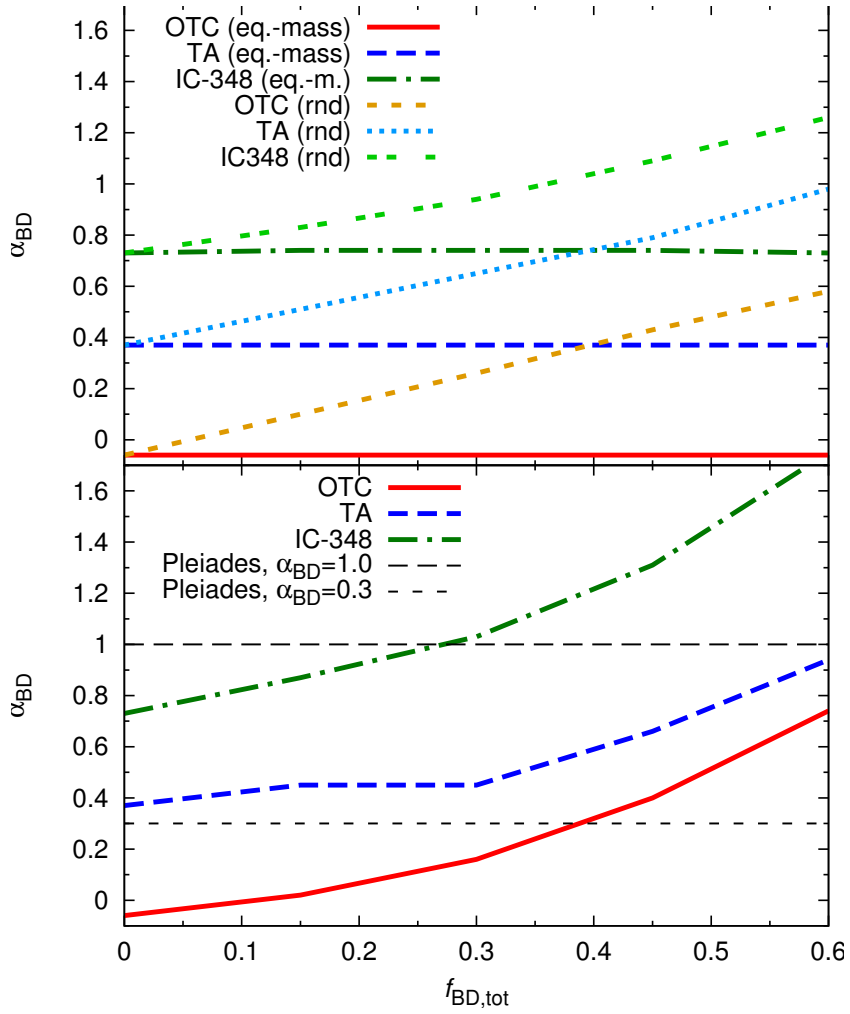

Figure 2.3: **Upper panel**: The best-fit BD IMF power-law indices for the ONC (solid line), TA (dashed line), and IC 348 (dash-dotted line) with equal-mass pairing and random pairing of BD binaries (dotted, narrow-dotted and double-dotted curves, respectively), as a function of the assumed BD binary fraction, $f_{\rm BD}$, fitted via the primary-object mass function for both BDs and stars (see text). The upper/lower uncertainty limits of $\alpha_{\rm BD}$ are about $+0.3/-0.3$ for the ONC, $+0.5/-2.8$ for TA and $+2/-0.6$ for IC 348. While $\alpha_{\rm BD}$ remains approximately constant for equal-mass pairing, there is a strong increase with increasing $f_{\rm BD}$ for the random pairing case. **Lower panel:** The BD IMF power-law indices for the case of equal-mass pairing, but this time fitted via the BD system MF (and the stellar primary MF). The upper/lower limits of $\alpha_{\rm BD}$ are about $+0.3/-0.3$ for the ONC, $+0.7/-3.5$ for TA and $+2.5/-0.6$ for IC 348. In contrast to the equal-mass case in the upper panel, $\alpha_{\rm BD}$ is now increasing with $f_{\rm BD}$. For comparison, the fixed $\alpha_{\rm BD} = 0.3$ (short-dashed horizontal line) and $\alpha_{\rm BD} = 1.0$ (long-dashed horizontal line) for the Pleiades have been added.

selected by chance from the IMF. The discontinuity (eq. 2.6) between the BD-like and the star-like IMF becomes slightly smaller for higher binary fractions while the BD-like IMF slope remains almost constant. The discontinuity between both populations is, however, still present.

The top panel of Fig. 2.3 shows the dependency of $\alpha_{\rm BD}$ on $f_{\rm BD}$ for the ONC, TA and IC 348 (the clusters for which $\alpha_{\rm BD}$ has actually been calculated from χ^2 minimisation) for both equal-mass pairing and random pairing. The IMFs have been fitted via the $\mathrm{IMF}_{\rm pri}$. It should be noted that $\alpha_{\rm BD} \geq 1$ for $f_{\rm BD} \gtrsim 0.4$ for random-pairing in IC 348, i.e. the turnover of the (bi-logarithmic) IMF in the substellar region vanishes, although the discontinuity remains (see Section 2.4.2). Similarly, the lower panel shows the trends with $f_{\rm BD}$ in the case of equal-mass pairing if the BD-like $\mathrm{IMF}_{\rm sys}$ is used for fitting.

The most remarkable feature is that $\alpha_{\rm BD}$ remains almost constant for equal-mass pairing in BD-like binaries. For random-pairing $\alpha_{\rm BD}$ increases with $f_{\rm BD}$ in a similar way for all three clusters. A similar growth is found even for equal-mass pairing if $\mathrm{IMF}_{\rm sys}$ is used for fitting. For comparison, the constant values assumed for the Pleiades are shown in the lower panel of Fig. 2.3 (straight dashed lines at $\alpha_{\rm BD} = 0.3$ and $\alpha_{\rm BD} = 1.0$).

The fitting of $m_{\rm max,BD}$ yields values slightly below 0.07 $M_\odot$ for the ONC and the Pleiades. This is probably due to the Gaussian smearing of $\log m$ that has been used for smoothing the fit. For TA and IC 348, however, $m_{\rm max,BD}$ is found to be around 0.1 $M_\odot$ and between 0.15 and 0.23 $M_\odot$, respectively. Furthermore, our results for the best-fit $\mathcal{R}_{\rm pop}$, the population ratio, and the magnitude of the discontinuity can be summarised as follows: For $f_{\rm BD} = 0$ the best-fit $\mathcal{R}_{\rm pop}$ is about 0.07 for the ONC and the Pleiades while it is about 0.15 for TA and IC 348. It increases for larger $f_{\rm BD}$, reaching about twice these values for the extreme binarity of $f_{\rm BD} = 0.6$. That is, if a realistic value of $f_{\rm BD} \approx 0.2$ is assumed, we expect about 1 BD-like body per 10 star-like ones for the ONC and the Pleiades, and about 1 BD-like body per 5 star-like bodies for the others. This result is remarkable given that e.g. Slesnick et al. (2004) state a *higher* BD-to-star ratio for the ONC than for TA and IC 348. The result can be interpreted as a consequence of the large mass overlap of the BD-like and the star-like regime in IC 348 (and a moderate overlap in TA), i.e. that many BD-like bodies are in actually very-low mass stars and thus are counted as normal stars. Another issue is whether the substellar peak in the ONC MF (see the thin dashed histogram in Fig. 2.2) is an artefact (Lada & Lada 2003) or a real feature. In the latter case, $\mathcal{R}_{\rm pop}$ would be significantly higher (about 75 %, given the histogram data) for the ONC than suggested by our results.

One may criticise the way of assigning a mass to an observed system. In TK07 the model-observed IMF has been created by simply adding the masses of all components, i.e. $\mathrm{IMF}_{\rm obs} = \mathrm{IMF}_{\rm sys}$. Because the observed data are being derived from luminosity functions rather than from mass functions, the correct way would be to convert luminosities into masses via the mass-luminosity relation (MLR). This would require rather complicated calculations because full-scale modelling would involve age-spreads and age-dependent MLRs with very significant uncertainties (Wuchterl & Tscharnuter 2003).

Instead, a simpler way to at least embrace the real relation is to repeat the analysis (or parts of it) by using the primary mass instead of the system mass. This corresponds to the extreme case that the contribution of less-massive companions is negligible. This

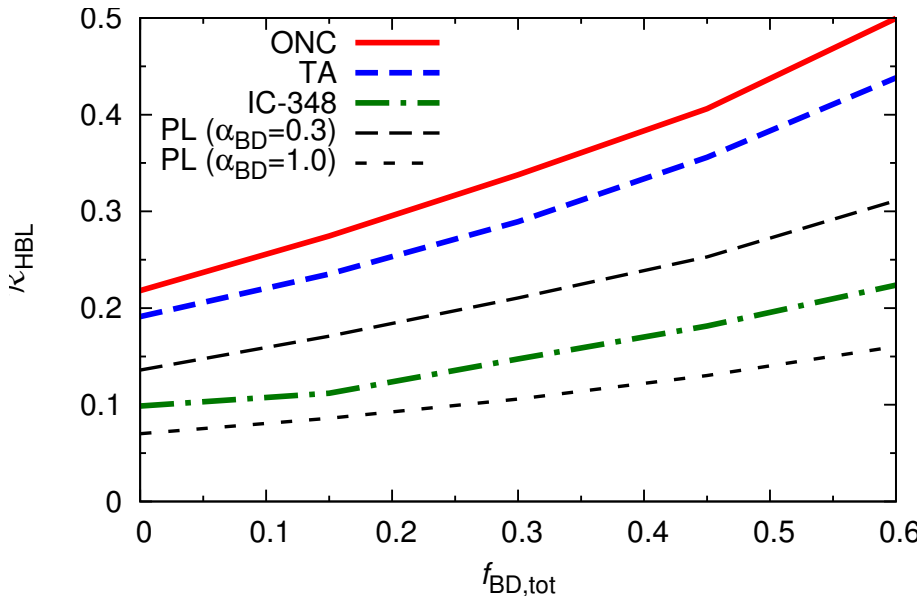

Figure 2.4: The ratio of BD-like to star-like bodies at the hydrogen-burning mass limit (HBL) as a function of the BD-like binarity, $f_{\rm BD}$, for the ONC (solid curve), TA (dashed curve), IC 348 (dash-dotted curve), as well as for the Pleiades for $\alpha_{\rm BD} = 0.3$ (thin dashed curve) and $\alpha_{\rm BD} = 1.0$ (thin dotted curve). For all clusters there is a similar trend towards a higher $\mathcal{R}_{\rm HBL}$ with increasing binary fraction. But even for the highest plausible binary fraction $\mathcal{R}_{\rm HBL} < 0.5$. A continuous IMF would require $\mathcal{R}_{\rm HBL} \equiv 1$.

method has been used in the present contribution with similar results as in TK07. In addition, similar calculations have been made for a substellar system IMF and for a stellar primary IMF, for equal-mass pairing of BDs, and for random pairing of stars.

2.4.2 The discontinuity in the low-mass IMF

A measure for the discontinuity at the HBL, $\mathcal{R}_{\rm HBL}$, is given by eq. 2.6. For a continuous IMF $\mathcal{R}_{\rm HBL} \equiv 1$, while values significantly different from 1 indicate a discontinuity. Fig. 2.4 displays $\mathcal{R}_{\rm HBL}$ as a function of $f_{\rm BD}$. For all clusters $\mathcal{R}_{\rm HBL}$ shows a similar steady increase. The uncertainties (not shown in the graph) can be estimated from those of $\alpha_{\rm BD}$ and are about $\pm 40\,\%$ for each value. Thus the discontinuity between the BD-like and the star-like IMF persists for both the system and the primary-body IMF for the BD-like population. It is largest (i.e. $\mathcal{R}_{\rm HBL}$ is smallest) for $f_{\rm BD} = 0$. The results from TK07 show that this even holds true if the system IMF fit is applied to the stellar population.

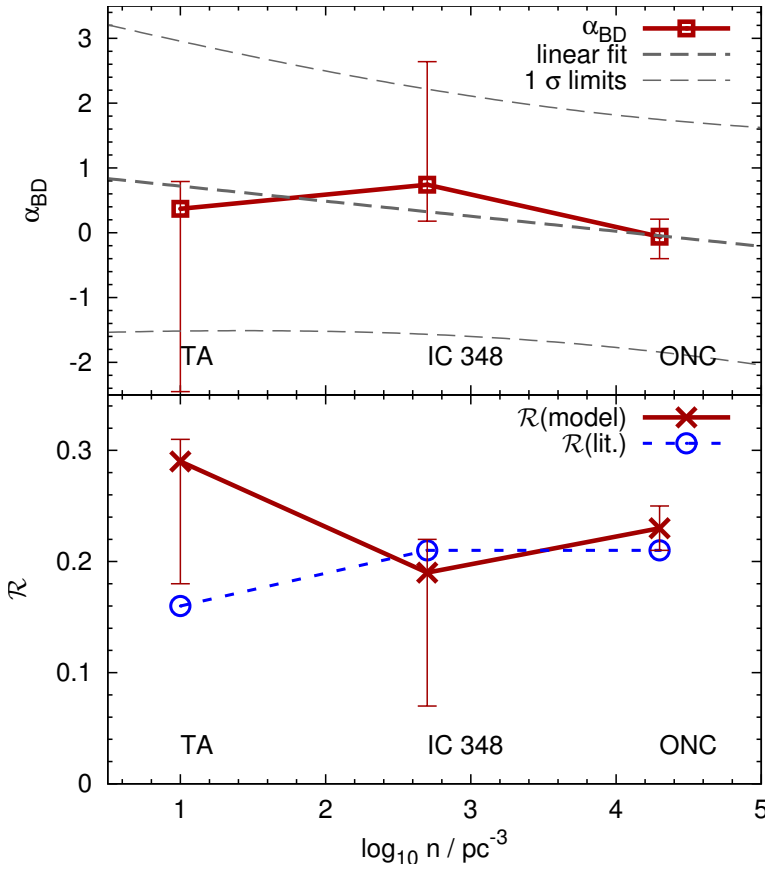

Figure 2.5: The power-law index $\alpha_{\rm BD}$ and the BD-to-star ratio $\mathcal{R}$ from our model (assuming equal-mass pairing for BDs) and from the literature are plotted in dependence of the logarithmic central stellar density of TA, IC 348 and the ONC. The references for $\mathcal{R}$ are Luhman (2006) for TA, Preibisch et al. (2003) for IC 348, and Slesnick et al. (2004) for the ONC.

2.4.3 IMF slope and BD-to-star ratio in relation to the stellar density

Certain theories of BD formation (e.g. Bonnell et al. 2008) suggest a dependency of the rate of BD formation on the star-cluster density. Correlating the BD IMF index, $\alpha_{\rm BD}$, and the BD-to-star ratio, $\mathcal{R}$, against the stellar density, n, may uncover such expected dependencies. For TA, $n = 1 - 10$ stars per pc^3 (Martín et al. 2001), $n \approx 500\,\mathrm{pc}^{-3}$ for IC 348 (Duchêne et al. 1999), and $n \approx 20000\,\mathrm{pc}^{-3}$ for the ONC (Hillenbrand & Hartmann 1998). The values of $\alpha_{\rm BD}$ found in this study are plotted against $\log_{10} n$ in Fig. 2.5 (upper panel). In addition, the BD-to-star ratio, $\mathcal{R}$, is shown in the lower panel, where

$$\mathcal{R} = \frac{N(0.02\,M_\odot \leq m \leq 0.075\,M_\odot)}{N(0.15\,M_\odot \leq m \leq 1 M_\odot)}\,. \tag{2.7}$$

The mass limits are chosen in accordance with Kroupa et al. (2003) and Thies & Kroupa (2007). The crosses connected with solid lines show the results of our modelling while the open circles with dashed lines are values taken from Luhman (2006) (TA), Preibisch et al. (2003) (IC 348), and Slesnick et al. (2004) (ONC).

For $\alpha_{\rm BD}$ a regression line has been calculated. However, only three clusters have been analysed in this study, and there are large uncertainties. Especially for TA and IC 348 the confidence range is rather large here. Thus, the linear fit is only poorly constrained and well in agreement with a constant $\alpha_{\rm BD}$. Furthermore, $\mathcal{R}$ also does not show a significant trend with increasing stellar density. From our analysis (Fig. 2.5) it follows that $\alpha_{\rm BD} \approx 0.3$ and $\mathcal{R} \approx 0.2$ for equal-mass pairing of BDs.

2.5 Summary

A discontinuity in the IMF near the hydrogen burning mass limit appears if the binary properties of BDs and VLMSs on the one hand, and of stars on the other, are taken into account carefully when inferring the true underlying single-object IMF. This implies that BDs and some VLMSs need to be viewed as arising from a somewhat different formation channel than the stellar formation channel, but this result has been obtained by TK07 under the assumption that BDs have a binary fraction of only 15 %. A higher binary fraction may close the gap between the stellar and the BD IMF. We refer to BDs and those VLMSs formed according to the putative BD channel as "BD-like" bodies, whereas stars and those BDs formed according to the stellar channel as star-like. The BD-like channel remains unknown in detail, but theoretical ideas have emerged (Sections 2.1, 2.2.2, and 2.4.3).

Here we have extended the analysis of TK07 for BD-like binary fractions up to 60 % for the Orion Nebula Cluster, the Taurus-Auriga association, IC 348 and the Pleiades by using slight modifications of the techniques introduced in TK07.

As a main result, we found that the discontinuity that comes about by treating BDs/VLMSs and stars consistently in terms of their observed multiplicity properties remains even for the highest BD binary fraction. These results suggest that the BD binary fraction, $f_{\rm BD}$, is not the dominant origin of the discontinuity in the IMF, and that, consequently, two separate IMFs need to be introduced.

It is re-emphasised that by seeking to mathematically describe the BD and stellar population in terms of the relevant mass- and binary distribution functions, it is unavoidable to mathematically separate BDs and VLMSs from stars. The two resulting mass distributions do not join at the transition mass near 0.08 $M_\odot$. The physical interpretation of this logically stringent result is that BDs and VLMSs follow a different formation history or channel than stars. This result is obtained independently by theoretical consideration of star-formation processes (Reipurth & Clarke 2001; Goodwin & Whitworth 2007; Stamatellos et al. 2007; Bonnell et al. 2008).

With this contribution we have quantified how the power-law index of the BD-like IMF and the BD-to-star ratio changes with varying binary fraction of BD-like bodies. The BD-like power-law index, $\alpha_{\rm BD} \approx 0.3$, remains almost constant if equal-mass pairing

of BD-like binaries is assumed, while $\alpha_{\rm BD}$ increases somewhat with increasing $f_{\rm BD}$ in the case of random pairing over the BD-like mass range. All values of $\alpha_{\rm BD}$ are between -0.1 and $+1.3$. We also find that although the stellar density differs from a few stars per pc^3 (TA) to about 20000 stars per pc^3, the resulting $\alpha_{\rm BD}$ is constant within the uncertainties. Similarly, the BD-to-star ratio does not show a trend with increasing stellar density. This suggests the star-formation and BD-formation outcome to be rather universal at least within the range of densities probed here.

3 Tidally induced brown dwarf and planet formation in circumstellar discs

(based on Thies et al., 2010 ApJ, 717, pp. 577-585. *Tidally Induced Brown Dwarf and Planet Formation in Circumstellar Disks*)

Most stars are born in clusters and the resulting gravitational interactions between cluster members may significantly affect the evolution of circumstellar discs and therefore the formation of planets and brown dwarfs. Recent findings suggest that tidal perturbations of typical circumstellar discs due to close encounters may inhibit rather than trigger disc fragmentation and so would seem to rule out planet formation by external tidal stimuli. However, the disc models in these calculations were restricted to disc radii of 40 AU and disc masses below 0.1 $M_\odot$. Here we show that even modest encounters can trigger fragmentation around 100 AU in the sorts of massive ($\sim 0.5\,M_\odot$), extended ($\geq 100\,\mathrm{AU}$) discs that are observed around young stars. Tidal perturbation alone can do this, no disc-disc collision is required. We also show that very-low-mass binary systems can form through the interaction of objects in the disc. In our computations, otherwise non-fragmenting massive discs, once perturbed, fragment into several objects between about 0.01 and 0.1 $M_\odot$, i.e., over the whole brown dwarf mass range. Typically these orbit on highly eccentric orbits or are even ejected. While probably not suitable for the formation of Jupiter- or Neptune-type planets, our scenario provides a possible formation mechanism for brown dwarfs and very massive planets which, interestingly, leads to a mass distribution consistent with the canonical substellar IMF. As a minor outcome, a possible explanation for the origin of misaligned extrasolar planetary systems is discussed. binaries: general — open clusters and associations: general — stars: formation — stars: low-mass, brown dwarfs — planetary systems: protoplanetary disks —

3.1 Introduction

The origin of brown dwarfs (BDs, to which we also include very low-mass stars $< 0.1 M_\odot$) as well as the formation of massive exoplanets is contentious. The most common idea is that BDs form like stars, and planets form by accretion onto a core formed from dust conglomeration within a circumstellar disc. However, there is increasing evidence that an alternative formation scenario for BDs and, possibly, some of the most massive exoplanets is required. BDs differ from low-mass stars in several ways. Firstly, there is

the 'brown dwarf desert' – a lack of BD companions to stars, especially at separations below about 30 AU within which companion planets and stars are common. In addition, the properties of BD-BD binaries are very different from star-star binaries, showing a significant lack of systems wider than ≈ 20 AU beyond which most stellar binaries are found. Furthermore, while typically every second star is a binary system only every fifth BD is a binary. Clearly we must ask ourselves why stars and BDs are so different if they form by the same mechanism. Indeed, in order to numerically set-up a realistic stellar and BD population, stars and BDs need to be according to different algorithmic pairing rules Kroupa et al. (2003). In other words, they follow different formation channels.

The fragmentation of extended circumstellar discs is one of the most promising alternatives to the standard scenario of star-like formation for BDs (Goodwin & Whitworth 2007). Research on circumstellar disc evolution has made great progress in recent years, but there are still many unanswered questions (Papaloizou & Terquem 2006; Henning 2008; Hillenbrand 2008). One issue that has gained surprisingly little attention in the past is the role of gravitational interactions between the disc and passing stars within the young host stellar cluster. Since stars are generally born in clusters (Forgan & Rice 2009), rather than as isolated objects, star-disc and disc-disc interactions (Boffin et al. 1998; Watkins et al. 1998a; Pfalzner et al. 2005; Thies et al. 2005) probably play an important role for the dynamical evolution of such discs and thus for massive planet and BD formation through fragmentation of the discs.

For a typical open star cluster hosting about 1000 stars within a half-mass radius of 0.5 pc, encounters closer than 500 AU will happen approximately every 10 Myr (Thies et al. 2005). They are even more frequent in denser clusters in which are thought to form at least half of the stars in the Galaxy. Encounters in star clusters are therefore expected to play a significant role in the evolution of extended discs of several 100 AU radii.

The formation of planets through core accretion is typically expected to happen within the innermost 100 AU of a circumstellar disc (Hillenbrand 2008), although there are many unanswered questions especially concerning the very first stages of core accretion (Henning 2008). Fragmentation has been proposed as an alternative way to form the most massive gas giant planets by Mayer et al. (2002); Boss (1997, 2004, 2006). In recent years, however, there has been a growing consensus that disc fragmentation cannot produce gas giant planets in the inner regions of discs for two reasons: (1) heating from the central star stabilises the innermost regions and thus inhibits fragmentation, and (2) these regions cannot cool fast enough to allow temporary gas clumps to collapse (Lodato et al. 2007; Stamatellos & Whitworth 2008; Cai et al. 2010). This picture changes greatly beyond about 100 AU where cooling becomes sufficiently efficient for gravitational collapse to occur. Consequently, disc fragmentation has been proposed as an alternative mechanism for the formation of BDs (Whitworth & Stamatellos 2006; Goodwin & Whitworth 2007). Most of these investigations, however, assume that the disc evolves in isolation.

Star-disc and disc-disc collisions have been investigated in previous studies (Boffin et al. 1998; Watkins et al. 1998a,b) but without a realistic treatment of the radiative heat transfer in the disc. From SPH computations Forgan & Rice (2009) deduce that close

encounters inhibit fragmentation in typical protoplanetary discs (assuming an initial radius of 40 AU) rather than inducing it. In contrast to that, a recent study of disc-disc collisions (Shen et al. 2010) has, however, shown that the direct compression of gas by the close encounters of stars hosting massive extended discs (disc mass $\approx 0.5\ M_\odot$, disc radius ≈ 1000 AU), may trigger the formation of substellar companions. However such massive, extended discs are probably short-lived (Eisner & Carpenter 2006) (in contrast to typical protoplanetary discs which are about ten times smaller and less massive), so that pairwise interactions of two discs of this kind are expected to be rare. The purely gravitational interaction of a low-mass star with no (or only a small) protoplanetary disc with a star hosting a massive disc would be much more likely. Although even these encounters may probably account for only a fraction of all BDs, especially in loose associations like Taurus-Auriga, they provide an additional channel of forming BDs out of discs that would otherwise probably dissolve without ever fragmenting. In this paper we address this issue. In Section 3.2, besides an estimate of the encounter probability, the model of the circumstellar disc is described. Section 3.3 depicts the computational methods and gives an overview of the model parameters studied in this work. The results are then presented in Section 3.4 and discussed in Section 3.5

3.2 Model basics

3.2.1 Encounter probability

The likelihood of a close stellar encounter with an impact parameter b depends on the stellar density of the star-forming environment and the impact parameter itself. The encounter event is then further characterised by the relative velocity of the two stars and thus the eccentricity of the path. The consequences on the circumstellar disc further depend on the mass of the perturber and the host star (i.e., the ratio of binding energy and magnitude of the perturbation) and the inclination of the disc plane wrt. the plane of the encounter hyperbola.

Stars can be born in a variety of environments from low-density groups like Taurus-Auriga (about 300 stars distributed in groups, each being ¡1 pc in radius and containing about a few dozen stars) up to ONC-type clusters (thousands of stars within 0.5 pc) or even in more massive and dense clusters (Kroupa 2005). An estimate of the encounter probability has been derived assuming a Plummer star cluster model of half-mass radius, $r_{1/2}$, total mass $M_{\rm tot}$, and an average stellar mass, $M_\star$. Note that two other radial scales are also often used to describe a Plummer model: the Plummer radius, $r_{\rm Pl} = \sqrt{2^{2/3}-1}r_{1/2} \approx 0.766 r_{1/2}$, and the gravitational scale radius, $r_{\rm grav} \approx 2.602 r_{1/2} \approx 3.395 r_{\rm Pl}$. From Thies et al. (2005), Section 1.3, the expected time, $t_{\rm enc}$, between two encounters within an encounter parameter, b, can be obtained from the characteristic crossing time $t_{\rm cr}$,

$$\frac{t_{\rm cr}}{\rm Myr} = 83 \left(\frac{M_{\rm tot}}{M_\odot}\right)^{-1/2} \left(\frac{r_{1/2}}{\rm pc}\right)^{3/2}\ , \tag{3.1}$$

and the average number, $n_{\rm enc}$, of encounter parameters below b, for a given number of stars, N,

$$n_{\rm enc}(<b) = N\frac{b^2}{{r_{\rm grav}}^2}\,. \tag{3.2}$$

$t_{\rm enc}$ is approximately given by

$$\frac{t_{\rm enc}}{\rm Myr} = \frac{2.4\cdot10^{13}}{N}\left(\frac{M_{\rm tot}}{M_\odot}\right)^{-1/2}\left(\frac{r_{1/2}}{\rm pc}\right)^{7/2}\left(\frac{b}{\rm AU}\right)^{-2}\,. \tag{3.3}$$

It has to be noted that the actual periastron distance, $R_{\rm peri}$, is always (and sometimes significantly) smaller than b due to gravitational focusing. The relation between $R_{\rm peri}$ and b for a given eccentricity, e, is

$$R_{\rm peri} = \sqrt{\frac{e-1}{e+1}}\,b\,. \tag{3.4}$$

For an ONC-type cluster with $N = 7500$, an average star mass $M_\star = 0.5\,M_\odot$, a total mass $M_{\rm tot} = 10000\,M_\odot$ (i.e., 30 % of the mass consists of stars and the rest of gas, see Kroupa et al. 2001), and a half-mass radius of $r_{1/2} = 0.5\,{\rm pc}$ we find that encounters below 500 AU occur on average every 11 million years. If a massive extended disc exists for about 1 Myr this means that about 9 per cent of all discs of this type will suffer such an encounter. See also Thies et al. (2005).

3.2.2 Disc model

The initial conditions for the disc are taken from Stamatellos & Whitworth (2008, 2009a). The disc model has a power law profile for temperature, T, and surface density, Σ from Stamatellos & Whitworth (2008), both as a function of the distance, R, from the central star,

$$\Sigma(R) = \Sigma_0\left(\frac{R}{\rm AU}\right)^{-q_\Sigma}\,, \tag{3.5}$$

$$T(R) = \left[T_0^2\left(\frac{R}{\rm AU}\right)^{-2q_T} + T_\infty^2\right]^{1/2}\,, \tag{3.6}$$

where $q_\Sigma = 1.75$, $q_T = 0.5$, and $T_0 = 300\,{\rm K}$. Σ_0 is chosen corresponding to a disc mass of 0.48 and 0.50 $M_\odot$ (see Table 3.3.3), i.e., $\Sigma_0 = 8.67\cdot10^4\ {\rm g\,cm^{-2}}$ and $\Sigma_0 = 9.03\cdot10^4\ {\rm g\,cm^{-2}}$, respectively. $T_\infty = 10$ K is a background temperature to account for the background radiation from other stars within the host cluster. This configuration leads to an initial Toomre stability parameter, Q, (Toomre 1964) between 1.3 and 1.4 between about 100 and 400 AU, leading to weak spiral density patterns but not to fragmentation. Q is given by

$$Q = \frac{c_{\rm s}\kappa}{\pi G\Sigma} \tag{3.7}$$

with $c_{\rm s}$ being the sound speed, and κ being the epicyclic frequency which can be, at least roughly, approximated by the Keplerian orbital frequency. The radiation of the

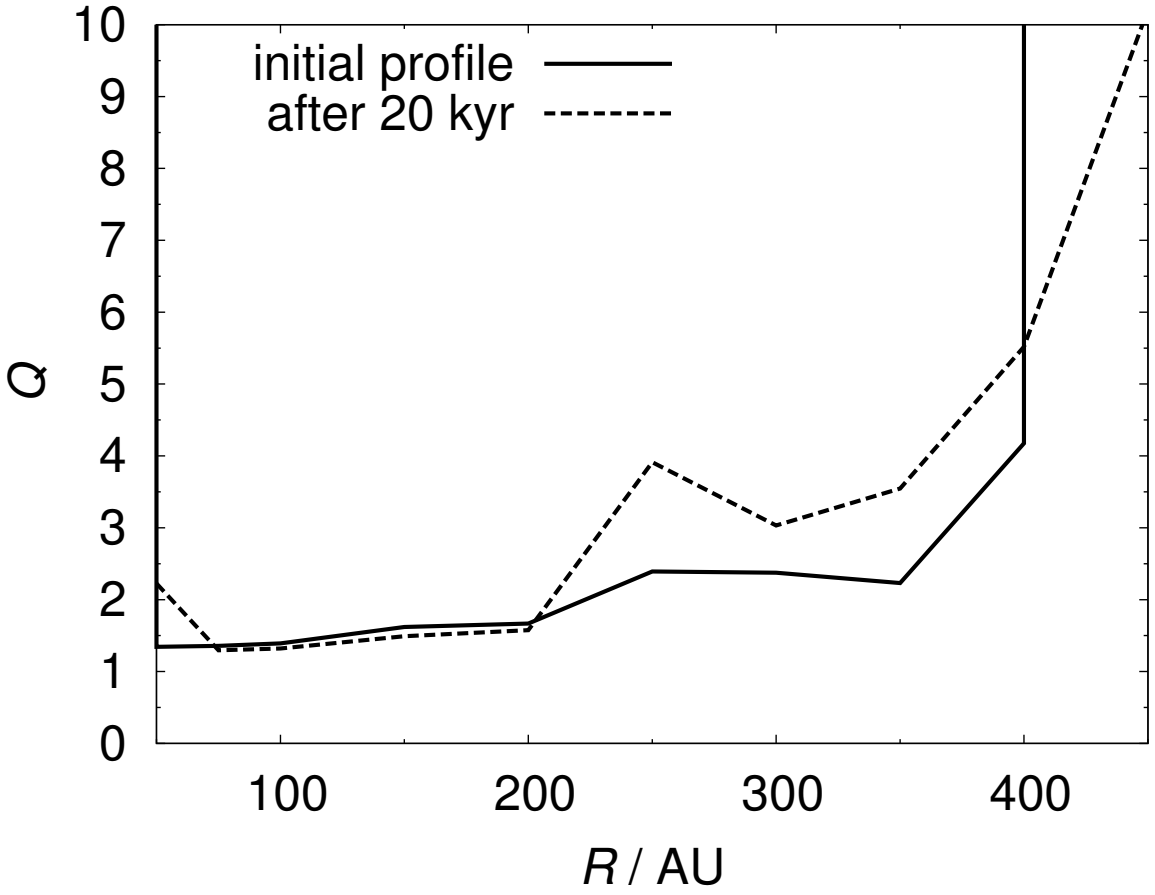

Figure 3.1: The Toomre parameter Q as a function of the radius from the central star for both the initial disc setup (solid line) and the settled disc after 20 kyr (dashed line). The profiles of both disc stages are nearly identical below about 200 AU while Q is slightly larger (i.e. the disc is more stable) between 200 AU and 400 AU, the outer rim of the initial disc. The region within 50 AU is skipped since it is initially partially void.

perturber is included in the same way as that of the central star, assuming a mass-to-luminosity relation of $L \propto M^4$ for low-mass stars. However, as long as the perturber is no more than about 0.5 $M_\odot$, corresponding to an early M-type or late K-type main sequence star, its influence on disc evolution is very small.

The disc is initially populated by SPH particles between 40 and 400 AU. Before starting the actual encounter computation the disc is allowed to "settle" for about 20 000 years (i.e., about two orbits at the outer rim) to avoid artefacts from the initial distribution function. During this settling the disc smears out at the inner and the outer border extending its radial range from a few AU up to $\gtrsim 500$ AU, eventually stabilising. The Q value is slightly increased beyond 200 AU relative to the initial setting while remaining largely unchanged below this radius, as can be seen in Figure 3.1. The actual surface density after the settling is therefore slightly smaller and thus the disc slightly more stable than in the initial setup. Any self-fragmentation of the unperturbed disc would have happened during the settling time when the Toomre parameter is lowest.

3.3 Methods

3.3.1 Smoothed particle hydrodynamics (SPH)

All computations were performed by using the well-tested DRAGON SPH code by Goodwin et al. (2004) including the radiative transfer extension by Stamatellos et al. (2007). Most of the numerical parameter settings have been adopted from Stamatellos et al. (2007); Stamatellos & Whitworth (2009a). Gravitationally collapsing clumps are treated by sink particles which form if the volume density exceeds $10^{-9}\,\mathrm{g\,cm^{-3}}$, and the clump is bound. The sink radius is 1 AU, in accordance with the studies mentioned above and in agreement with the local Jeans criterion. In addition, the central star and the perturbing star are both represented by sink particles.

There are ongoing discussions whether fragmentation can be triggered artificially due to the numerical behaviour of SPH and grid-based hydrocodes. Hubber et al. (2006) find that smoothed particle hydrodynamics (SPH) does not suffer from artificial fragmentation. However, Nelson (2006) suggest that SPH may artificially enhance fragmentation due to a pressure-underestimation if the smoothing radius, h, is considerably larger than about 1/4 of a vertical scale height of a circumstellar disc. Stamatellos & Whitworth (2009b) show that this criterion is fulfilled for 150,000 or more particles, for the types of disc studied in this paper.

Commerçon et al. (2008) have performed calculations of fragmenting protostellar clouds with the adaptive mesh refinement (AMR) code RAMSES and the SPH code DRAGON (which we have been using for this study) and compared the results at different resolutions given by the number N of grid cells and particles, respectively. For about $N = 5 \cdot 10^5$ cells/particles fragmentation in both codes appeared nearly equal. With $N = 2 \cdot 10^5$ the results were very similar to the high-resolution AMR computations while being still acceptable for many purposes at $N = 1 \cdot 10^5$. Stamatellos & Whitworth (2009b) briefly review the resolution criteria with respect to their models using 150 000

in that paper and 250 000 to 400 000 particles earlier (Stamatellos & Whitworth 2009a).

The three most important resolution criteria are the resolution of the local Jeans mass, $M_{\rm J}$, (and thus the Jeans length), the local Toomre mass and the vertical scale height of the disc. In particular, the local Jeans mass,

$$M_{\rm J} = \frac{4\pi^{5/2}}{24} \frac{c_{\rm s}^3}{\sqrt{G^3\,\rho}}\,, \tag{3.8}$$

must be resolved by at least a factor of $2 \times N_{\rm neigh} = 100$, corresponding to 0.5 $M_{\rm J}$ for the 100,000 particle discs and 0.2 $M_{\rm J}$ for the 250,000 particle discs. Since the global disc setup as well as the evolution after the perturbation (Section 3.4) is quite similar to that used by (Stamatellos & Whitworth 2009b), as similar range of Jeans masses of the forming clumps, i.e., $\sim$ 2–20 $M_{\rm J}$, can be reasonably assumed for our models and has actually been tested for the models E/X002 and E/X009 for all forming objects. The minimum $M_{\rm J}$ during the clump formation is typically between 4 and 6 $M_{\rm J}$ and does never go below about 2 $M_{\rm J}$. Therefore, $M_{\rm J}$ is resolved by a safe factor of at least 4 in the low-resolution case and 10 in the high-resolution case. Accordingly, the minimum Toomre mass of 2.5 $M_{\rm J}$ is adequately resolved as well as the vertical scale height (by at least a few smoothing lengths).

3.3.2 Radiative transfer model

In Thies et al. (2005) the possibility of fragmentation has been estimated via the Toomre criterion for both isothermal and adiabatic equations of state, both resulting in perturbed regions with highly unstable conditions ($Q < 1$). However, Toomre instability does not necessarily lead to actual fragmentation.

In realistic models of radiative transfer, such as the one used here, the thermal response of the gas to density changes is between near-isothermal in regions with efficient cooling (outside about 100–200 AU) and near-adiabatic in regions with long cooling times (the inner parts of the disc). Shen et al. (2010) have shown that direct disc-disc collisions may lead to fragmentation of massive extended discs at some 400 AU even for a "thick disc approximation", i.e., the near-adiabatic case.

The Stamatellos et al. (2007) method uses the density and the gravitational potential of each SPH particle to estimate an optical depth for each particle through which the particle cools and heats. The method takes into account compressional heating, viscous heating, radiative heating by the background, and radiative cooling. It performs well, in both the optically thin and optically thick regimes, and has been extensively tested by Stamatellos et al. (2007). In particular it reproduces the detailed 3D results of Masunaga & Inutsuka (2000), Boss & Bodenheimer (1979), Boss & Myhill (1992), (Whitehouse & Bate 2006), and also the analytic results of Spiegel (1957). Additionally the code has been tested and performs well in disc configurations as it reproduces the analytic results of Hubeny (1990).

The gas is assumed to be a mixture of hydrogen and helium. We use an equation of stare by Black & Bodenheimer (1975); Masunaga et al. (1998); Boley et al. (2007) that

accounts (1) for the rotational and vibrational degrees of freedom of molecular hydrogen, and (2) for the different chemical states of hydrogen and helium. We assume that ortho- and para-hydrogen are in equilibrium.

For the dust and gas opacity we use the parameterisation by Bell & Lin (1994), $\kappa(\rho, T) = \kappa_0 \ \rho^a \ T^b$, where κ_0, a, b are constants that depend on the species and the physical processes contributing to the opacity at each ρ and T. The opacity changes due to ice mantle melting, the sublimation of dust, molecular and H^- contributions, are all taken into account.

3.3.3 Overview of Calculations

We have conducted thirteen SPH calculations using 100,000 and eight using 250,000 SPH particles (i.e., 21 models in total) corresponding to about nine CPU months in total on 16-core machines. The model identifiers that begin with an "E" or "F" refer to the low resolution models while the models with "X" or "Y" are the high resolution ones. Subsequent letters with identical numbers correspond to follow-up calculations (beginning at the moment of the closest encounter) with identical model settings. Due to the dynamical interaction of the parallel computing CPUs a slight random perturbation is imposed to the subsequent evolution such that the outcome differs within the statistical noise. The high resolution calculations are set up with parameters of preceding lower-resolution models that showed fragmentation. Therefore, the fact that all high resolution computations show fragmentation is due to the parameter selection. The low-resolution calculations are used as a parameter survey while the high resolution ones are follow-ups to selected low-resolution ones. Please note that not all non-fragmenting models are listed here but only those which represent the borders of the parameter space between fragmentation and no fragmentation.

We chose a 0.5 $M_\odot$ perturbing star as a typical member of a star cluster (Kroupa 2001) for the majority of models, but we also performed calculations with perturbers down to 0.3 $M_\odot$. The encounter orbit is slightly inclined ($\iota = 10°$ against the initial disc plane) with varying eccentricities from $e = 1.1$ (near-parabolic) to $e = 2$ (hyperbolic), corresponding to a relative velocity of 0.4–2.7 $\mathrm{km\,s^{-1}}$ at infinity. For these parameters the disc typically fragments to form a few very-low-mass stars and substellar-mass objects. A calculation with $e = 3$ has been performed but yielded no fragmentation. The same holds true for encounters at 600 AU or more. Depending on the eccentricity the calculations start 5000–10000 years before periastron to ensure a sufficiently low initial interaction. The calculations continue for 15 000 years after encounter for the models E/X/Y002 and at least 20 000 for the others. The masses and orbital radii of the objects formed in the calculation are determined at this time. After 15 000 years the accretion process of the objects has largely finished while dynamical evolution may still lead to major changes of the orbital parameters (and even to ejections of some bodies) if the calculations would have been continued over a longer time interval. For this reason, the orbital separations computed in this study have to be taken as a preliminary state.

It has to be noted that the orbit is altered slightly during the passage due to the transfer of mass and angular momentum. Furthermore, since the encounter dissipates

Calculations Summary

Model	$N/1000$	$M_\star$ ($M_\odot$)	M_d ($M_\odot$)	M_{pert} ($M_\odot$)	R_peri (AU)	e	ι (deg)	m_env (M_J)	N_form	N_ej	Binaries?
E002	100	1.00	0.50	0.50	500	1.1	10	11.7	4	1	—
X002	250	1.00	0.50	0.50	500	1.1	10	12.0	5	2	1 (≈ 4 AU)
Y002	250	1.00	0.50	0.50	500	1.1	10	10.2	3	—	—
E003	100	0.75	0.48	0.50	500	1.1	10	16.1	3	2	1 (≈ 2 AU)
X003	250	0.75	0.48	0.50	500	1.1	10	12.6	4	1	—
E004	100	0.75	0.48	0.50	500	1.5	10	5.6	2	—	—
X004	100	0.75	0.48	0.50	500	1.5	10	11.0	3	—	—
E006	100	0.75	0.48	0.50	500	2.0	10	4.8	2	—	—
X006	250	0.75	0.48	0.50	500	2.0	10	4.4	3	—	1 (≈ 4 AU)
E007	100	0.75	0.48	0.50	500	3.0	10	2.1	0	—	—
E008	100	0.75	0.48	0.50	600	1.5	10	2.8	0	—	—
F008	100	0.75	0.48	0.50	600	1.1	10	6.5	0	—	—
E009	100	0.75	0.48	0.50	500	1.5	30	3.0	3	—	—
X009	250	0.75	0.48	0.50	500	1.5	30	7.6	4	—	1
E010	100	0.75	0.48	0.50	550	1.5	10	4.1	3	—	—
X010	250	0.75	0.48	0.50	550	1.5	10	8.8	4	—	—
E011	100	0.75	0.48	0.50	500	1.5	45	7.6	6	—	—
F011	100	0.75	0.48	0.50	500	1.5	45	4.2	2	—	—
X011	250	0.75	0.48	0.50	500	1.5	45	6.1	2	—	—
E015	100	0.75	0.48	0.40	400	1.5	45	7.9	3	—	—
E016	100	0.75	0.48	0.30	400	1.5	30	10.4	2	—	—
Total $N = 100\,000$ (10 of 13 models showing fragmentation):									30	3	1
Total $N = 250\,000$ (8 of 8 modes showing fragmentation):									28	3	3
Grand total (18 of 21 models showing fragmentation):									58	6	4

Table 3.1: Overview of our SPH computations. The columns (from left to right) show the computation ID, the number of gas particles in thousands, the mass of the central star, its disc and the perturber star. Then follows the periastron distance of the encounter, the eccentricity and inclination. The four rightmost columns show the amount of gas captured by the perturber in a circumstellar envelope within a radius 40 AU, m_env, the number of formed companions in total, N_form, and the number of bodies that got ejected during the calculation, N_ej, as well as the number of binary systems. In all models except for E015 and E016 the perturbing star has 0.5 $M_\odot$ and passes the central star on an initially hyperbolic orbit with initial eccentricity between 1.1 and 3.0 and inclination to the disc plane between 10° and 45°.

energy the post-encounter speed is typically lower than the pre-encounter speed and in some cases both stars may be captured in an eccentric binary (which actually happened to the companions 1a and 1b in calculation E003; see Table 3.3.3 and Figures 3.3 and 3.4). We found, however, that these effects are small.

3.4 Results

Outcome of Individual Calculations

100 000 particles			250 000 particles		
Model ID E002	m ($M_\odot$)	Separation (AU)	Model ID X002	m ($M_\odot$)	Sep. (AU)
1	0.021	332–342	1	0.013	ejected
2	0.080	ejected	2	0.046	ejected
3	0.100	20–30	3	0.057	155–225
4	0.131	50–100	4a	0.088	70–110
			4b	0.099	70–110
E003			X003		
1a	0.013	130–500	1	0.021	50–100
1b	0.086	130–500	2	0.022	200
2	0.130	29–42	3	0.055	ejected
			4	0.154	130–200
E004			X004		
1	0.134	160–190	1	0.026	150–220
2	0.162	60–90	2	0.096	50–170
			3	1.032	25
E006			X006		
1	0.063	35–70	1a	0.033	150
2	0.154	120–220	1b	0.046	150
			2	0.148	60
E009			X009		
1	0.026	16	1	0.049	20
2	0.099	50	2	0.064	230
3	0.133	140	3	0.073	230
			4	0.138	60
E010			X010		
1	0.066	190	1	0.031	190
2	0.117	80	2	0.058	40
2	0.092	80	2	0.106	40
			3	0.128	80
E011			X011		
1	0.031	110	1	0.073	100–180
2	0.038	300	2	0.107	50–80

Model/Object	m ($M_\odot$)	Separation (AU)	Model/Object	m ($M_\odot$)	Sep. (AU)
3	0.038	700			
4	0.048	230			
5	0.074	15–20			
6	0.098	125			
F011			Y002		
1	0.090	150–400	1	0.080	≈ 110
2	0.168	60–100	2	0.108	100–600
			3	0.137	≈ 50
Additional calculations with 100 000 particles					
E015			E016		
1	0.070	ejected	1	0.093	13–30
2	0.103	10–29	2	0.149	55–98
3	0.134	70–101			

Table 3.2: List of the companions formed during individual calculations within 15 000–20 000 years after the flyby, sorted by mass. The table shows the masses and the approximate minimum and maximum separations from the central star. Note that bodies 4a and 4b in X002 got bound in a VLMS binary with a mutual distance of about 4 AU through a triple encounter while 1a and 1b in E003 got bound through dissipational capture. The binary capture of 1a and 1b in X006 probably involved both mechanisms.

3.4.1 General findings

As the unperturbed disc is marginally stable it does not fragment until the passage of the perturbing star. The first visible effects of a typical fly-by are the appearance of tidal arms and a mass transfer to the passing star (which acquires a small disc). About 2000–3000 years after the periastron passage parts of the tidal arms become gravitationally unstable, and spiral-shaped over-densities begin to form (see the snapshots from model X002 in Figure 3.2[1]). Some of these continue to contract into a runaway collapse and form bound objects represented by sinks (see Section 3.3). This typically happens at radii between 100 and 150 AU from the central star with some clumps forming even around 200 AU. Temporary overdensities do also occur within less than 100 AU but, however, dissolve quickly. This is probably due to the heating from the central star and the less effective cooling in these regions as already being mentioned in the Introduction and by Whitworth & Stamatellos (2006); Goodwin & Whitworth (2007). At radii larger than about 200 AU, on the other hand, the gas density is apparently too low for gravitationally bound clumps for form.

[1]Supplementary content like movies from our calculations can be downloaded from the AIfA download page, http://www.astro.uni-bonn.de/~webaiub/german/downloads.php

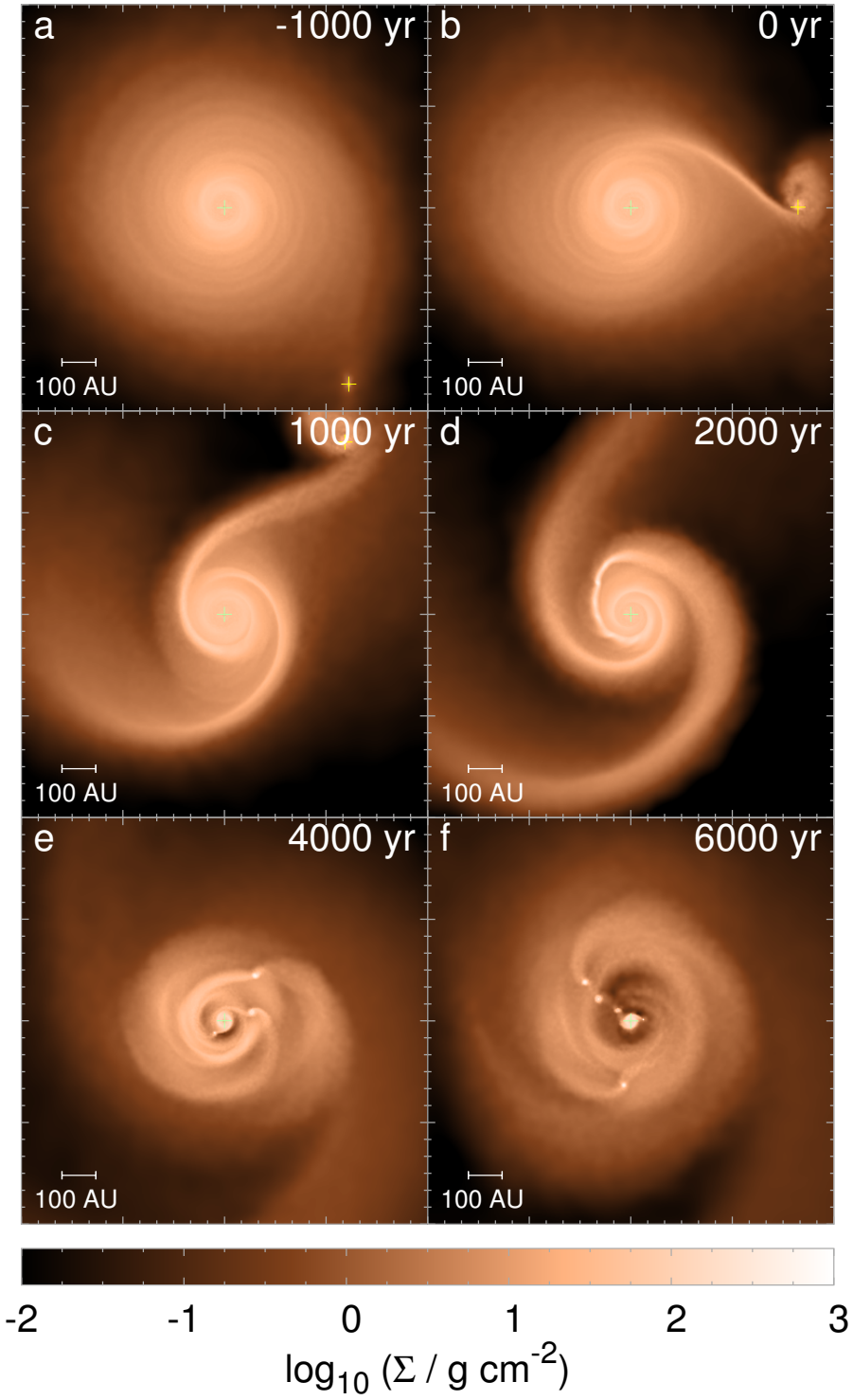

Figure 3.2: Snapshots of a circumstellar disc modelled with 250,000 SPH particles, around a Sun-type star being perturbed by a close star-star encounter (model X002, Table 3.3.3). The time stamp in each frame refers to the time of the encounter.

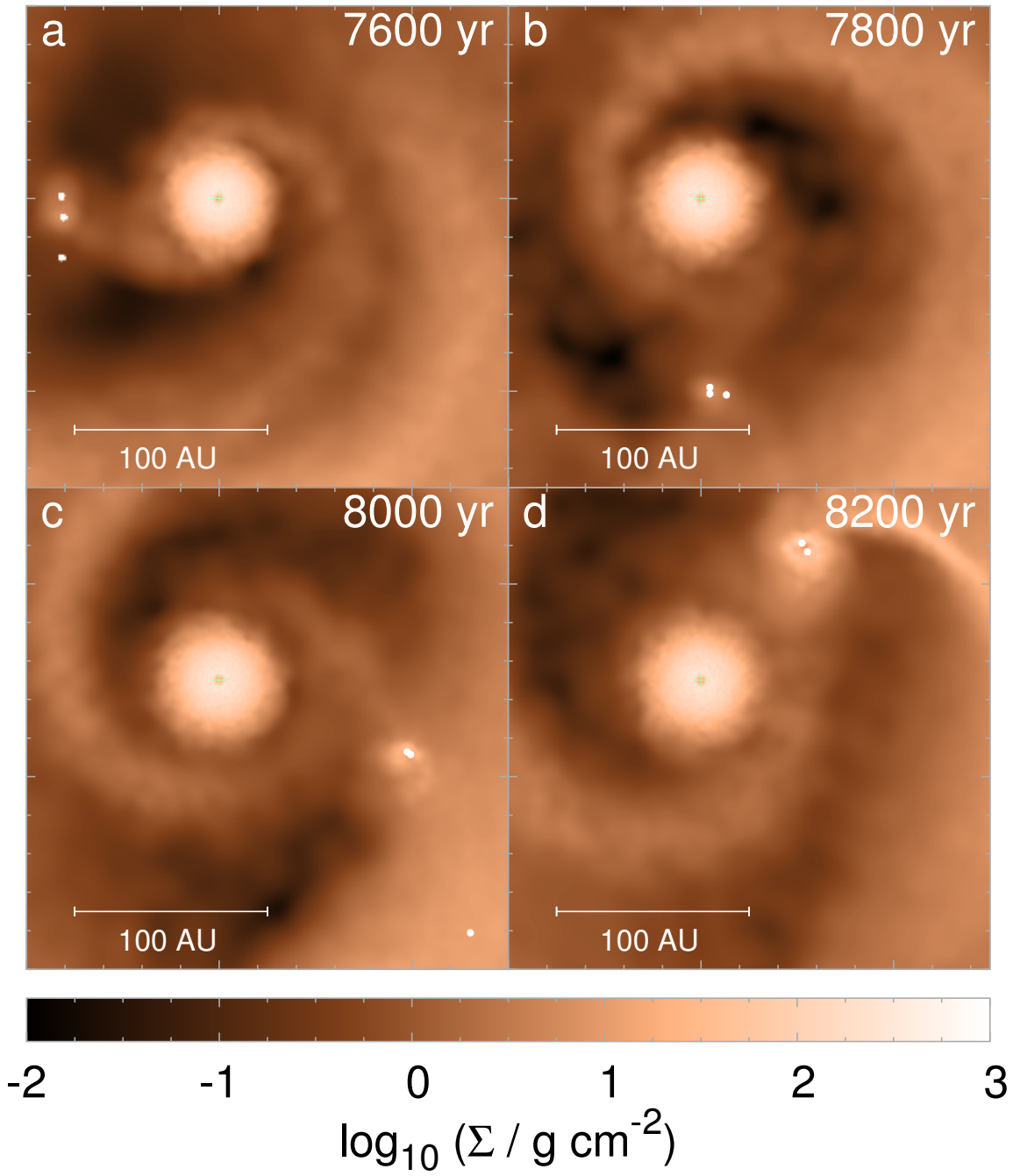

Figure 3.3: Snapshots of a forming binary around about 8000 years after the fly-by in model X002 (see also Figure 3.2). The components of the remaining VLMS pair have masses of 0.08 $M_\odot$ and 0.09 $M_\odot$, subsequently accreting another 0.01 $M_\odot$ each. The escaping third body has 0.05 $M_\odot$ and is eventually ejected.

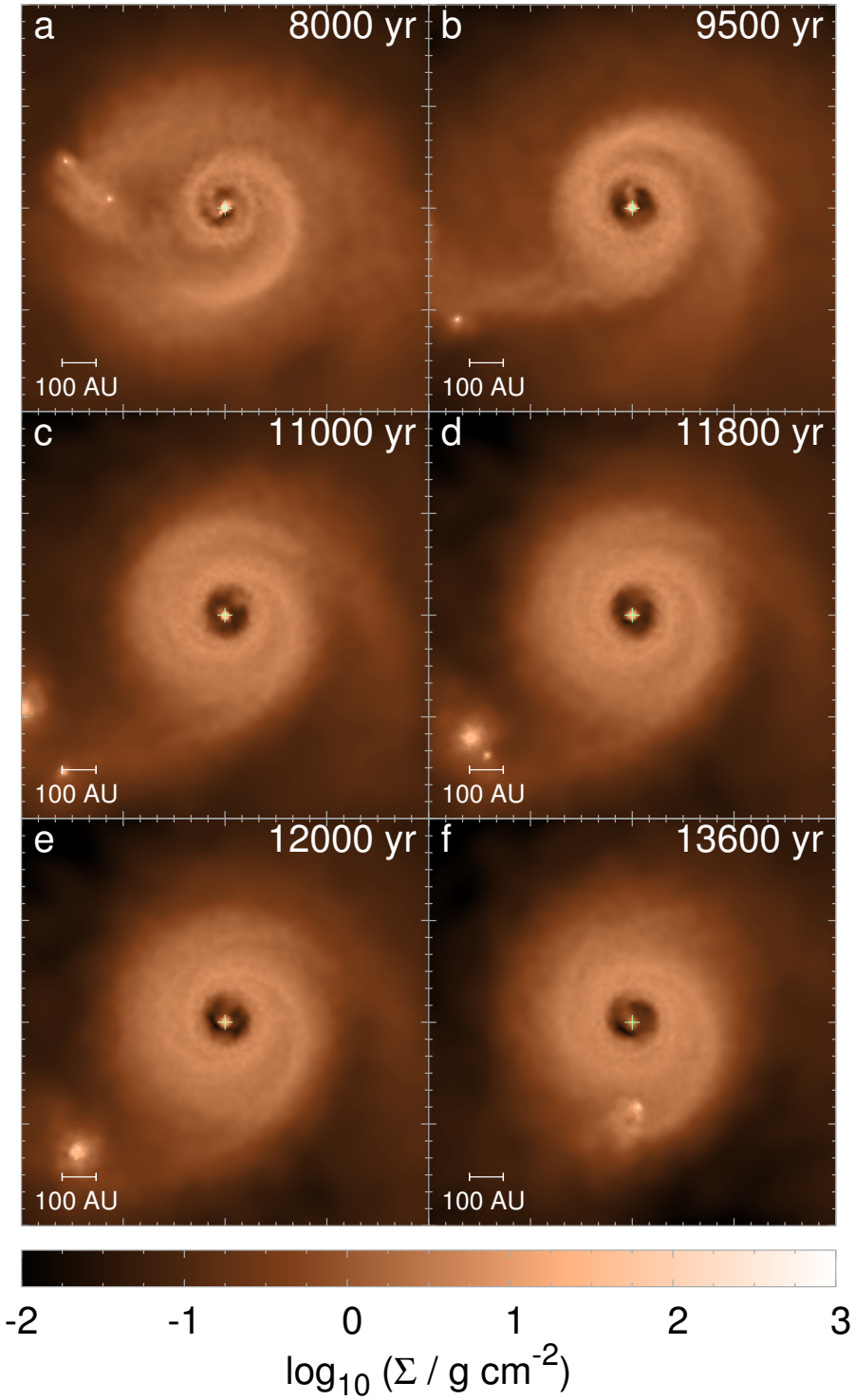

Figure 3.4: Snapshots of another forming binary around about 12000 years after the fly-by. The components of the remaining VLMS-BD pair have very unequal masses of 0.09 $M_\odot$ and 0.013 $M_\odot$ (with a mass ratio $q = 0.14$). In contrast to the binary formed in X002 (Figure 3.2) these bodies became bound due to a frictional encounter of their accretion envelopes.

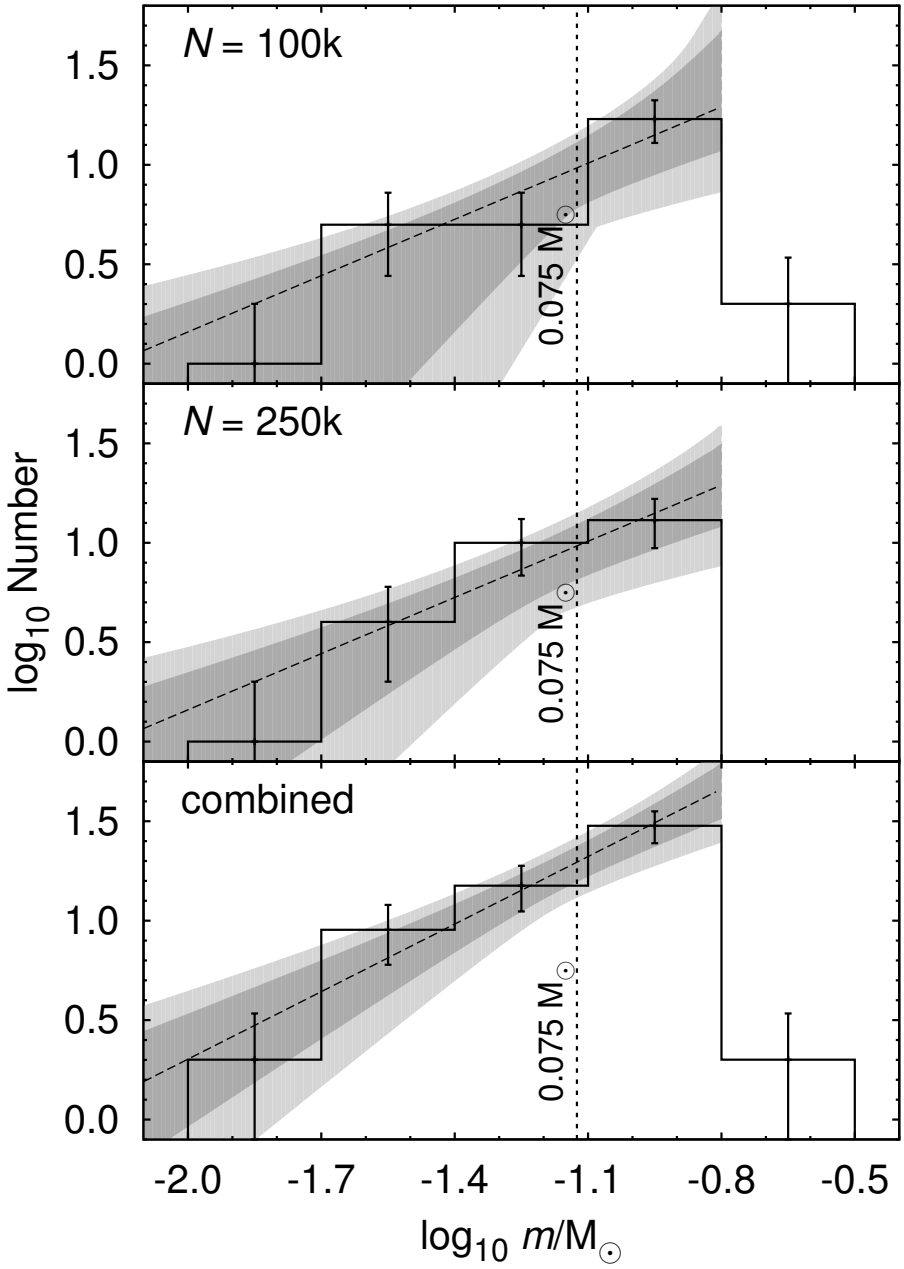

Figure 3.5: Mass distribution of the bodies created in the 100 000 particle models (top frame), the 250 000 particle models (middle frame), and both combined (bottom frame). The majority of companions is found in the mass interval between 0.08 and 0.16 $M_\odot$ while most of the rest is in the substellar regime. The substellar mass function corresponds to a power law index of $\alpha = +0.1^{+0.3}_{-1.5}$ for the 100k models, $\alpha = +0.1^{+0.3}_{-0.6}$ for the 250k models, and $\alpha = -0.1^{+0.3}_{-0.4}$ for both combined (see text for further explanations). The dark and light grey-shaded regions refer to the 1 and 2 σ confidence limits of the fit while the errorbars correspond to the 1 σ Poisson errors. The vertical dotted line marks the hydrogen-burning mass limit of 0.075 $M_\odot$ (Chabrier & Baraffe 2000).

Each of the calculations typically produces between two and five (six on one case) low-mass objects with masses between those of very massive planets (0.01 $M_\odot$) and very low-mass stars (0.13 $M_\odot$). Additionally, mass is accreted onto the central star, and also mass is transfered to the perturber during the encounter. In the model shown in Figure 3.2 five objects with masses between 0.013 $M_\odot$ and 0.10 $M_\odot$ form; two of them being bound in a binary system. In addition, 0.016 $M_\odot$ of gas accretes onto the central star within 15 000 years, and 0.0028 $M_\odot$ = 2.8 Jupiter masses (M_J) of gas transfers to the perturber (into the representing sink particle) while about 0.012 $M_\odot$ ($\approx 12\,M_\mathrm{J}$) is captured around the perturber as a circumstellar envelope. In our analysis, any gas that is present within a radius of 40 AU but outside the sink radius is counted as circumstellar material of the perturber and shown in the ninth column of Table 3.3.3. This mass capture is typical, ranging between 2 and 16 M_J.

In total, 28 bodies between 0.01 and 0.15 $M_\odot$ formed in eight high resolution calculations, while the ten 100 000 particle calculations that showed fragmentation, yielded 30 bodies between 0.01 and 0.16 $M_\odot$ (see Tables 3.3.3 and 3.4). Thus, there is no statistically significant relation between the resolution and the number of formed bodies. Similarly, no clear trend towards lower minimum masses of the companions for the high resolution can be derived from the current data. The average mass of the lowest-mass member is 0.056 $M_\odot$ for the 100 000 particle models while it is 0.044 $M_\odot$ for the 250 000 ones. Similarly, the average mass of the highest-mass is 0.097 $M_\odot$ and 0.083 $M_\odot$, respectively. Table 3.4 does also show the separations of the objects at the end of each calculation. It has to be noted that these can differ largely from the initial separation at the moment of formation. Dynamical interaction between the objects and the disc as well as mutual encounters push some bodies at wide and eccentric orbits or even eject them while others migrate closer to the star. The closest separation observed in our calculations is about 10 AU in model E015 after 15 000 years of evolution. The overall outcome is very similar to that of unperturbed self-fragmenting disc as shown in Stamatellos & Whitworth (2009b) except for the lower disc mass. This is quite plausible since the main difference between the two scenarios is the cause for the density patterns which undergo fragmentation. While Toomre density waves are the source of fragmentation in self-fragmenting discs, the gravitationally induced fragmentation occurs in tidal arms. In both cases, a dense bar-like in the disc reaches the density limit for fragmentation and thus the underlying physics is essentially the same.

Figure 3.5 shows the mass distribution of the n bodies created all calculations with 100 000 particles (top frame), 250 000 particles (middle frame) and both combined (bottom frame). A power law mass function $dn/dm = k(m/M_\odot)^{-\alpha}$ can be fitted to this distribution. This has been done in this figure for the substellar regime (dashed line). In the bi-logarithmic scaling, the slope of $d\log n/d\log m$ corresponds to $1-\alpha$ due to the differentiation of the logarithm (see Thies & Kroupa 2007 for details). The linear fit to the mass function for all calculation outputs combined appears to have a slope of $0.9^{+0.3}_{-0.4}$ ($< 0.16\ M_\odot$) corresponding to power law index of $\alpha = -0.1^{+0.3}_{-0.4}$. If the calculations are separated by resolution, the 100 000 particle models correspond to $\alpha = +0.1^{+0.3}_{-1.5}$ while the 250 000 particle models similarly yield $\alpha = +0.1^{+0.3}_{-0.6}$. The slightly flatter IMF in the separate mass functions may be interpreted as a weak resolution-dependence of the

average created mass which gets smeared out in the combined mass function. However, the difference between the slopes of 0.2 is within the 1σ uncertainty The uncertainty, based on the Poisson errors of the log mass bins, is indicated by a shaded region. Above 0.12 $M_{\odot}$ there is a sharp drop in the mass distribution that can be treated as a truncation. Similar results have been obtained by Stamatellos & Whitworth (2009a) and Shen et al. (2010). Interestingly, this is also in good agreement with both the sub-stellar IMF deduced by Kroupa (2001) as well as with the separate substellar IMF deduced in Thies & Kroupa (2007, 2008). However, more calculations are needed to provide statistically robust tests of the IMF. Furthermore, there is no weighting with respect to the different likelihood of the different encounter settings (i.e., inclination, fly-by distance etc.). Since the outcome of the computations does not show a specific dependency on the orbital parameters (except for whether there is fragmentation) such a weighting might introduce an artificial bias by amplifying the random noise of higher-weighted models.

3.4.2 Binary formation

In the same way as in the models of Stamatellos & Whitworth (2009a) of isolated circumstellar discs, very low-mass binary systems can also form in gentle three-body encounters between low-mass objects in the disc. Such a triple in-orbit encounter occurred during the X002 computation about 8,000 years after the fly-by, as shown in Figure 3.3 where a 4 AU binary system composed of 0.09 $M_{\odot}$ and 0.10 $M_{\odot}$ objects forms through a triple encounter. This binary remains bound to the host star in an orbit of about 100 AU. These separations are consistent with the observations of VLMS binaries according to which the most probable separation is around 3 AU (see, e.g., Figure 10 in Stamatellos & Whitworth 2009a). Another binary-forming mechanism was unveiled during calculation E003 (see Table 3.4). A 2 AU binary, consisting of a VLMS of 0.09 $M_{\odot}$ and a BD with 0.013 $M_{\odot}$, formed through a grazing encounter of circum-substellar accretion envelopes, which subsequently evolve into a circumbinary disc. The event is shown in a sequence plot in Figure 3.4. In two similar events in run X006, two accreting clumps merged to a single one of about 0.03 $M_{\odot}$ 9600 yr after the fly-by, and 6000 yr later this body and a third one got captured into a binary of about 5 AU separation, probably involving both triple encounter and grazing collision. The masses at the end of the calculation are 0.03 and 0.04 $M_{\odot}$.

Binaries formed via these processes may later be separated from their host star in a subsequent encounter with another star as already discussed for single substellar companions (Kroupa 1995a; Goodwin & Whitworth 2007), or, possibly, by dynamical interaction with more massive companions in the same system. These models produce 55 systems of BDs and VLMSs, and 3 binaries giving a binary of $3/55 = 0.05$, whereby the binaries have semi-major axes of 4, 2 and 5 AU. Thus, while the separations are quite consistent with the observed VLMS and BD binaries, the present theoretical binary fraction is somewhat low.

3.4.3 The role of eccentricity and inclination

In a previous study (Thies et al. 2005) we found that the strength of the perturbation increases with decreasing eccentricity and inclination. This agrees with results of an SPH parameter study by Pfalzner et al. (2005). While disc-disc collisions produce most objects due to shock formation (Shen et al. 2010), coplanar encounters increase the effectiveness of the tidal perturbations which cause our discs to fragment. This is a consequence of the low relative velocity between the perturber and the perturber-facing parts of the disc in coplanar encounters, and thus a longer tidal exposure time. While drag forces in disc-disc collisions are larger for larger collisional velocities the tidal force does not depend on the velocity, and therefore the total amount of tidally transferred momentum for a given flyby distance is larger for slower encounters, i.e., for those with lower eccentricity.

3.5 Discussion

Our computations show that the tidal perturbations of massive (otherwise stable) discs can form massive planets and BDs. Previous computations had assumed the interaction of two massive discs (Shen et al. 2010), reducing the probability of such an event dramatically. Our scenario only requires a single extended disc. This scenario can produce very low-mass companions at large distances from the primary star, and may help explain recent direct detections of massive planets orbiting at > 100 AU, far beyond where core accretion could have formed them[2], as well as intermediate (Liu et al. 2002) and distant (Stamatellos et al. 2007; Stamatellos & Whitworth 2009a) BD companions to stars. Like Stamatellos & Whitworth (2009a) we are also able to form BD binaries through three body encounters within the disc, and in addition, through dissipative encounters. But the required disc mass is considerably smaller, by about 30–40 %, since even initially stable discs do fragment upon perturbation in our calculations. The mass function of companions formed by this process is in good agreement with that of self-fragmentation and with the separate substellar IMF deduced in Thies & Kroupa (2007). However, the volume of the current results does not allow robust statistical tests of the normalisation of this sub-stellar IMF relative to the stellar IMF. Nevertheless, the obtained results are in remarkable agreement both with the form of the substellar IMF and the binary properties in the BD and VLMS regime, although the binary fraction is somewhat low (Section 3.4.2). More computations will have to be performed at different resolutions (up to a million particles) to enhance quantity as well as quality of the data.

3.5.1 How often do such encounters occur?

Furthermore, it has to be noted that triggered fragmentation is probably responsible only for a fraction of disc-fragmentation events while a good fraction may be triggered simply by over-feeding of an accreting disc towards self-fragmentation. Although the

[2]See also the Extrasolar Planets Encyclopaedia, http://exoplanet.eu/

borders of the parameter subspace suitable for triggered fragmentation are not yet fully determined the current findings show that encounters of a higher inclination than 45 degrees, outside 600 AU or with eccentricities above 2 are generally unlikely to trigger fragmentation for the disc type studied here. The same holds true for perturbers of less than 0.3 $M_\odot$.

By combining all these limits of the parameter space one can estimate the fraction of random encounters with a mutual periastron below 500 AU that are suitable for fragmentation of the analysed disc type. If a characteristic velocity dispersion of $\sim 2\,\mathrm{km\,s^{-1}}$ and an upper stellar mass limit of 10 $M_\odot$ within the host cluster is assumed only about 3 % of all encounters below 500 AU lead to fragmentation. However, discs with even only slightly larger mass or lower background temperature may be pushed much easily to fragmentation, probably enlarging the parameter space significantly. Furthermore, other perturbing effects like stellar winds or supernova shock waves, which might influence large volumes within the host cluster at once, are not covered by this study, nor are the effects of dust.

3.5.2 Consequences for planet formation

All objects formed in our calculations have masses above 0.01 $M_\odot$ or 10 M_J and are thus above the masses typically assumed for planets. However, we cannot rule out at the moment that also objects below 0.01 $M_\odot$ may form through fragmentation, especially around lower-mass host stars which heat the inner disc region much less than more massive ones. Another critical point may be the resolution limits (although the local Jeans mass is well resolved even in the inner disc region, as discussed in Section 3.3.1).

It has to be emphasised, that planet formation probably typically takes place in the inner disc region through core-accretion (Hillenbrand 2008) which are less influenced by the perturbation unless companions formed through it migrate into these inner regions. There might still be significant impacts on the outcome of planet formation for stellar encounters, though. Even temporary gravitational instabilities that do not collapse into a brown dwarf or planet directly may induce the formation of substellar companions down to Kuiper-Belt objects by induced vorticity and subsequent dust trapping (Barge & Sommeria 1995; Klahr & Bodenheimer 2003, 2006). Also the development of baroclinic vortices may be altered under the influence of tidal perturbations, either inhibiting or promoting the formation of dust aggregates. This mechanism may even work in typical protoplanetary discs and is subject of our ongoing research. According to solar system architecture (Heller 1993; Eggers et al. 1997; Kenyon & Bromley 2004) and radionuclide evidence (Takigawa et al. 2008; Sahijpal & Gupta 2009; Gaidos et al. 2009; Gounelle & Meibom 2008, however, disagree) the highly probable origin of our Sun in a large star-forming region further emphasises the importance of such scenarios.

Another fact worth to be discussed is the capture of disc material by the perturbing star. As mentioned in Section 3.4 about 0.003 $M_\odot = 3\ M_\mathrm{J}$ are accreted by the perturber in a typical 500 AU encounter like model E/X002, while the amount of accreted gas can be as large as 10 M_J, as in models E/X003 (see Table 3.3.3). An even larger amount can be contained in a circumstellar disc or envelope around the perturber. Although

being smaller than typically assumed for the Minimum-Mass Solar Nebular (MMSN, see Crida 2009) this may still be sufficient for the formation of Jupiter- or Saturn-type planets around the perturber. Since the orientation of this encounter-related accretion disc is not correlated to the stellar rotation of the perturber, this scenario may provide an explanation for highly inclined or even retrograde planets which have recently been detected (Narita et al. 2009; Johnson et al. 2009). If the captured gas is accreted onto a pre-existing circumstellar disc of the perturber star this might even lead to the formation of planetary systems with multiple mutually inclined (or even retrograde) orbital planes.

We have to emphasise at this point that gas capture from a massive extended circumstellar disc is only one of several possible gas capture scenarios, and is being observed in our work as a spin-off besides the main topic of this article. As the more general case, capture of material from any dense gas aggregate in the hosting star-forming region after the formation of the protostar itself may be a possible channel to form non-aligned planets. As the most general formulation, we note that the whole process of planet formation from the pre-stellar cloud in the context of stellar encounters in young star clusters to a fully established planetary system appears to be a discontinuous one in many cases, probably limiting the probability of regularly-shaped planetary systems with Solar system-like architecture. This issue will be investigated in detail in future work.

One issue not treated by our calculations is the varying protostar and disc mass during the accretion process. According to Machida et al. (2010) the growing disc may become temporarily unstable when the mass of the protostar is still negligibly small ($\sim 10^{-3}\,M_{\odot}$). In their nested-grid calculations, the disc fragments in the region of < 100 AU, and even within 10 AU. However, their simulations do not include a realistic treatment of radiative transfer. It is subject to future investigations whether accreting discs under perturbation may develop into planetary systems with Solar-type architecture.

Furthermore, the influence of magnetic fields are completely ignored in our calculations. Liverts et al. (2010) show that both hydromagnetic and thermomagnetic effects may amplify density waves in the disc into instability, and may provide an effective viscosity via turbulence which may assist accretion onto the star.

Observations of tidally perturbed fragmenting discs would surely be the best confirmation of this scenario. Due to the short duration of the flyby of only about 10,000 years the chance of such an event to be 'caught in the act' is small. It may, however, be possible to identify encounter-triggered fragmentation if observers succeed in detecting the typical tidal arms around the disc-hosting star as well as smaller amounts of non-circular filaments around a close-by star indicating it as a candidate perturber star. Such structures may be detectable with future high-resolution instruments like ALMA in star-forming regions like the ONC. Another possibility is to target FU Orionis stars which are thought to be undergoing enhanced accretion, such enhanced accretion may be caused by the perturbation of discs by a close encounter.

3.6 Summary and Conclusions

In a series of SPH calculations we have shown that massive ($\sim 0.5\,M_\odot$), extended ($\geq 100\,\mathrm{AU}$) circumstellar discs can be stable when isolated, but fragment when perturbed by a moderately close and slightly inclined stellar encounter. Binaries formed in two cases via triple encounters of companions and via grazing encounters of accreting envelopes. This agrees with binary formation in self-fragmenting discs (Stamatellos & Whitworth 2009a). We further found that the mass distribution of companions formed in discs is in agreement with the canonical substellar IMF as a separate population (Kroupa 2001; Kroupa & Bouvier 2003a; Thies & Kroupa 2007, 2008). We have, however, to note that direct tidally induced fragmentation is probably only responsible for a fraction of all disc fragmentation events due to the relatively small orbital parameter subset that is suitable for fragmentation of discs of about 0.5 $M_\odot$. More massive discs are expected to be more prone to fragmentation even due to weak perturbations, but are also more likely to reach the limit for self-fragmentation. This study, however, shows that tidal perturbations do not necessarily inhibit fragmentation but are instead capable of inducing fragmentation in disc that otherwise would silently disperse or be accreted by the central star without ever experiencing fragmentation. The perturber star may accrete gas from the target circumstellar disc and may form planets on misaligned or even counter-rotating orbits with respect to the stellar spin. Future work will analyse discs with different masses and more or less massive host stars as well.

Outlook

The current work already provides an important insight into the nature and possible origin of brown dwarfs and giant planets. Future improvements of the IMF models will mostly depend on the availability of new observational data. Star cluster surveys with higher sensitivity as well as higher spatial resolution (or more reliable data reduction for binary fraction) will be required to address the question of the universality of the low-mass and very-low-mass IMF and the discontinuity between the stellar and substellar regime. On the other hand, the numerical models have to be improved for both more realistic physics and higher resolution. The future availability of high-performance computing hardware is a crucial point to this issue.

The very next step will be a dedicated study to the multi-stage accretion scenario for misaligned planets. The aim will be a prediction of the distribution of orbital inclinations for planetary systems with negligible subsequent evolution. In an improved study, also the statistical effects of the Kozai mechanism on this distribution will be taken into account, and the results will be compared with current and future observational data on misaligned transiting planets.

Another interesting issue is concerning planet formation in multiple stellar systems. A few binaries are already known to host planets (Raghavan et al. 2006). While the aspects of orbital stability of planets in binary systems are quite well understood today the formation of planets, i.e. coagulation and/or disc fragmentation in a permanently perturbed disc is still a matter of investigation. Guedes et al. (2008) deduce a substantial likelihood of terrestrial planet formation in the nearby α Cen system which is a moderately close binary with a semimajor axis of 23.5 AU and an eccentricity of 0.52. They further discuss the feasibility of detecting even terrestrial planets on AU-scale orbits around solar-type stars by a dedicated long-term radial-velocity (RV) survey. For the case of α Cen B (but also feasible for most nearby stars) they deduce a good prospect of success for detection of Earth-type planets within a few years of observation. However additional data will be needed to determine the actual orbital alignments and thus the true masses, because RV surveys do not provide information about the inclination. My future studies will therefore also account for the behaviour of discs in binary systems. These will have to include dust dynamics to investigate the mechanism of dust trapping in self-forming and induced vortices (Barge & Sommeria 1995). Last but not least the timescale problem of Uranus and Neptune in our Solar System will be revisited by these advanced hydrodynamical means.

Bibliography

Adams F. C., Fatuzzo M., 1996, ApJ, 464, 256

Barge P., Sommeria J., 1995, A&A, 295, L1

Barrado y Navascués D., Stauffer J. R., Jayawardhana R., 2004, ApJ, 614, 386

Basri G., Reiners A., 2006, AJ, 132, 663

Bate M. R., 2005, MNRAS, 363, 363

Bate M. R., Bonnell I. A., 2005, MNRAS, 356, 1201

Bate M. R., Bonnell I. A., Bromm V., 2003, MNRAS, 339, 577

Bell K. R., Lin D. N. C., 1994, ApJ, 427, 987

Black D. C., Bodenheimer P., 1975, ApJ, 199, 619

Boffin H. M. J., Watkins S. J., Bhattal A. S., Francis N., Whitworth A. P., 1998, MNRAS, 300, 1189

Boley A. C., Hartquist T. W., Durisen R. H., Michael S., 2007, ApJ, 656, L89

Bonnell I. A., Clark P., Bate M. R., 2008, MNRAS, 389, 1556

Bonnell I. A., Larson R. B., Zinnecker H., 2007, in Reipurth B., Jewitt D., Keil K., eds, Protostars and Planets V The Origin of the Initial Mass Function. Univ. Arizona Press, Tucson, pp 149–164

Boss A. P., 1997, Science, 276, 1836

Boss A. P., 2004, ApJ, 610, 456

Boss A. P., 2006, ApJ, 641, 1148

Boss A. P., Bodenheimer P., 1979, ApJ, 234, 289

Boss A. P., Myhill E. A., 1992, ApJS, 83, 311

Bouvier J., Stauffer J. R., Martin E. L., Barrado y Navascues D., Wallace B., Bejar V. J. S., 1998, A&A, 336, 490

Bouy H., Brandner W., Martín E. L., Delfosse X., Allard F., Basri G., 2003, AJ, 126, 1526

Briceño C., Luhman K. L., Hartmann L., Stauffer J. R., Kirkpatrick J. D., 2002, ApJ, 580, 317

Burgasser A. J., Kirkpatrick J. D., Reid I. N., Brown M. E., Miskey C. L., Gizis J. E., 2003, ApJ, 586, 512

Burgasser A. J., Reid I. N., Siegler N., Close L., Allen P., Lowrance P., Gizis J., 2007, in Reipurth B., Jewitt D., Keil K., eds, Protostars and Planets V Not Alone: Tracing the Origins of Very-Low-Mass Stars and Brown Dwarfs Through Multiplicity Studies. Univ. Arizona Press, Tucson, pp 427–441

Burrows A., Hubbard W. B., Saumon D., Lunine J. I., 1993, ApJ, 406, 158

Cai K., Pickett M. K., Durisen R. H., Milne A. M., 2010, ApJ(accepted)

Chabrier G., 2002, ApJ, 567, 304

Chabrier G., 2003, PASP, 115, 763

Chabrier G., Baraffe I., 2000, ARA&A, 38, 337

Close L. M., Siegler N., Freed M., Biller B., 2003, ApJ, 587, 407

Commerçon B., Hennebelle P., Audit E., Chabrier G., Teyssier R., 2008, A&A, 482, 371

Crida A., 2009, ApJ, 698, 606

Dobbie P. D., Pinfield D. J., Jameson R. F., Hodgkin S. T., 2002, MNRAS, 335, L79

Duchêne G., 1999, A&A, 341, 547

Duchêne G., Bouvier J., Simon T., 1999, A&A, 343, 831

Duquennoy A., Mayor M., 1991, A&A, 248, 485

Eggers S., Keller H. U., Kroupa P., Markiewicz W. J., 1997, Planet. Space Sci., 45, 1099

Eislöffel J., Steinacker J., 2007, ArXiv Astrophysics e-prints

Eisner J. A., Carpenter J. M., 2006, ApJ, 641, 1162

Fischer D. A., Marcy G. W., 1992, ApJ, 396, 178

Forgan D., Rice K., 2009, MNRAS, 400, 2022

Gaidos E., Krot A. N., Williams J. P., Raymond S. N., 2009, ApJ, 696, 1854

Goodwin S. P., Kroupa P., 2005, A&A, 439, 565

Goodwin S. P., Kroupa P., Goodman A., Burkert A., 2007, in Reipurth B., Jewitt D., Keil K., eds, Protostars and Planets V The Fragmentation of Cores and the Initial Binary Population. Univ. Arizona Press, Tucson, pp 133–147

Goodwin S. P., Whitworth A., 2007, A&A, 466, 943

Goodwin S. P., Whitworth A. P., Ward-Thompson D., 2004, A&A, 414, 633

Gounelle M., Meibom A., 2008, ApJ, 680, 781

Grether D., Lineweaver C. H., 2006, ApJ, 640, 1051

Güdel M., Padgett D. L., Dougados C., 2007, in Reipurth B., Jewitt D., Keil K., eds, Protostars and Planets V The Taurus Molecular Cloud: Multiwavelength Surveys with XMM-Newton, the Spitzer Space Telescope, and the Canada-France-Hawaii Telescope. Univ. Arizona Press, Tucson, pp 329–344

Guedes J. M., Rivera E. J., Davis E., Laughlin G., Quintana E. V., Fischer D. A., 2008, ApJ, 679, 1582

Guenther E. W., Wuchterl G., 2003, A&A, 401, 677

Guieu S., Dougados C., Monin J.-L., Magnier E., Martín E. L., 2006, A&A, 446, 485

Haisch K. E., Lada E. A., Lada C. J., 2001, ApJ, 553, L153

Heller C. H., 1993, ApJ, 408, 337

Henning T., 2008, Physica Scripta Volume T, 130, 014019

Hillenbrand L. A., 2008, Physica Scripta Volume T, 130, 014024

Hillenbrand L. A., Carpenter J. M., Feigelson E. D., 2001, in Montmerle T., André P., eds, ASP Conf. Ser. 243: From Darkness to Light: Origin and Evolution of Young Stellar Clusters The Orion Star-Forming Region. pp 439–+

Hillenbrand L. A., Hartmann L. W., 1998, ApJ, 492, 540

Hubber D. A., Goodwin S. P., Whitworth A. P., 2006, A&A, 450, 881

Hubeny I., 1990, ApJ, 351, 632

Jeffries R. D., Maxted P. F. L., 2005, Astronomische Nachrichten, 326, 944

Joergens V., 2006, A&A, 446, 1165

Johnson J. A., Winn J. N., Albrecht S., Howard A. W., Marcy G. W., Gazak J. Z., 2009, PASP, 121, 1104

Kenyon M. J., Jeffries R. D., Naylor T., Oliveira J. M., Maxted P. F. L., 2005, MNRAS, 356, 89

Kenyon S. J., Bromley B. C., 2004, Nature, 432, 598

Klahr H., Bodenheimer P., 2003, ApJ, 582, 869

Klahr H., Bodenheimer P., 2006, ApJ, 639, 432

Konopacky Q. M., Ghez A. M., Rice E. L., Duchene G., 2007, ArXiv Astrophysics e-prints

Kraus A. L., White R. J., Hillenbrand L. A., 2006, ApJ, 649, 306

Kroupa P., 1995a, MNRAS, 277, 1491

Kroupa P., 1995b, MNRAS, 277, 1522

Kroupa P., 1995c, MNRAS, 277, 1507

Kroupa P., 2001, MNRAS, 322, 231

Kroupa P., 2005, Nature, 434, 148

Kroupa P., Aarseth S., Hurley J., 2001, MNRAS, 321, 699

Kroupa P., Bouvier J., 2003a, MNRAS, 346, 369

Kroupa P., Bouvier J., 2003b, MNRAS, 346, 343

Kroupa P., Bouvier J., Duchêne G., Moraux E., 2003, MNRAS, 346, 354

Kroupa P., Gilmore G., Tout C. A., 1991, MNRAS, 251, 293

Kroupa P., Petr M. G., McCaughrean M. J., 1999, New Astronomy, 4, 495

Kroupa P., Tout C. A., Gilmore G., 1993, MNRAS, 262, 545

Kumar M. S. N., Schmeja S., 2007, A&A, 471, L33

Lada C. J., 2006, ApJ, 640, L63

Lada C. J., Lada E. A., 2003, ARA&A, 41, 57

Lafrenière D., Jayawardhana R., Brandeker A., Ahmic M., van Kerkwijk M. H., 2008, ApJ, 683, 844

Law N. M., Hodgkin S. T., Mackay C. D., 2007, ArXiv e-prints, 704 (submitted to MNRAS)

Liu M. C., Fischer D. A., Graham J. R., Lloyd J. P., Marcy G. W., Butler R. P., 2002, ApJ, 571, 519

Liverts E., Mond M., Urpin V., 2010, MNRAS, 404, 283

Lodato G., Meru F., Clarke C. J., Rice W. K. M., 2007, MNRAS, 374, 590

Lodieu N., Pinfield D. J., Leggett S. K., Jameson R. F., Mortlock D. J., Warren S. J., Burningham B., Lucas P. W., et al. 2007, MNRAS, 379, 1423

Luhman K. L., 2004a, ApJ, 617, 1216

Luhman K. L., 2004b, ApJ, 614, 398

Luhman K. L., 2006, ApJ, 645, 676

Luhman K. L., Allers K. N., Jaffe D. T., Cushing M. C., Williams K. A., Slesnick C. L., Vacca W. D., 2007, ApJ, 659, 1629

Luhman K. L., Briceño C., Stauffer J. R., Hartmann L., Barrado y Navascués D., Caldwell N., 2003, ApJ, 590, 348

Luhman K. L., Stauffer J. R., Muench A. A., Rieke G. H., Lada E. A., Bouvier J., Lada C. J., 2003, ApJ, 593, 1093

Lupton R., 1993, Statistics in Theory and Practice, first edn. Princeton University Press, Princeton, New Jersey

Machida M. N., Inutsuka S., Matsumoto T., 2010, ApJ(submitted)

Malkov O., Zinnecker H., 2001, MNRAS, 321, 149

Martín E. L., Barrado y Navascués D., Baraffe I., Bouy H., Dahm S., 2003, ApJ, 594, 525

Martín E. L., Dougados C., Magnier E., Ménard F., Magazzù A., Cuillandre J.-C., Delfosse X., 2001, ApJ, 561, L195

Masunaga H., Inutsuka S., 2000, ApJ, 531, 350

Masunaga H., Miyama S. M., Inutsuka S., 1998, ApJ, 495, 346

Matsumoto M., Nishimura T., 1998, ACM Trans. Model. Comput. Simul, 8, 3

Mayer L., Quinn T., Wadsley J., Stadel J., 2002, Science, 298, 1756

Mayor M., Queloz D., 1995, Nature, 378, 355

McCarthy C., Zuckerman B., Becklin E. E., 2003, in Martín E., ed., Brown Dwarfs, IAU Symposium 211 There is a Brown Dwarf Desert of Companions Orbiting Stars between 75 and 1000 AU. ASP, San Francisco, pp 279–+

Metchev S., Hillenbrand L., 2005, Memorie della Societa Astronomica Italiana, 76, 404

Moraux E., Bouvier J., Stauffer J. R., Cuillandre J.-C., 2003, A&A, 400, 891

Moraux E., Kroupa P., Bouvier J., 2004, A&A, 426, 75

Muench A. A., Lada E. A., Lada C. J., Alves J., 2002, ApJ, 573, 366

Nakajima T., Oppenheimer B. R., Kulkarni S. R., Golimowski D. A., Matthews K., Durrance S. T., 1995, Nature, 378, 463

Narita N., Sato B., Hirano T., Tamura M., 2009, PASJ, 61, L35

Natta A., Testi L., Muzerolle J., Randich S., Comerón F., Persi P., 2004, A&A, 424, 603

Nelson A. F., 2006, MNRAS, 373, 1039

Padoan P., Nordlund Å., 2002, ApJ, 576, 870

Padoan P., Nordlund Å., 2004, ApJ, 617, 559

Papaloizou J. C. B., Terquem C., 2006, Reports on Progress in Physics, 69, 119

Pfalzner S., Vogel P., Scharwächter J., Olczak C., 2005, A&A, 437, 967

Preibisch T., Stanke T., Zinnecker H., 2003, A&A, 409, 147

Press W. H., Teukolsky S. A., Vetterling W. T., Flannery B. P., 1992, Numerical Recipes in Fortran 77, second edn. Cambridge University Press, Cambridge

Price N. M., Podsiadlowski P., 1995, MNRAS, 273, 1041

Raghavan D., Henry T. J., Mason B. D., Subasavage J. P., Jao W., Beaulieu T. D., Hambly N. C., 2006, ApJ, 646, 523

Reid I. N., Gizis J. E., Hawley S. L., 2002, AJ, 124, 2721

Reid I. N., Lewitus E., Allen P. R., Cruz K. L., Burgasser A. J., 2006, AJ, 132, 891

Reipurth B., 2000, AJ, 120, 3177

Reipurth B., Clarke C., 2001, AJ, 122, 432

Reipurth B., Guimarães M. M., Connelley M. S., Bally J., 2007, AJ, 134, 2272

Sahijpal S., Gupta G., 2009, Meteoritics and Planetary Science, 44, 879

Salpeter E. E., 1955a, ApJ, 121, 161

Salpeter E. E., 1955b, ApJ, 121, 161

Scholz A., Jayawardhana R., Wood K., 2006, ApJ, 645, 1498

Shen S., Wadsley J., Hayfield T., Ellens N., 2010, MNRAS, 401, 727

Slesnick C. L., Hillenbrand L. A., Carpenter J. M., 2004, ApJ, 610, 1045

Spiegel E. A., 1957, ApJ, 126, 202

Stamatellos D., Hubber D. A., Whitworth A. P., 2007, MNRAS, 382, L30

Stamatellos D., Whitworth A. P., 2008, A&A, 480, 879

Stamatellos D., Whitworth A. P., 2009a, MNRAS, 392, 413

Stamatellos D., Whitworth A. P., 2009b, MNRAS, 400, 1563

Stamatellos D., Whitworth A. P., Bisbas T., Goodwin S., 2007, A&A, 475, 37

Sterzik M. F., Durisen R. H., 2003, A&A, 400, 1031

Takigawa A., Miki J., Tachibana S., Huss G. R., Tominaga N., Umeda H., Nomoto K., 2008, ApJ, 688, 1382

Thies I., Kroupa P., 2007, ApJ, 671, 767

Thies I., Kroupa P., 2008, MNRAS, 390, 1200

Thies I., Kroupa P., Theis C., 2005, MNRAS, 364, 961

Toomre A., 1964, ApJ, 139, 1217

Umbreit S., Burkert A., Henning T., Mikkola S., Spurzem R., 2005, ApJ, 623, 940

Watkins S. J., Bhattal A. S., Boffin H. M. J., Francis N., Whitworth A. P., 1998a, MNRAS, 300, 1205

Watkins S. J., Bhattal A. S., Boffin H. M. J., Francis N., Whitworth A. P., 1998b, MNRAS, 300, 1214

Weidner C., Kroupa P., 2004, MNRAS, 348, 187

Weidner C., Kroupa P., 2006, MNRAS, 365, 1333

Whitehouse S. C., Bate M. R., 2006, MNRAS, 367, 32

Whitworth A., Bate M. R., Nordlund Å., Reipurth B., Zinnecker H., 2007, in Reipurth B., Jewitt D., Keil K., eds, Protostars and Planets V The Formation of Brown Dwarfs: Theory. Univ. Arizona Press, Tucson, pp 459–476

Whitworth A. P., Stamatellos D., 2006, A&A, 458, 817

Whitworth A. P., Zinnecker H., 2004, A&A, 427, 299

Wuchterl G., Tscharnuter W. M., 2003, A&A, 398, 1081

Acknowledgements

This thesis would not have been completed without the support of many people, first of all the University of Bonn and my supervisor Prof. Dr. Pavel Kroupa, and the colleagues in his and other research groups at the Argelander-Institute for Astronomy. In particular, Prof. Dr. Holger Baumgardt (now in Australia), Prof. Dr. Michael Fellhauer (now in Chile), Prof. Norbert Langer and Prof. Peter Schneider for providing me great insights into astronomy and astrophysics of star clusters, brown dwarfs and planets, but also for letting me participate in the current debates on extra-galactic astronomy and cosmology. I further wish to thank also Dr. Simon Goodwin (Sheffield), Dr. Dimitris Stamatellos and Prof. Anthony Whitworth (Cardiff) for allowing and assisting me so kindly in using their `DRAGON` software. Special acknowledgements are addressed to the Deutsche Forschungsgemeinschaft for supporting my PhD by DFG grants KR1635/12-1 and KR1635/25-1.

I also wish to thank Dr. Ole Marggraf and Dr. Oliver Cordes as well as the other members of the AIfA computer group, without whose technical skills and personal commitment no productive work would have been possible at the institute, as well as Günter Lay who passed away far too early. And, of course, Andreas Bödewig, Elisabeth Danne, Kathy Schrüfer and Christina Stein-Schmitz for their indispensible help and support in all technical and administrative issues. My further thanks to all the other colleagues and (present and former) AIfA members and visitors for many discussions about science and life at and outside the AIfA, in particular (but in no way exclusively) Claudia Brüns, Ylva Schuberth, Jan Pflamm-Altenburg, Dr. Sambaran Banerjee, Dr. Gisela Maintz, Dr. Michael Geffert, Prof. Wolfgang Kundt, and many others.

Im am deeply indebted to my parents Margaretha and Klaus, who is now looking at us from beyond the cosmic background, my brother Mario and my cousin Henning, as well as his parents and my aunt Wiebe and uncle Wilfried. Their motivation and moral support have proven indispensable for me to overcome all the difficulties and challenges beyond science, and not to become desperate because of the amounts of hurdles over my six years in Bonn. In addition, Mario's and Henning's computational skills have proven helpful many times. Special thanks are also devoted to Jochen Schweizer, and the Reverends Stefanie Graner and Michael Verhey for their great support in dark times, as well as to Klaus Baehr and other members of the Friedenskirche Bonn, as well as Renate Glitsch and her parents, Andreas Kreide, Stefan Preiss and many others, who opened my eyes for many interesting aspects of life beyond astronomy. I also acknowledge the members of the examination committee for allowing me to defend my PhD.

Last, but not least, I wish to thank my office mates over time, Peter Kahabka, Alessio Fangano, Michael Brockamp and Fabian Lüghausen for everyday support. And, of course, the one who triggered the Big Bang and allowed us to explore its exhaust.